CRITICAL REVIEWS IN ENVIRONMENTAL SCIENCE AND TECHNOLOGY
2020, VOL. 50, NO. 9, 903–978
https://doi.org/10.1080/10643389.2019.1642832

Chemical and biological immobilization mechanisms of potentially toxic elements in biochar-amended soils

Tharanga Bandara[a], Ashley Franks[b,c], Jianming Xu[d,e], Nanthi Bolan[f,g,h], Hailong Wang[i,j] and Caixian Tang[a]*

[a]*Department of Animal, Plant and Soil Sciences, Centre for AgriBioscience, La Trobe University, Melbourne Campus, Bundoora, Victoria 3086, Australia;*
[b]*Department of Physiology, Anatomy and Microbiology, La Trobe University, Melbourne Campus, Bundoora, Victoria 3086, Australia;*
[c]*Centre for Future Landscapes, La Trobe University, Melbourne Campus, Bundoora, Victoria 3086, Australia;*
[d]*Institute of Soil and Water Resources and Environmental Science, College of Environmental and Resource Sciences, 866 Yuhangtang Road, Hangzhou 310058, China;*
[e]*Zhejiang Provincial Key Laboratory of Agricultural Resources and Environment, Zhejiang University, 866 Yuhangtang Road, Hangzhou 310058, China;*
[f] *Global Centre for Environmental Remediation (GCER), Advanced Technology Centre, Faculty of Science, The University of Newcastle, Callaghan, NSW 2308, Australia*
[g] *Cooperative Research Centre for High Performance Soil (Soil CRC), The University of Newcastle, Callaghan, NSW, 2308, Australia*
[h] *The Australian Centre for Cannabinoid Clinical and Research Excellence (ACRA), The University of Newcastle, Callaghan, NSW, 2308, Australia*
[i]*Biochar Engineering Technology Research Centre of Guangdong Province, School of Environmental and Chemical Engineering, Foshan University, Foshan, Guangdong 528000, China;*
[j]*Key Laboratory of Soil Contamination Bioremediation of Zhejiang Province, Zhejiang A & F University, Hangzhou, Zhejiang 311300, China*

*corresponding author
Caixian Tang
E-mail: C.Tang@latrobe.edu.au
Tel: +61390327416
Fax: +61390327605

Chemical and biological immobilization mechanisms of potentially toxic elements in biochar-amended soils

The application of biochars for the remediation of water and soils contaminated with potentially toxic elements (PTEs) has seen a recent growing interest. The mechanisms of chemical immobilization of PTEs with biochars in aqueous media have been well defined. However, immobilization mechanisms by which biochars interact with PTEs in soil matrix are more complex. The biological immobilization mechanisms and their interactions with PTEs in biochar-amended soils are not as well defined. This review presents an overview of factors governing interactions of biochars with PTEs as well as the synergistic effect of biochars and microorganisms in biological immobilization processes. The effectiveness of biochars in improvement of microbial immobilization of PTEs mainly depends on biochar properties, application rates and soil environments such as organic matter content, clay type and content, pH and redox potential. Although some modified biochars appear to be better than the pristine biochars for immobilization of PTEs, their potential adverse impacts on soil microbial activity should be considered. This review highlights the most common analytical methods to discover molecular interaction mechanisms between biochar and PTEs and future research areas required for the understanding of biochar-PTE interactions in polluted soil systems.

Keywords: Biochar; potentially toxic elements; chemical mechanisms; microbes; advance techniques; modification; priming effect

1. Introduction

Contamination of potentially toxic elements (PTEs) in soil is a major environmental, agricultural and public health concern worldwide (Bolan et al., 2014; Jin et al., 2019; Ok et al., 2010; Shaheen, El-Naggar, et al., 2019; Yousaf et al., 2018). Many anthropogenic activities, e.g., use of agrochemicals, mining, explosive and industrial sources, municipal waste, and power generation, discharge and accumulated PTEs into the soil environment (Ali et al., 2017; El-Naggar, Shaheen, et al., 2019; Igalavithana, Kim, et al., 2019; Liu, Xu, et al., 2018; Oh & Yoon, 2016; Wood, Tang, Franks, & Liu, 2016). Potentially toxic elements can be transported through water or the atmosphere before being deposited and concentrated into soils and sediments. Unlike other pollutants, PTEs are persistent in the ecosystems and concentrate in the biosphere through trophic levels of the food web (Bandara, Herath, Kumarathilaka, Seneviratne, et al., 2017; Rinklebe, Antoniadis, Shaheen, Rosche, & Altermann, 2019). The accumulation of PTEs in water bodies and agricultural soils threaten the food quality and security. Prevention and reduction of PTEs in a soil are essential for the secure of the future environment.

The mobility and bioavailability of PTEs are governed by soil characteristics, such as organic matter content, pH, cation exchange capacity, and redox potential (Awad et al., 2018; Bolan et al., 2014; Chen, Yang et al., 2019; El-Naggar, Shaheen, et al., 2019; Lu et al., 2014; Salam et al., 2019; Yuan et al., 2017). Conventional techniques for soil remediation including soil washing, chemical precipitation and soil flushing have been employed worldwide, but themselves contribute to soil degradation and are not economically feasible at a large scale (Houben, Evrard, & Sonnet, 2013; Liu, Xu, et al., 2018; Meng et al., 2017; Yuan, Wang, Pan, Shen, & Wu, 2018). To be broadly feasible it is important that techniques are efficient, low-cost and environmentally-friendly allowing environmental or agricultural application.

More recently, biochars have been gaining recognition as a potential *in-situ* immobilization amendment for the remediation of PTEs (Qi, Kuppusamy, et al., 2017; Shaheen, Niazi, et al., 2019; Tack, Rinklebe, & Ok, 2019; Yuan et al., 2017; Wei et al., 2018; Zhang, Zhang, et al., 2019). Biochars are comprised of solid carbonaceous materials originated from pyrolysis of biomass under low-oxygen environment and used for soil amendment or other environmental applications (Dong et al., 2015; He et al., 2015; He et al., 2018; Hyväluoma et al., 2018; Lehmann et al., 2011; Li, Khan, et al., 2018; Li, Song, Singh, & Wang, 2018; Weng et al., 2017). The addition of biochars increases water and nutrient retention in soils and carbon sequestration, facilitates growth and habitat for soil biota, increases microbial abundance, changes microbial community composition, promotes waste recycling, and reduces bioavailability of soil contaminants (Abiven, Schmidt, & Lehmann, 2014; Ahmad et al., 2014; Dai, Zhang, et al., 2017; Igalavithana, Mandal, et al., 2017; Igalavithana, Kim, et al., 2019; Wu et al., 2019; Yang et al., 2016; Yuan et al., 2019; Zhang, Guo, et al., 2018).

The immobilization capacity of biochar in soil is dependent on the interaction between soil properties, PTEs and the biochar (Igalavithana, Kim, et al., 2019; Lu et al., 2014; Qi, Dong, et al., 2017; Zhang et al., 2013). Therefore, mechanisms of PTE and biochar interactions in soil matrix are expected to be more complex than those in aqueous media. It is imperative to identify and understand the biochar-PTE interactions in soil systems to allow the efficient use of biochars to amend contaminated soils. Biochars undergo an irreversible process in soil and change soil physical and chemical properties which affect biological processes and overall soil health. Compounds present in biochars, such as free radicals, volatile organics, minerals, labile substrates and nutrients, reshape the microbial community and influence the soil enzyme activities (Ahmad, Ok, Kim, et al., 2016; Igalavithana, Kim, et al., 2019; Nie et al., 2018; Sanchez-Hernandez, Rios, Attademo, Malcevschi, & Cares, 2019; Yang, Lu, et al., 2017; Zhu, Chen, Zhu, & Xing, 2017). Recently, many advanced techniques such as fourier transform infrared spectroscopy (FTIR), X-ray photoelectron spectroscopy (XPS), X-ray diffraction (XRD), and X-ray absorption spectroscopy (XAS) have been engaged to identify molecular-binding mechanisms of PTEs and biochar (e.g., Wei et al., 2018; Wu et al., 2016; Wu, Li, et al., 2017). Particularly, synchrotron-

based techniques are being more commonly used for *in-situ* measurements of distribution and speciation of PTEs with the needs for less sample preparation (Kopittke, Wang, Lombi, & Donner, 2017; Liu, Ptacek, Blowes, & Finfrock, 2019).

To the best of our knowledge, there is no comprehensive review dealing with both chemical and biological immobilization mechanisms of PTEs in the biochar-amended soil environment. Therefore, this paper aims to address the following aspects: 1) the major factors affecting the effectiveness of biochars in the immobilization of PTEs; 2) the effects of biochars on plant growth and uptake of PTEs; 3) the key mechanisms of biochar interactions with PTEs in the soils; 4) the possible interactions of biochars, PTEs and microbes in the soils environment; 5) the technologies are employed to the identification of these mechanisms; and 6) the potential use of modified biochars for the immobilization of PTEs in soil. These aspects are brought together to highlight important future areas of research.

2. Biochar production and characterization

Biochars have more specific properties such as high surface area and pore volume, high number of surface functional groups, and low O/C ratio (El-Naggar, Lee, et al., 2019; El-Naggar, Shaheen, et al., 2019). These unique properties primarily depend on feedstock type and production conditions (Table S1) and govern the ability to remediate PTEs (Rangabhashiyam & Balasubramanian, 2019; Wu et al., 2016; Wu, Li, et al., 2017). Pyrolysis, gasification, torrefaction and hydrothermal carbonization are the major technologies used for the conversion of biomass into biochar (Shaheen, Niazi, et al., 2019; Song et al., 2018; Zhang, Zhu, Shen, & Liu, 2019). This section mainly focuses on biochars produced from pyrolysis and hydrothermal carbonization because these biochars have high surface area and surface functional groups (Shaheen, Niazi, et al., 2019), which are important surface characteristics controlling the interactions with PTEs.

Pyrolysis is the most widely employed technique in biochar production. Three pyrolysis methods are reported; slow pyrolysis at low temperature (350-550^{o}C), slow pyrolysis at high temperature (600-900^{o}C) and fast pyrolysis (Vithanage, Herath, Joseph, et al., 2017). Recently, microwave irradiation of biomass is also commonly used to produce biochars, and compared to the conventional pyrolysis, microwaves supply energy directly into biomass that prevents partial carbonization of biomass (Haeldermans et al., 2019). Microwave irradiation produces high-quality products and utilize less energy compared to heat pyrolysis (Li, Dai, et al., 2016; Mao et al., 2019; Wahi et al., 2017). However, microwave irradiation is still limited to laboratory studies due to economic feasibility, large-scale production and technological limitations.

Hydrothermal carbonization is a process of thermochemical conversion of high-moisture biomass into hydrochar. This process has less emission and produces higher amount of C compared to the pyrolysis process (Fang, Zhan, Ok, & Gao, 2018; Melo et al., 2019; Shaheen, Niazi, et al., 2019; Song et al., 2018). However, Han et al. (2017) demonstrated that hydrochar produced from animal manure had low sorption capacities of Cd(II) and Sb(III) due to lack of negative charges and surface polar functional groups compared to the pyrochar. Fang et al. (2018) and Kambo and Dutta (2015) reviewed more details about production, properties and applications of hydrochar.

The yield of produced biochars depends on the size of the biomass particle, density of the feedstock materials, and the content of lignin, cellulose, hemicellulose and minerals (Antal and Gronli, 2003). Biomass with higher lignin and less moisture is considered as most suitable feedstock for high biochar yield (Tripathi, Sahu, & Ganesan, 2016). Biochars produced at low temperatures (<300^{o}C) show a relatively low pH, small surface area, low ash content and low aromaticity, but contain more acidic functional groups and higher CEC. High temperatures (> 600^{o}C) lead to more aromatic graphite structure, high surface area, high pore volume and high ash content which are important in PTE sorption.

Pyrolysis temperature, as well as residence time, significantly affect biochar characteristics with an increase in pH and percentage of ash (Figure 1). Generally, with increasing pyrolysis temperature, biochars mostly exhibit alkali pH due to the removal or loss of acidic functional groups, separation of alkali salts from the organic compounds and the ash component with alkali metals (Al-Wabel, Al-Omran, El-Naggar, Nadeem, & Usman, 2013; Bandara, Herath, Kumarathilaka, Hseu, et al., 2017).

Biochars from legume plants have a higher pH compared to the biochars from non-legumes at the same temperature, which is related to ash, or ash alkalinity or excess cations (Tang, Weligama, & Sale, 2013; Yuan & Xu, 2011). Heating procedure also contributes to biochar pH. Biochars derived from wheat straw from slow and fast pyrolysis at 625ºC resulted in pH 10.1 and 6.8, respectively (Bruun, Ambus, Egsgaard, & Hauggaard-Nielsen, 2012).

As a result of degradation of organic components in biomass during pyrolysis, a substantial amount of ash provides sources of metals, silicates, and some essential plant nutrients (Bachmann et al., 2016). Biochars derived from grass, animal manure and sludge contain more ash compared to the biochars derived from woody biomass (Table S1). The feedstocks which contain a higher inorganic fraction and low C such as straw, shells and husks of grains, animal manure and herbaceous biomass, result in biochars with higher ash content compared to feedstocks that are low in inorganic fraction (woody biomass) (Arán, Antelo, Fiol, & Macías, 2016).

The majority of biochars show a reduction of oxygen to carbon (O/C) ratio with increasing pyrolysis temperature (Figure 2). A possible reason for this reduction is a progressive dehydration and decarboxylation with higher temperature is the formation of highly-condensed aromatic carbons (Bandara, Herath, Kumarathilaka, Hseu, et al., 2017). Low O/C ratios indicate a lower degree of polarity or more hydrophobicity. Generally, increasing pyrolysis temperature decreased H and N contents of biochars. However, increasing the temperature from 200 to 800ºC increased the N concentration in biochars of conocarpus waste, which could be due to the incorporation of N into the biochar structure (Al-Wabel et al., 2013). Therefore, the behaviour of N in biochars shows inconsistency with pyrolysis temperature while C content increases and other elements (O and H) decreases with increasing temperature.

The surface area and pore volume of biochar are considered as major physical properties governing the immobilization of PTEs. During pyrolysis of biomass, microspores are formed due to dehydration process that is a major structural change. Biochars produced at low temperature showed a low surface area compared to those produced at high temperature (Figure 2). Biochars produced from switchgrass and alfalfa showed a small surface area compared to the woody biochars formed at a higher temperature (600ºC), highlighting the effect of feedstock type on the surface area (Wang, et al., 2015a). Other than temperature, residence time plays an important role in surface area and pore volume and when residence time exceeded 2 h at 500-900ºC the surface area and pore volume rapidly decreased (Cha et al., 2016).

Overall, the immobilization of PTEs by biochar depends on the biochar type, production condition and technology, which is used for biochar production. Biochars derived at low temperature contain more nutrients, surface functional groups and labile C that are important for surface complexation of PTEs and microbial growth. On the other hand, biochars derived at higher temperatures have more surface area and fixed C, which favour PTE immobilization by physical sorption and are resistant to microbial mineralization. More detailed information can be found in the supplementary materials.

3. Effects of biochar on plant uptake of PTEs

The application of biochars is considered as an effective method for decreasing bioaccumulation of PTEs in plants. Its effectiveness depends on biochar characteristics, PTE type, soil type and plant species. However, some biochars may have negative effects on plant growth due to the presence of toxic compounds.

Recent meta-analyses conducted by Chen et al. (2018) and Peng, Deng, Peng, and Yue (2018) critically discussed the effects of biochars on plant uptake of PTEs in contaminated soils. Chen et al. (2018) evaluated 74 publications which were published before on March 2016, while Peng et al. (2018) evaluated 97 publications published before December 2016. Overall, they observed that biochar addition decreased the bioaccumulation of PTEs in the plants. However, the extent of decrease depends on biochar type and addition rate, soil type, PTE type and concentration, and plant species. For instance, Chen et al. (2018) observed biochars decreased the plant accumulation of Cd, Pb, Cu and Zn concentration by 38, 39, 25 and 17%, respectively. The bioaccumulation of PTEs in the plant decreased to a greater extent in soils with coarse-texture and high organic carbon than those with fine- and medium-texture and low organic carbon. Biochar addition rate of > 3% decreased plant uptake of PTEs more than the rate of 1.1-3% and

≤ 1%. In general, biochar addition decreased the bioaccumulation of Cd and Cu more in cereals and vegetables than legumes. Biochars decreased the bioaccumulation of Pb to the greatest extent in maize and the smallest in wheat. In comparison, biochars decreased the bioaccumulation of Zn only in vegetables, legumes and hyperaccumulators and had no significant effects on it in rice, wheat, maize and grasses. Moreover, the authors observed that biochars derived at 400-500°C decreased bioaccumulation PTEs in plants more effectively and economically than those derived at higher temperatures (>600°C).

Similarly, Peng et al. (2018) showed that biochars produced from animal manure, decreased the Cd and Pb bioaccumulation in plants more significantly (decreased by 65% and 85%, respectively) than those derived from wood, herbaceous, biosolids and lignocellulosic waste (by 21-14%, 27-45%, 10-45%, and 42-61%, respectively). Overall, the addition of biochars negatively correlated with bioaccumulation of PTEs and hence, biochars can be a potential soil amendment to decrease food-chain contamination.

The potential negative effects of biochar on plant growth have also been reported (Kookana, Sarmah, Van Zwieten, Krull, & Singh, 2011). Intani, Latif, Islam, and Muller (2019) showed that the application of fresh corn-cob biochar produced via slow pyrolysis (450°C) decreased seed germination, plant height, and fresh and dry weights of *Lepidium sativum* plants. However, heat-treated (105°C for 24 h) and washed (shaken with de-ionized water for 24 h) biochars decreased the potential toxicity for plant growth. Furthermore, the authors revealed that with increasing application rates from 10 to 30 t/ha, shoot fresh weight decreased by 41%, 72% and 75% in the washed, heat-treated and fresh biochars, respectively. Similarly, Li et al. (2015) reported that high dosage (16.0 g biochar/beaker) of corn-stover biochar decreased the seed germination, growth, and antioxidant enzyme activities in the roots and leaves of tomato. Furthermore, the enhanced malondialdehyde content and altered root-tip morphology at higher biochar dosages were observed due to serious lipid peroxidation in the tomato seedlings. The application of biochars at 5% (w/w) decreased rice plant growth due to the higher electrical conductivity in salt-affected soils (Hafeez et al., 2019). The negative effects of biochar application on seed germination and plant growth are often attributed to toxic compounds such as heavy metals, polycyclic aromatic hydrocarbons and free radicals present in biochars (Kookana et al., 2011; Quilliam, Rangecroft, Emmett, Deluca, & Jones, 2013; Wang, Xia, et al., 2018). Recently, Ruan et al. (2019) critically reviewed the formation, characterization and effects of environmentally-persistent free radicals (EPFRs) in biochars. Biochars with high amounts of EPFRs inhibited seed germination, and the growth of root and shoot, and damaged the plasma membrane due to OH free radicals. Therefore, future research needs to focus more on biochar-induced plant toxicity before biochar is applied to the large scale.

4. Mechanistic understanding of biochar interaction with PTEs in soils

Two aspects appear necessary to describe the interactions between biochars and PTEs in the soil system; 1) direct influence of biochars on PTEs, 2) indirect immobilization of PTEs (Figure 3). The structural specificity of biochars governs the direct mechanisms on PTE interactions such as chemical and physical interactions, and precipitation. Biochars also change the soil environment by changing the chemical, physical and biological properties that favour immobilization of PTEs (Table 1). These mechanisms are discussed together in relation to various PTEs in the environment.

4.1. Cadmium

The possible immobilization mechanisms that are involved in the Cd and biochar interactions include: cation exchange; precipitation; surface complexation with functional groups; and electrostatic interaction (Figure 4). However, immobilization mechanisms highly depend on the biochar type and application rate, soil type, Cd concentration and the aging process. Cation exchange, precipitation as $CdCO_3$ and co-precipitation with $CaCO_3$, are the main mechanisms contributing to Cd sorption by olive pomace-derived biochars (Pellera & Gidarakos, 2015). Alkali nature of biochars can promote the formation of $Cd_3(PO_4)_2$, $CdCO_3$, K_4CdCl_6, Cd_3P_2 and $Cd(OH)_2$ in pore water which are highly insoluble (Zhang, Wang, et al., 2015). Cd(II) ions are easily bound

to form strong surface complexes on the surface of biochars rich in O-containing functional groups such as –OH and –COOH (Sun, Lian, Liu, Zhu, & Song, 2014). EDX semi-quantitative analysis, FTIR analysis, and XPS morphological analysis showed that surface complexation was the main mechanism of Cd interaction with rice-husk biochar produced at 400°C due to the large amount of O-containing functional groups, while the generation of stable compounds with inorganic salts (Si, S, Cl etc.) might also contribute to the interaction (Tan, Wang, Zhang, & Huang, 2017). Furthermore, the aromatic graphite structure of biochars rich in delocalized lone-pair π electrons favours Cd-π bonding (Zhang, Wang, et al., 2015). The addition of biochars at 40 t/ha into the Cd-contaminated paddy soil effectively deceased the bioavailable fraction of Cd by 70, 85, 54 and 43% in consecutive four rice growth seasons compared to the non-amended treatment (Chen, Guo, et al., 2016). The sustainable effect of Cd immobilization decreases with time, which may be accounted for by the aging process of biochars. By contrast, a laboratory incubation study revealed that the Cd adsorption capacity of 12 month-aged biochars in Oxisol and Inceptisol was higher than fresh biochars (Nagodavithane, Singh & Fang, 2014). Specific adsorption was the major mechanism in aged biochars rather than cation exchange. Initially, Cd precipitates within biochar particles as $CdCO_3$, and with aging, Cd is immobilized via organic functional groups (Rechberger et al., 2019). Similarly, Xu, Xu, Tsang, & Cao (2018) observed that aged biochars had little impact on biochar alkalinity and Cd immobilization via surface completion with O-containing functional groups. Aging of biochars increases organic functional groups and decreases surface area by dissolution and re-precipitation of minerals (Padhye 2017).

The solubility and bioavailability of Cd are strongly related to types of biochars and soils. The application of wheat-straw-derived biochar promoted the formation of carbonate, (oxy)hydroxide and organically-bound Cd phases (Cui, Noerpel, Scheckel, & Ippolito, 2019). Based on the XAS analysis, the authors concluded that organic functional groups on wheat-straw-biochar surface played a major role in Cd immobilization. Pal and Maiti (2019) reported that biochar derived from tea waste effectively decreased the exchangeable and carbonate-bound fractions of Cd and increased the Cd in the residual fraction. On the other hand, biochars rich in alkali metals are easily exchanged with Cd (II) (Yin et al., 2016).

Other than major surface interaction mechanisms, pH value of biochars plays a crucial role in determining PTE availability in contaminated soils (Egene, Van Poucke, Ok, Meers, & Tack, 2018). Alkaline biochars increased negative charges on soil and biochar surfaces, which enables the entrapment of heavy metal cations on their surfaces and promotes the adsorption mechanism (Bashir et al., 2017). Van Poucke et al. (2018) reported that the combined effect of pH and Cd complexation capacity of biochar play an important role in decrease Cd solubility in contaminated soil. For strongly acidic soils, it would be suitable to use biochar with more acidic functional groups, while it is more appropriate to use alkaline biochars produced at higher temperatures for soils with moderate acidity (Qian et al., 2019). Li, Khan, et al. (2018) observed the application of biochar significantly modified the soil dissolved organic matter and subsequently decreased the mobility and bioaccumulation of Cd in a paddy soil.

4.2. Lead

Sorption mechanisms of lead (Pb) into biochars are fundamentally influenced by production temperature and feedstock composition of biochars, and soil solution pH (Ahmad, Lee, et al., 2014; Ahmad, Ok, Kim, et al., 2016; Li, Wang, et al., 2019). As with other divalent metals, Pb showed the similar mechanisms of interaction with biochars, e.g., electrostatic interaction, cation exchange, precipitation, and complexation (Figure 4). Precipitation is the major mechanism when biochars added to Pb-contaminated soil (Kumarathilaka et al., 2018). Biochars could increase soil pH, thus enhancing Pb precipitation. The formation of pozzolanic reaction products induced by increased solubility of Al and Si under high pH are considered responsible for Pb precipitation (Moon et al., 2013). Animal manure-based biochars predominantly form precipitates due to richness with PO_4^{3-} and CO_3^{2-} minerals. Especially, biochars derived at low pyrolysis temperature (400-500°C) favour stabilizing Pb (Chen et al., 2018; Uchimiya, Bannon, Wartelle, Lima, & Klasson, 2012). The overall process of Pb precipitation with PO_4^{3-} and CO_3^{2-} minerals is outlined in (1) and (2) (Cao, Ma, Gao, & Harris, 2009);

$$6HPO_4^{2-} + 9Pb^{2+} + 6OH^- \longrightarrow Pb_9(PO_4)_6 + 6H_2O \quad (1)$$

$$2HCO_3^- + 3Pb^{2+} + 4OH^- \longrightarrow Pb_3(CO_3)_2(OH)_2 + 2H_2O \quad (2)$$

The majority of Pb(II) precipitated as hydroxypyromorphite ($Pb_5(PO_4)_3(OH)$) with a lesser amounts sorbed to biochars (Cao, Ma, Liang, Gao, & Harris, 2011). Lower biochars pH lead to precipitation of Pb as $Pb_2(CO_3)_2$ while higher biochars pH favour the formation of $Pb_3(CO_3)_2(OH)_2$ (Shen, Zhang, Jin, McMillan, & Al-Tabbaa, 2017). Biochar surfaces rich in alkali metals such as Ca and Mg easily exchange with positively charged Pb(II) ions. The exchangeable Pb negatively correlated with soil pH and CEC in soils amended with soybean- and pine needle-derived biochars, resulting in decreased mobility via cation exchange with Ca(II) and Mg(II) on the biochar surfaces (Ahmad, Ok, Kim, et al., 2016). On the other hand, the surface of biochars rich in π-electrons interact with Pb(II) deficient in π-electrons, resulting in Pb-π electrostatic interaction. O-containing functional groups such as –OH and –COOH play a vital role in Pb immobilization through surface complexation. For instance, legume-straw biochars showed more non-electrostatic adsorption mainly due to higher abundance of acidic functional groups (Jiang, Xu, Gu, & Jiang, 2014). Incorporation of legumes-straw biochars decreased the solubility and bioavailability of Pb(II) compared to the non-legume-straw biochars. In a recent study, Igalavithana, Kwon, et al. (2019) observed that biochars produced under CO_2 atmosphere had an enhanced ability of Pb immobilization due to the formation of –Si-O-Si- (siloxanes) on the biochar surface compared to the biochar produced under N_2 environment. Therefore, the atmosphere of pyrolysis conditions during biochar production also plays a significant role in biochar properties and Pb immobilization.

The application of biochar increased the dissolved organic carbon (DOC) and thereby increased the adsorption of soluble DOC-metal complexes on the biochar surface (Vithanage, Herath, Almaroi, et al., 2017). Biochars could effectively decrease the water-soluble, exchangeable and carbonate-bound Pb, but enhance the amorphous iron-oxide fraction (Boostani, Najafi-Ghiri, Hardie, & Khalili, 2019). Similarly, Salam et al. (2019) observed that the biochar derived from rice-straw and rapeseed residues at high temperature (500^{o}C) decreased the bioavailability of Pb and redistributed Pb to most stable geochemical fractions under high soil moisture (80% of field capacity).

4.3. Chromium

Chromium (Cr) is a highly redox-sensitive metal consisting of several oxidation statuses (-2 to +6), with Cr(III) and Cr(VI) being the most dominant species in soil environment (Arshad et al., 2017). Among them, Cr(VI) is considered as more toxic form compared to the Cr(III), due to high solubility, mobility, and strong oxidation ability (Xia et al., 2019). According to the available literature, reduction, electrostatic interaction, porous diffusion and complexation with surface functional groups or precipitation are the responsible mechanisms in Cr(VI) remediation in polluted soils (Figure 4).

Biochars are effective in Cr(VI) reduction in the polluted environment. The presence of π-electrons on the aromatic graphite structure of biochars donate elections for the Cr(VI) reduction to Cr(III) and resulting Cr(III) form surface complexation with surface functional groups of biochars (Choppala, Bolan, Megharaj, Chen, & Naidu, 2012; Xia et al., 2019). Likewise, oxygen-containing acidic functional groups are also effective in Cr(VI) reduction via donating protons (Choppala et al., 2012; Li, Dong, et al., 2017). Modified biochars have been shown to increase percentage reduction of Cr(VI) compared to the non-modified biochars. For example, animal manure-derived biochars, modified with chitosan and zerovalent iron, reduced Cr(VI) effectively due to the enhancement of oxygen-containing surface functional groups, which could act as the proton donor for reduction process (Mandal, Sarkar, Bolan, Ok, & Naidu, 2017). More detailed mechanisms related to the modified biochar and Cr immobilization will be discussed in Section 7.

4.4. Mercury

Mercury (Hg) is a highly toxic heavy metal because of its persistence nature and ability of accumulation in the food chain (Gao, Han, Hao, & Zhou, 2016). The organic form of Hg, [e.g., methylmercury (MeHg)] is more toxic and bioaccumulative than inorganic forms (Liu, Ptacek, Blowes, & Gould, 2018). The ionic Hg(II) can be converted into MeHg by sulfate-reducing

bacteria, iron-reducing bacteria and methanogens under anoxic conditions (e.g., sediments and wetlands) (Bussan, Sessums, & Cizdziel, 2016; Liu, Ptacek, et al., 2018). Methylmercury primarily damages the central nervous system and damage is irreversible due to destruction of neuronal cells (Liu et al., 2019). The process of formation of MeHg and dimethyl mercury under reducing conditions is out lined in (3), (4) and (5).

$$Hg^{o} \leftrightarrow \quad Hg^{2+} + 2e \tag{3}$$

$$Hg^{2+} + CH_3^- \rightarrow CH_3Hg^+ \tag{4}$$

$$CH_3Hg^+ + CH_3^- \rightarrow (CH_3)_2Hg \tag{5}$$

The accumulation of MeHg in rice grains is a major health concern, especially in Asian countries (Qiu, Feng, Wang, & Shang, 2006). The return of straw is a common practice in many rice farms and can potentially accelerate the transformation of inorganic Hg to MeHg species (Zhang, Liu, Lei, Wang, & Zhong, 2018). The application of rice-straw biochar decreased the accumulation of MeHg in rice plants (Zhang, Liu, et al., 2018). Biochar could decrease the phytoavailability of MeHg in soils and enhance plant biomass resulting in biodilution of MeHg. Similarly, Shu, Wang, and Zhong (2016) observed that the addition of rice-straw biochar (600ºC) immobilized MeHg in soils due to the large surface area and high organosulfur content of the biochar and biodilution of MeHg in rice grains due to increased grain biomass. Liu, Ptacek, et al. (2018) evaluated four biochars and their abilities and mechanisms to remove Hg and MeHg from contaminated sediments. The study revealed that the biochar derived from switchgrass at 300ºC was the most efficient material for Hg stabilization compared to those derived from poultry manure and oak. Furthermore, the formation of Hg-sulfide and precipitation on or within biochar particles are the responsible mechanisms of Hg stabilization. Xing et al. (2019) recently showed that rice-husk biochar (480-660ºC) effectively decreased Hg(II) concentration in soil pore water, thereby decreased Hg(II) concentrations in rice grains compared to the wheat-straw biochar (350-450ºC). They also observed that Hg(II) concentration in pore water was correlated negatively with sulfate concentration, but positively with soil DOC concentration. Biochars produced at a low temperature generally consist of a higher amount of DOC and may therefore enhance the mobility of Hg(II) in paddy soils (Figure 4). Biochar-derived DOM is a key factor which regulates the mobility of Hg(II) in the environment by forming soluble Hg-DOM complexes. Liu, Ptacek, Blowes, and Gould (2018) reported that a biochar produced at 300ºC formed more Hg-DOM complexes compared to the biochar produced at 600ºC. The concentration of Hg-DOM complexes was higher in manure-based biochar compared to the wood- and agricultural residue-based biochar. Liu, Ptacek, Blowes, and Gould (2018) concluded biochars derived from wood and agricultural residues at high temperature (600ºC) would be suitable for minimizing Hg(II) mobilization. A biochar derived from pinewood (~830ºC) decreased the formation of MeHg in Hg-contaminated sediments by 88% compared to the control (Bussan et al., 2016). There was no significant effect of biochar on the formation of dimethyl mercury compared to the control. In contrast, Beckers et al. (2019) reported biochar decreased the release of Hg from the floodplain soil, but did not affect methylation and ethylation of Hg. O'Connor et al. (2018) observed modification of rice husk biochar with sulfur has good potential to stabilize Hg in contaminated soils. Modification increased the biochar S content from 0.2 to 13.0% and Hg(II) adsorptive capacity by 73%. Recently, a synchrotron-based study conducted by Liu et al. (2019) observed co-existence of Hg with S, Cu, Fe, Mn and Zn on the surface and inside of the biochar particles. The study also showed that Hg initially remained as soluble, colloidal, Hg-O like unstable forms in the sediment, and it was then immobilized to form HgS on the surface or within the biochar particle. The Hg adsorption capacity of biochars was increased with aging due to hydroxylation and carboxylation on the biochar surfaces (Zhang, Yang, Ju, Liu, & Zheng, 2019).

4.5. Arsenic

The dynamics of arsenic (As) in biochar-treated soils is different from the previously mentioned PTEs. While the addition of biochars changes soil chemical properties that are favourable for immobilization of cationic heavy metals such as Cd, Pb and Hg, these changes in soil properties are more favourable for mobilization of anionic metalloids such as As. For example, the addition of alkaline biochars enhanced soil pH and thus increased the negative sites in soil particles, which favoured As mobilization (Hartley, Dickinson, Riby, & Lepp, 2009). Moreover, mobilization is

caused due to the electrostatic repulsion and the competition between As and the PO_4^{3-} for the sorption sites of biochars (Ahmad et al., 2017). Biochars could reduce Fe and Mn species by donating electrons (Yuan et al., 2017), and under reduced conditions, As is more mobile and bioavailable (Beesley et al., 2013). The addition of biochars increased soil pH, dissolved organic carbon, P in pore water and soil microbial activity, which in turn increased the mobility of As in soil (Figure 5) (Beesley et al., 2014; Choppala, Bolan, Kunhikrishnan, & Bush, 2016; Gregory, Anderson, Camps Arbestain, & McManus, 2014).

Bioaccumulation of As is most common when the soils are amended by biochars. Rice husk-derived biochars significantly increased the bioaccumulation of As and its species in various tissues of alfalfa plant by increasing mobilization of As through increasing the available concentration of Si and P in soil (Ibrahim, Khan, Hao, & Li, 2016). If the concentration of soluble P is low (Olsen P < 14 μg/g) in the soil, As could be sorbed to the biochar surfaces without competition (Beesley & Marmiroli, 2011). The addition of peanut-shell and sewage-sludge biochars significantly decreased the accumulation of As in bean plants, which might be due to the competitive interaction of As with P and S present in the biochars (Ibrahim, Li, Khan, Chi, & Xu, 2017). Biochars derived from orchard prune residue increased the solubility and mobility of As in a mine soil, while uptake of As into tomato plants decreased, indicating a possible water contamination rather than food chain contamination (Beesley et al., 2013). Compared to the biochar derived from pine sawdust, the raw sawdust showed the ability to decrease the mobility and phytoavailability of As under various redox conditions, likely due to the abundance of O-containing surface functional groups and acidic properties (Beiyuan et al., 2017). The dynamics of As in biochar-amended soils is quite complicated and more detailed studies are necessary for the identification of mechanisms involving in As mobilization or immobilization. More detailed information about As and biochar interactions in soil and water was critically reviewed by Vithanage, Herath, Joseph, et al. (2017) and Alkurdi et al. (2019). Furthermore, engineered biochars have good potential to immobilize As in soil and the mechanisms related to the modified biochar and As immobilization will be discussed in Section 7.

4.6. Antimony

The effect of biochars on Sb remediation in soils is still not well understood. There are very few experiments illustrating the mechanism of biochars-Sb interactions. The biochar derived from oak wood at 400°C decreased phytoavailable Sb by 53% which might be due to sorption of Sb onto iron (hydr)oxides of biochars forming inner-sphere complexation (Ahmad, Lee, et al., 2014). Pine-needle biochars generated at 300°C decreased Sb mobility by 15.1% in a shooting-range soil, which was attributed to the sorption onto amine functional groups present in the biochar surfaces (Ahmad et al., 2017). Biochars produced at a higher temperature (700°C) mobilize the Sb mainly due to anionic electrostatic repulsion to negatively-charged surfaces. Biochars derived from buffalo weed at 300 and 700°C enhanced the desorption of Sb from the soil, due to repulsive electrostatic interaction and competition between negatively charged PO_4^{3-} ions (Rajapaksha et al., 2015). Cotton hull-derived biochars (oxidized with H_2SO_4 and HNO_3) enhanced more negatively charged carboxylic functional groups which promote the desorption of Sb oxyanions (Uchimiya, Bannon, & Wartelle, 2012). While negatively-charged surface functional groups (-COOH, -OH) are more efficient in the interaction with cations such as Cd and Pb, functional groups (R-NH_x) at a positively charged surface are efficient in the interaction with oxyanions such as As(V) and Sb(V) (Figure 5).

Immobilization of oxyanions with biochars in the soil system is not fully understood. According to the available literature, positively-charged surface functional groups of biochars contribute to surface complexation of anions (Banik, Lawrinenko, Bakshi, & Laird, 2018). Most of the biochars generated at low temperatures are rich in negatively-charged surface functional groups, while only nitrogen-rich biochars have positively-charged amine groups (Xiao, Chen, Chen, Zhu, & Schnoor, 2018). Selection of feedstock and production conditions, and modification through nitrogenous compounds such as NH_3 (Mian et al., 2018; Xiong et al., 2013), have a good potential for improving anion immobilization by biochars.

4.7. Multi metal- contaminated soil

Soil is usually contaminated with multiple PTEs rather than one single element (Wijayawardena, Megharaj, & Naidu, 2016). Therefore, the behaviour of PTEs to biochar addition may have different immobilization mechanisms. Meng et al. (2018) observed that the addition of biochar produced from co-pyrolysis of rice straw and swine manure significantly decreased bioavailable PTEs in the order of Pb > Cu > Zn > Cd. They showed biochar addition was not equally effective for individual PTEs depending on PTE concentration, speciation and binding mechanisms. Similarly, Wang, Alidoust, Yang, and Isoda (2018) observed that the addition of 10% bamboo biochar decreased PTE concentration in soybean shoots in the order of Pb > Mn > Cd > Zn > Cu > Ni. The affinity of Pb, a hard Lewis acid, with surface functional groups of the biochar was higher than those of Cd and Zn, soft Lewis acids. The addition of 5% rice-straw biochar decreased the concentrations of DTPA-extractable metals in the order of Zn > Pb > Cu > Cd (Lu et al., 2017). While Pb was immobilized by forming insoluble $Pb_5(PO_4)_3OH$, Cu mobility was reduced due to the decrease of DOC in soil. Moreover, the mechanisms of Cd and Zn immobilization in soil are difficult to predict due to contrasting results. As explained earlier, the addition of biochar immobilized Pb, Zn and Cu via surface complexation and precipitation but mobilised As and Sb due to electrostatic repulsion and phosphate competition (Ahmad et al., 2017). Zhang, Zhang, et al. (2019) reported that the tobacco-stem-derived biochar was effective in decreasing the phytoavailability of Cr, Cu, and Pb in the soil, due to increased soil pH and P supply. In the case of anions, the effect of biochar on the immobilization depends on the anionic species. For example Choppala et al. (2016) demonstrated that while biochar addition was effective in alleviating Cr toxicity by reducing Cr(VI) to Cr(III), the biochar-induced reduction of As(V) to As(III) increased the mobility and toxicity of As in soils. The results indicate that biochars have different impacts on cationic and anionic PTEs in contaminated soils. Overall, future research is needed to focus on soils contaminated with multi-elements.

5. Biochar-microorganism interactions on immobilization of PTEs

Changes in soil chemical and physical properties upon biochar application can influence microbial properties. Part of the PTE immobilization process of biochars is achieved by facilitating, stimulating and enhancing detoxification ability of native soil microorganisms (Zhu et al., 2017). Microbial responses to biochars are highly diverse due to the variations in biochar properties, contaminant type and severity, native soil microorganisms and the environment (Zhu et al., 2017). The changes of microbial abundance and diversity due to biochar addition have been well studied (Huang et al., 2018; Lehmann et al., 2011; Palansooriya et al., 2019). However, it is still unclear how microorganisms regulate the immobilization of PTEs in biochar-amended soil.

As discussed above, biochars immobilize PTEs through chemical or physical sorption and precipitation processes. On the other hand, some PTEs are oxyanions such as As and Sb which can be desorbed or mobilized upon the addition of biochars. Moreover, biochars release toxic compounds (VOCs, PTEs etc.) and nutrients which in turn affect the microbial activities. Therefore, the following sections focus on the interaction mechanisms of biochars and microbes that are involved in immobilization of PTEs in soil. Only limited references are available to discuss the biochar-microbe interactions in soil ecosystems contaminated with PTEs.

5.1. Importance of soil microbes in remediation of polluted environments

Soil microorganisms comprise a large portion of the genetic diversity on Earth and play a vital role in the soil ecosystem functioning (Zhang, Chen, & Ruan, 2018). Soil microorganisms include bacteria, fungi, archaea, actinomycetes, algae and protozoa. The soil microbes that are present in the contaminated soil are adapted to PTE toxicity, with some evolving efficient biological utilization (ingest, solubilize or assimilate) or detoxification mechanisms (Abdu, Abdullahi, & Abdulkadir, 2017). The PTEs together with lack of nutrients, water or appropriate electron acceptors limit the growth of microorganisms (Harms, Schlosser, & Wick, 2011). Some microbes are capable of utilization or transformation to different PTE species that are less toxic, more or less water-soluble, easily volatilized and less bioavailable through the bioremediation process (Chibuike & Obiora, 2014; Harms et al., 2011). Especially, native microorganisms in PTE-rich environments are capable of adopting detoxifying mechanisms such as biosorption,

biotransformation, bioaccumulation or biomineralization of PTEs (Bolan, Choppala, Kunhikrishnan, Park, & Naidu, 2013; Dixit et al., 2015). Some microbes have specific genes that are capable of accumulating PTEs to a certain level and transforming them into less toxic forms (Abdu et al., 2017). For instance, *Bacillus subtilis*, *Pseudomonas putida* and *Enterobacter cloacae* are successful in the reduction of highly toxic and mobile Cr(VI) to immobile and less toxic Cr(III) (Chibuike & Obiora, 2014).

The biochemical role of microbes in bioremediation process is to mobilize or immobilize PTEs in the soil. The bioavailability of PTEs in soils can be enhanced by microbial processes such as bio-weathering of rock and minerals, biocorrosion, methylation, and bioleaching (Gadd, Rhee, Stephenson, & Wei, 2012). The soil microbes that are associated with plants play an important role in phytoextraction process by mobilizing PTEs in plant rhizosphere (Wood, Tang, & Franks, 2016). The microbial biosorption is a two-step process and initially heavy metals are binding to cell walls and then gradually transported through the cell membrane (Jing & Kjellerup, 2016). On the other hand, microbes can produce biofilms that are complex communities of microbes with a variety of extracellular polymeric substances (Jing & Kjellerup, 2016). The extracellular polymeric substances are rich with cationic and anionic functional groups, aromatic amino acids and polysaccharides which form physical and chemical interactions between biofilms and heavy metals (Bandara, Herath, Kumarathilaka, Seneviratne, et al., 2017). Microorganisms play a vital role in the speciation, mobility and toxicity of PTEs by regulating redox reactions of PTEs (Bolan et al., 2014). For example, Minamata disease in Japan is caused by the ingestion of sea-foods containing methylmercury compounds that are formed by microbial biomethylation of mercury salts (Bolan et al., 2013). Hence, microorganisms play an important role on biogeochemistry of PTEs in the soil environment.

5.2. Effects of biochars on the microbes

Biochar addition could positively or negatively affect soil microorganisms. On the negative side, biochars could release some toxic compounds (PTEs, VOCs, or EPFRs) to the soils or mobilized anionic PTEs (As, Sb) from the soil. Positively, biochars provide nutrients and habitats for soil microorganisms and immobilize PTEs from the polluted soils. The overall effects depend on the nature of biochar, soil environment, PTEs and microorganisms. In this section, we discussed the pros and cons of biochars on microbial activities.

5.2.1. Microbial response to biochar addition

The immobilization of PTEs facilitates the growth of soil microbes. For instance, the application of wine lees-derived biochars into a paddy soil contaminated with multi-metals changed native microbial community and enhanced the bacterial diversity but decreased the bacterial richness (Xu, Xia, et al., 2017). The relative abundance of *Actinobacteria*, *Proteobacteria*, *Firmicutes*, *Cyanobacteria* and *Plancomycetes* increased with biochars application rates (0.5, 1 and 2% w/w), while *Gemmatimonadetes* decreased at a higher application rate (2% w/w). Reduction of heavy-metal toxicity and the enhancement of available N and P through biochar application are the major responsible mechanisms for enhancing bacterial abundance (Xu, Xia, et al., 2017). The addition of wheat-straw biochars at 10, 20 and 40 t/ha to a Cd- and Pb-polluted paddy soil, increased populations of fungi by 370, 460, 930%, and of actinomycetes by 20, 19, 39%, respectively, and such increases inversely correlated to concentrations of acid-soluble Cd and Pb in the soil (Cui et al., 2013). Table 2 presents more details about the major microbial responses to biochar addition in PTE-contaminated soils.

Synergistic effects of microorganisms together with biochars on immobilization of PTEs in contaminated soils have been studied. The addition of biochars and fungal-bacterial co-inoculation significantly reduced the bioavailability of Ni, Mn, and Cr in a serpentine soil (Bandara, Herath, Kumarathilaka, Seneviratne, et al., 2017). Compared to the biochar-alone treatments, biochars and fungal-bacterial co-inoculation slightly increased the bioavailability of heavy metals, probably due to reduction reaction of Fe or Mn oxides/hydroxide induced by microbial activity. Similarly, the application of plant-growth-promoting *Neorhizobium huautlense* T1-17 and rice-stem biochars in a Cd and Pb co-polluted soil significantly decreased the bioaccumulation of heavy metals in edible tissues by increasing the proportion of indole acetic

acid (IAA)-producing bacteria and reducing bioavailability of heavy metals in rhizosphere soils (Wang, Chen, He, & Sheng, 2016). However, *Pseudomonas aeruginosa* (2% v/v) was more effective than biochars (1%) in the decrease of Cd accumulation in rice grains (Suksabye, Pimthong, Dhurakit, Mekvichitsaeng, & Thiravetyan, 2016). Moreover, both treatments lowered Cd concentration in rice grains compared to the non-amended treatment, indicating the potential use of bioremediation techniques. The combined effectiveness of pig-manure biochars with inoculation of *Bacillus subtilis* in remediation of multi-metals was greater than application of individuals (Wang, Sun, Ren, Li, & Mao, 2017). In contrast, the combined application of corn-stalk biochars with arbuscular mycorrhizae fungi had no significant interaction on remediation of heavy metals in long-term biosolids-amended soils (Qiao, Crowley, Wang, Zhang, & Li, 2015). The addition of biochars with arbuscular mycorrhizas to the mine-residue soils significantly desorbed Pb probably through mineral dissolution by activities of arbuscular mycorrhizas and root exudates (González-Chávez, Carrillo-González, Hernández Godínez, & Evangelista Lozano, 2017). Combined application of a fungal strain isolated from multi-metal-polluted mine soil (*Lecythophora* sp. DC-F1) with sawdust biochar effectively decreased Hg(II) content of lettuce plant by 67% compared to the non-amended soil (Chang et al., 2019). However, the total fungal number decreased by fungal strain DC-F1 may be due to an antimicrobial property.

5.2.2. Contrasting effects of biochar on microbes and enzymes

All the biochemical reactions in the soil environment are catalyzed by soil enzymes. The soil enzymes are considered as a highly sensitive bio-indicator of any anthropogenic or natural disturbance in the soil, and thus can be used as a sensitivity measurement of soil microbial activity (Vithanage et al., 2018). Contrasting observations on soil enzymatic activities have been reported with the addition of biochars into contaminated soils (Table 3). Application of biochars derived from willow wood at 350 and 600oC significantly increased soil dehydrogenase activity (DHA), with no significant difference between application rates of 30 and 60 t/ha (Gregory et al., 2014). Igalavithana, Lee, et al. (2017) observed that biochars derived from vegetable waste and pine cone at 200oC enhanced DHA compared to the biochars derived at 500oC. The labile C component in biochars derived from low temperatures acted as a bioavailable C source to microbes resulting in higher DHA.

Biochar stimulated enzyme activities are associated with decreased concentrations of bioavailable PTEs. An increasing addition rate of wheat-straw biochars decreased Cd and Pd bioavailability and increased the activities of cellulase, neutral phosphatase, urease and sucrase in Cd- and Pb-polluted soils (Cui et al., 2013). Similarly, rice-straw biochar significantly increased soil urease activity by decreasing bioavailable concentrations of heavy metals (Huang et al., 2017).

The addition of biochar increases the enzyme activity via increasing soil pH. The addition of rice-straw and dairy-manure-derived biochars significantly increased the activity of denitrifying reductase and functional gene abundance in a Cd-polluted soil (Chen, Zhang, Zhang, & Zhang, 2017). However, the activities of alkaline phosphatase and invertase decreased with increasing application rate (up to 5% w/w). Similarly, the addition of biochars derived from Gliricidia sepium at 700oC to the serpentine soils at a rate of 5% (w/w) significantly decreased the activities of DHA, polyphenol oxidase and catalase (Bandara, Herath, Kumarathilaka, Seneviratne, et al., 2017). The decrease of enzymatic activities at higher application rates could be attributed to the toxicity of biochars or sorption behaviour of enzymes or substrates onto the porous structure. According to the above studies, the behaviour of soil enzymes upon biochar addition showed the highly variable responses, depending on biochar type and application rate, soil type, PTE type and concentration, enzyme type as well as analytical method.

5.2.3. Biochar as a nutrient source and habitat for microorganisms

The degree of changes in soil chemical or physical properties upon biochar incorporation depends on the characteristics of biochars. The porous structure and higher surface area of biochars provide the habitat for microorganisms by reducing environmental stresses (Lehmann et al., 2011; Moore et al., 2018). On the other hand, biochars contained sufficient amounts of labile substrates and nutrients to support microbial growth and reproduction (Ahmad, Ok, Rajapaksha, et al.,

2016). For instance, the increases of dissolved organic carbon, electrical conductivity and NH4+ concentration of soils after addition of biochars enhanced the growth of Fe(III)-reducing bacteria and increased Fe(III) reduction and As release (Wang, Xue, et al., 2017). The manure-based biochars produced at 700oC had higher aromatic C, surface area, porous structure, and higher content of minerals than those produced at 300oC. Therefore, they can act as electron transporters which contribute to microbial colonization and absorption of soluble organic matter and gases, and provide essential nutrients for growth and reproduction (Dai, Barberán, Li, Brookes, & Xu, 2017). Soil pH and organic matter play a significant role in maintaining microbial abundance and diversity in soil. Enhancement of soil organic carbon and soil pH with biochar treatment affects microbial growth and metabolism in contaminated soils (Cui et al., 2013; Moore et al., 2018). As discussed above, the degree of pH enhancement by biochar depends on feedstock type, pyrolysis conditions and application rate. For instance, the addition of biochar derived from rice husk into the PTEs-contaminated sediment at 1 and 5% increased pH up to 7.3 and 8.5, respectively (Huang et al., 2017). The study revealed that higher microbial abundance at 1% amendment compared to the 5% amendment. The growth inhibition of some species of bacteria and fungi with higher application rate (5%) of biochars could be attributed to the increase in soil pH.

5.2.4. Impact of toxic compounds of biochar on microbes

Some biochars inherently contain toxic compounds, depending on feedstock materials and production conditions. Potentially toxic elements, polycyclic aromatic hydrocarbons, polychlorinated dibenzodioxins, polychlorinated dibenzofurans and some volatile compounds such as xylenols, cresols, acrolein and formaldehyde are toxic to the microorganisms (Hussain et al., 2017). Biochars produced by fast pyrolysis contain more volatile organic compounds (VOCs) compared to biochars produced by slow pyrolysis (Gurtler, Boateng, Han, & Douds, 2014). The VOCs of biochars could be toxic to the microorganisms in short-term and subsequently, the VOCs can be metabolized (Sun et al., 2015). However, Thangarajan et al. (2018) recently demonstrated that these toxic compounds in biochars can serve as nitrification inhibitors, thereby decreasing the nitrous oxide emission in biochar-amended soils. Therefore, future research should focus on how biochar-induced toxic compounds regulate soil microorganisms in PTE-contaminated soils.

5.2.5. Effects of biochar on the microbes through desorption of PTEs

Desorption of PTEs can increase their concentrations in soil solution and hence bioavailability. Arsenic and Sb are the most common metalloids that tend to be mobilized due to addition of biochars. Generally, As is associated with Fe or Mn oxides/hydroxides in soil. Adding biochar to the soil accelerates the reduction of Fe or Mn oxides/hydroxides (Kim et al., 2018; Zhu, Qiao, & Yan, 2019). As a result, As associated with Fe or Mn oxides/hydroxide is released to the soil solution. On the other hand, biochars could increase the abundance of Fe-reducing bacteria (*Clostridium*, *Bacillus,* and *Caloramator*) which facilitate the release of As associated with Fe oxyhydroxides (Wang, Xue, Juhasz, Chang, & Li, 2017). Moreover, biochars could increase soil pH and CEC, and consequently enhance As mobilization. Ahmad et al. (2017) found that the biochars derived from soybean stover, peanut shell and pine needles at 300 and 700ºC mobilized Sb and As in a shooting-range soil due to electrostatic repulsion and competition with phosphate. Biochar application induced reduction of As(V) to As(III) and thereby enhance its mobility (Xu, Yan, et al., 2019). Similarly, the application of biochars generated at high temperature (700ºC) increased Sb mobilization in a shooting-range soil (Rajapaksha et al., 2015). Lomaglio et al. (2017) observed that the addition of woody biochar derived at 500ºC to a mine-site soil increased the mobility of As and Sb while decreased the mobility of Pb. The increase in the mobility of Sb was attributed to increased soil pH in the biochar treatment, which induced the mobilization of humic acids. The mobilized humic acids might displace the Sb from organic/inorganic binding sites. The addition of biochar derived from rice hull at 500ºC increased concentrations of the dissolved Cd, Ni, Zn and Cu in a mine soil under oxic conditions (El-Naggar, Shaheen, Ok, & Rinklebe, 2018). Therefore, mobilization of PTEs by biochars may potentially change the microbial activity and future research on this aspect is needed.

5.3. Effect of microbial process on biochar

Due to their aromatic carbon structure, biochars are resistant to microbial decomposition and thus indirectly alter microbial communities by serving as a physical habitat and by changing the chemical and physical properties of soils (Bamminger et al., 2016). Recently, it has been suggested that some biochars are susceptible to decomposition through abiotic or biotic processes (Jiang, Denef, Stewart, & Cotrufo, 2016). The major abiotic processes have been reported to be chemical oxidation, photo-oxidation or solubilisation, with biotic process being reported to involve microbial incorporation or oxidative respiration of carbon (Kuppusamy, Thavamani, Megharaj, Venkateswarlu, & Naidu, 2016). The contribution of abiotic oxidation of freshly added biochars to the soil was higher than biotic oxidation in a short-term incubation (Cheng, Lehmann, Thies, Burton, & Engelhard, 2006). The degree of decomposition mainly depends on the product characteristics of biochars and the environmental conditions. The rate of biochar decomposition also depends on pyrolysis temperature, feedstock type, soil water content, time, concentration of native organic carbon in soil and soil pH (Luo, Durenkamp, De Nobili, Lin, & Brookes, 2011; Wang, Xiong, & Kuzyakov, 2016).

The mineralization process strongly depends on feedstock type. Among the biochars derived from maize stover, rice straw, pearl millet stalk, and wheat straw, maize-stover biochars showed the highest stability and resistance to mineralization because of their higher proportion of C=C aromatic stretching (Purakayastha, Kumari, & Pathak, 2015). Maize-residue, rye-residue and oak-wood biochars were mineralized by 0.78, 0.72 and 0.26% at the end of 60-day incubation, respectively (Hamer, Marschner, Brodowski, & Amelung, 2004). Maize and rye residues mainly consist of cellulose and hemicellulose materials that are susceptible to decomposition while oak wood is rich in lignin material that is resistant to degradation (Hamer et al., 2004). Biochars that are dominated by aliphatic compounds are more susceptible to the mineralization than those dominated by aromatic compounds (Rittl et al., 2015). Biochars derived at higher pyrolysis temperature (i.e., 600^{o}C) form more recalcitrant aromatic graphite structure which resists to microbial degradation. Increasing pyrolysis temperature decreased the concentration of labile matter of biochars while increased aromatic carbon concentration and C:N ratio, resulting in slow mineralization (Ameloot, De Neve, Graber, & Verheijen, 2013). Increasing pyrolysis temperature decreases molar O/C ratio of biochars, indicating higher stability of biochars generated at high temperatures (700^{o}C) (Bandara, Herath, Kumarathilaka, Hseu, et al., 2017). Increasing soil temperature (15 to 35^{o}C) increases the activity or changes composition of microbial community by changing biochemical pathways and thus, increases the mineralization of biochars (Sun, He, Zhang, Shao, & Xu, 2016). Mineralization of biochars could facilitate microbial growth and reproduction, while decreasing the stability of biochars in the soil system.

The effects of biochars on decomposition of native soil organic matter are also an important aspect in relation to the microbial mineralization. The increased decomposition of native soil organic matter due to the addition of biochars is called “priming effect”. The priming effect can be negative, positive or no effect, depending on properties of biochars (Zheng, Wang, Luo, Wang, & Xing, 2018). The biochar derived from mixed wood shaving had a negative priming effect in the sandy loam soil of pH 7.66 while those from paper sludge plus wheat husk and sewage sludge showed positive priming effects (Cely, Tarquis, Paz-Ferreiro, Méndez, & Gascó, 2014). Especially, the C content, aromaticity, toxic substances, volatile matter and surface properties of biochars and the environmental conditions interactively affect the mineralization of native soil organic matter. Biochars derived from grasses at low temperatures (250 and 400^{o}C) had positive priming effects in an Alfisol during the first 90 days and had negative priming effects during 250-500 days of incubation (Zimmerman, Gao, & Ahn, 2011). In contrast, biochars derived from woody materials at higher temperatures (525 and 650^{o}C) did not affect SOC priming during the first 90 days but had negative priming effects observed in soil amended with biochars during 250-500 days of incubation (Zimmerman et al., 2011).

The addition of corn-straw biochars into a coastal wetland soil had a negative priming effect (Zheng et al., 2018). It has been reported that biochar increased the microbial C-use efficiency and soil aggregate stability by shifting bacterial community towards to low C-turnover taxa. Wang, Xiong, et al. (2016) reported that the negative priming was more common for studies with a duration less than six months. The addition of biochars into low fertility or sandy soils

increased the susceptibility of native soil organic matter to the microbial mineralization. The mineralization of native soil organic matter also depends on the age of biochars in soil. The addition of aged biochars into a paddy soil improved microbial activity and C sequestration by negative priming while fresh biochars decreased the soil enzymatic activities and microbial respiration, however, motivated positive priming (Wang, Dokohely, Xiong, & Kuzyakov, 2016). Repeated biochar additions induced positive priming effects by altering soil microbial community (Luo, Lin, Durenkamp, & Kuzyakov, 2017). Therefore, aging of biochars protects native soil organic matter and thus enhances C sequestration. Su et al. (2017) reported that microbial community is the major driver of priming effects and C dynamics in biochar-amended soil. However, no studies have focused on how biochar-induced priming effects change the bioavailability of PTEs in contaminated soils. Thangarajan, Chowdhury, Kunhikrishnan, and Bolan (2014) observed that the biochar-amended soil had significantly lower priming effect than biosolid-, compost-, or poultry manure-amended soils due to its low dissolved organic matter.

5.4. Microbial immobilization mechanisms of PTEs in biochar-amended soils

The exact immobilization mechanisms of PTEs by microorganisms in biochar-amended soils are not fully understood. In this section, we propose the most likely immobilization mechanisms that occur. As shown in Figure 6, the immobilization of PTEs by microorganisms involves three identical steps. The first step is the biochar-induced PTE immobilization. This immobilization would decrease the bioavailability of the PTEs and decrease toxicity to soil microorganism (Choppala et al., 2012). The second step is biochar-induced microbial growth. After biochar changes the soil environment by decreasing PTE toxicity and providing nutrients and habitat, soil microorganisms will fill the available environmental niches. Some dormant species, due to PTE toxicity, will no longer be inhibited (Xu et al., 2018). At this stage, microorganisms may metabolize some VOCs and utilise PTEs as electron donors and acceptors. Biochar is able to donate π-elections to microbes that are electron acceptors (Joseph et al., 2010; Yuan et al., 2017). At the final step, microorganisms are involved in the PTE immobilization process. Microbes can change the oxidation states of PTEs through reduction or oxidation of PTEs (Wood and Wang, 1983). Saquing, Yu, and Chiu (2016) proposed that biochar acts as a rechargeable reservoir of bioavailable electrons (electron shuttle) in reduced environments. Pyrogenic C facilitated microbial extracellular reduction of Fe(III)-(oxyhydr)oxides (Yuan et al., 2017; Wu et al., 2018). In another study, the addition of activated C facilitated microbial reduction of As-bearing ferrihydrite and precipitation of vivianite and siderite which are effective in the immobilization of As(III) and As(V) (Wu et al., 2018). Similarly, Kappler et al. (2014) reported that the microbial reduction of Fe(III)-(oxyhydr)oxides depended on the biochar dosage; 5 and 10 g/L stimulated both rate and extent of microbial reduction while 0.5 and 1 g/L had a negative effect. Therefore, microorganisms can contribute to the conversion of PTEs to a less soluble/ toxic form.

Biochars derived at high temperature (700ºC) facilitate adherence and growth of microbial biofilm (Ding, Zeng, Wang, Du, & Zhu, 2011). Biofilm formation could facilitate the immobilization of PTEs by mass transfer of metals, bio-sorption and precipitation (Bandara, Herath, Kumarathilaka, Seneviratne, et al., 2017). Microbial biofilm consists of many extracellular polymeric substances (EPS) such as aromatic amino acids, polysaccharides, and cationic and anionic functional groups, leading to chemical and physical interactions with PTEs (Bandara, Herath, Kumarathilaka, Seneviratne, et al., 2017). Frankel et al. (2016) observed that a biofilm-associated biochar immobilized four-time more Fe, Al and As by than a sterile biochar in aqueous media.

Overall, our proposed immobilization mechanisms provide new knowledge and future research direction to identify microbial-induced PTEs immobilization process in biochar-amended soils. The addition of biochars alters the soil microbial activities by decreasing PTE bioavailability and providing habitable places and nutrients. The survival of microbes depends on the species, the amounts of pollutants and toxic compounds present in the biochar material. Moreover, biochar-associated microorganisms are able to immobilize PTEs via providing electrons for redox reactions and facilitating extracellular polymeric substances to bio-sorption. Potentially toxic elements, biochars, and microbes are interrelated to govern the overall output.

6. The analytical methods for identification of mechanisms

Many analytical methods have been utilized for characterization of biochar materials, including the analyses of elemental composition, surface functional groups, surface morphology and molecular species (Amin et al., 2016). Understanding mechanisms of biochar, PTE and microbe interactions is imperative prior to field application in order to assist sustainable remediation process. This section mainly discusses techniques that are employed to identify the interaction mechanisms of biochar, PTEs and microorganisms.

6.1. Fourier transform infrared spectroscopy (FTIR)

The FTIR is the most widely employed method for the characterisation of biochar surfaces. Especially, this technique determines surface functional groups and adsorbed or deposited species at a biochar surface. This technique has been used extensively to identify various mechanisms involved in the interactions between biochars and PTEs (Li, Zheng, et al., 2019; Wu et al., 2019). For instance, a new peak of CO_3^{2-} stretching was observed after Pb(II) adsorption onto wheat-straw biochar produced at 700ºC, due to formation of $Pb_3(CO_3)_2(OH)_2$ (Shen et al., 2017). Yu, Zhou, Huang, Song, and Qiu (2015) observed that O-H, C=O, Mn-O and Si-O were the responsible surface functional groups for As adsorption on Mn-oxide-modified biochar. The addition of biochars to Cr(VI)-contaminated soils reduced Cr(VI) to Cr(III) as confirmed by the FTIR analysis (Choppala, Bolan, Kunhikrishnan, Skinner, & Seshadri, 2015). The release of –OH ions, involvement of amine groups, stretching of C-O group in amides and involvement of N-H groups, hydrolysis of aldehydes/ketones and formation of carboxyl groups and bending of aromatic C-H bonding involved in Cr(VI) reduction process. Likewise, the FTIR analysis revealed that the application of biochars to Cu-spiked Alfisol and Spodosol modified the peaks of spectra and provided the direct evidence of Cu complexation with surface functional groups of biochar (Bakshi, He, & Harris, 2014). The FTIR analysis is a useful technique for the identification of functional groups involved in the microbial immobilization of PTEs. For instance, FTIR analysis showed a weak peak of CO_3^{2-} after biochar addition to *Bacillus cereus* NS4 medium containing with Ni(II) because biochar decreased the microbial calcite precipitation process and inhibited the Ni(II) immobilization (Zhang, Kumari, Fang, & Achal, 2019). Zhu, Zhang, Tang, Zhu, and Wu, (2018) reported that –OH, and –C=O groups were involved in the biosorption of As(III) by periphytic biofilm. Seneviratne et al. (2016) showed that amine ($-NH_2$) and nitro (-NO) functional groups present in the *Bradyrhizobium japonicum* were responsible for the process of heavy-metal biosorption. Moreover, FTIR results showed stronger biosorption of Pb than of Cu and Ni. Similarly, FTIR spectral analysis revealed that carboxyl (-COOH) and phosphate groups in microbial biofilm contributed to biosorption of Ni (Seneviratne, Vithanage, Madawala, & Seneviratne, 2015).

6.2. X-ray diffraction (XRD)

The XRD is a widely used technique for the identification of the crystalline structure of the biochar. Especially, mineral compounds present in the biochar play a vital role in precipitation and adsorption of PTEs. XRD analysis revealed that the number of minerals (e.g., quartz, calcite, feldspar, and anhydrite) present in the biochar increased with increasing pyrolysis temperature (Azargohar, Nanda, Dalai, & Rao, 2013). It also revealed that the biochar derived from rice husk was dominated with inorganic components such as KCl, $CaCO_3$, and SiO_2 while the biochar derived from bamboo biomass was dominated with SiO_2 (Weng et al., 2017). The XRD analysis of four biochars after exposure to Pb(II) revealed the formation of $PbCO_3$ on British hardwood biochar, and $Pb_3(CO_3)_2(OH)_2$ on biochars derived from wheat straw, rice husk and softwood pellets (Shen et al., 2017). With incubation time, the peaks of less stable $PbCO_3$ and $Pb_3(CO_3)_2(OH)_2$ decreased and the peak of more stable hydroxypyromorphite ($Pb_5(PO_4)_3OH$) increased after dairy-manure biochar was added to Pb-polluted soils (Cao et al., 2011). Periphytic biofilm was effective in As(III) immobilization due to the presence of calcite on the biofilm surface (Zhu et al., 2018). The XRD analysis showed the disappearance of calcite peak after treated with As(III), indicating the interaction of As(III) with calcite. Zhang, Kumari, et al. (2019) reported that biochar inhibited the microbial calcite precipitation and suppressed the Ni(II)

immobilization. The XRD analysis showed that microbial calcite precipitation process led to the immobilization of Ni(II) in the form of $NiCO_3$ and that the $NiCO_3$ peak lowered after biochar addition due to dissolution of $CaCO_3$ by biochar. Phosphate-solubilizing bacteria enhanced Pb(II) immobilization by rice-husk and sludge biochars through formation of pyromorphite on the biochar surfaces (Chen et al., 2019). The XRD analysis also showed that Pb existed as $PbCO_3$ or $Pb_3(OH)_2(CO_3)_2$ on the surface of biochar particles without P-solubilizing bacteria but as pyromorphite ($Pb_5(PO_4)_3OH$, $Pb_{10}(PO_4)_6(OH)_2$) with the addition of P-solubilizing bacteria. Synchrotron-based XRD technique is used for the determination of material structure, crystal and molecular structure (Rao et al., 2017). It has a well-defined wavelength, high flux, and collimation to enhance sensitivity and resolution of different peaks (Kopittke et al., 2017).

6.3. Scanning electron microscope-energy dispersive X-ray spectroscopy (SEM-EDX)

The SEM-EDX is a useful technique to estimate the elemental distribution and composition of biochar surfaces (Igalavithana, Mandal, et al., 2017) as well as microbial cells in relation to the immobilization of PTEs (Wang, Wu, et al., 2019). For example, by using SEM-EDX, Igalavithana et al. (2018) reported that Pb and Cd were stabilized on the biochar surface via surface complexation with O-containing functional groups. They also observed that Pb was associated with Al, Fe, Si, Ca, Mg and K, and Cd associated with Si, Al, Ca and K present in the biochar surface. Chen et al. (2019) showed the application of P-solubilizing bacteria could promote the transformation of unstable Pb-minerals to Pyro-minerals on the biochar surfaces. In contrast, Zhang, Kumari, et al. (2019) observed that lower amount of Ca in biochar-added samples by inhibiting microbial-induced calcite formation, which in turn decreased the Ni(II) immobilization.

6.4. Nanoscale secondary ion mass spectrometry (NanoSIMS)

The nanoSIMS can obtain chemical imaging of surface distribution of elements with sensitivities from the ppb to ppm range and lateral resolution below 50 nm (Penen et al., 2016). Mueller et al. (2013) reviewed the potential use of nanoSIMS to investigate the plant, microbe and element interactions in soil. For instant, Newsome, Lopez Adams, Downie, Moore, and Lloyd (2018) used nanoSIMS imaging to describe the extracellular electron transport process during the microbial Fe(III) reduction. Moreover, they highlighted the importance of nanoSIMS imaging in tracing the fate of PTEs associated with Fe/Mn oxides and related microorganisms. The nanoSIMS has been used to monitor C stability in biochar-amended soil (DeCiucies, Whitman, Woolf, Enders, & Lehmann, 2018; Hernandez-Soriano, Kerré, Kopittke, Horemans, & Smolders, 2016). Therefore, this technique has potential to identify biochar, PTE and microbial interactions and associated mechanisms in the soil environment.

6.5. X-ray photoelectron spectroscopy (XPS)

XPS is widely employed in the analysis of elemental compositions, chemical states or electronic state of the materials. For instance, XPS spectra can be used for the identification of surface functional groups, and it was implied that HNO_3 acid oxidation of biochars led to the increased oxygen-containing surface functional groups (Li, Ye, et al., 2016). Choppala et al. (2016) observed that, based on XPS analysis, biochar reduced Cr(VI) to Cr(III) by 33% and As(V) to As(III) by 12% within seven days of incubation while remained Cr and As presented as Cr(VI) and As(V). The XPS spectra obtained from soils amended with sludge-derived biochar indicated that As(III) was converted to stable As(V) (30.5% increased) and that this transformation was highly time-dependent (Fang, Tsang, Zhou, Zhang, & Qiu, 2016). Sludge-derived biochars contained 33% of Fe which catalyses As(III) co-oxidation. Similarly, XPS analysis revealed that As(III) partially oxidized to As(V) by Mn oxides and Fe-Mn-oxides in As(III)-contaminated soils amended with manganese-oxides-modified biochars (Yu et al., 2015). Rees et al. (2017) observed that Pb and Cd were mainly distributed in carbonate phase of biochar and their concentrations were proportional to Ca concentration.

6.6. X-ray fluorescence microscopy (μ-XRF)

A synchrotron-based μ-XRF technique is widely used for the elemental mapping in bulk samples. The major advantage of this method is that in the presence of high energy of the X-rays, atoms of elements are excited and photoelectrons released; therefore multi-elemental maps can be easily generated (Kopittke et al., 2017). The potential use of this technique in biochar research is the identification of PTE distribution of biochar particles. Determination of PTEs in biochar particles is imperative before environmental application specially for biochars produced from sewage sludges or animal manures. For instance, the μ-XRF analysis revealed that poultry- and swine-manure biochars contain the elevated amounts of Cu, Zn, and As that were heterogeneously distributed during pyrolysis process while less amounts of Pb were homogeneously distributed (Lin, Xu, Wang, et al., 2017). In addition, Cu, Hg and Fe were distributed along pore edges and on particle surfaces or penetrated into solid phase of the biochar derived from switchgrass pyrolysed at 600 and 300ºC, respectively (Liu, Ptacek, Blowes, Finfrock, & Gordon, 2016).

6.7. X-ray absorption spectroscopy (XAS)

The chemical speciation of PTEs determines their mobility and bioavailability in the soil. In this context, XAS is a non-destructive analytical method and provides the information of speciation and bonding types. The XAS spectrum fundamentally divides into two energy regions called x-ray absorption near spectroscopy (XANES) or extended X-ray absorption fine structure (EXAFS) and near edge X-ray absorption fine structure (NEXAFS) (Lombi & Susini, 2009).

XANES analysis indicated that iron oxides and aluminium oxides strongly adsorbed As(V) by surface complexation and electrostatic interactions in a red-mud amended with rice-straw biochar (Wu, Huang, et al., 2017). Another study showed that biochar addition did not alter the As oxidation states in soil and As existed as less mobile arsenate in both amended and non-amended soils (Strawn, Rigby, Baker, Coleman, & Koch, 2016). The XANES analysis revealed that immobilization mechanism of Zn by biochars in soils amended with aged sewage sludge was attributed to precipitation as Zn phosphate [$Zn_3(PO_4)_2$] and hopeite ($Zn^{[6]}Zn_2^{[4]}PO_4.4H_2O$) (Wagner, Kaupenjohann, Hu, Kruse, & Leinweber, 2015). The addition of poultry-litter and sludge biochars into the Typic Udic Ferrisols with 60% of water-holding capacity or flooded conditions caused complete dissolution of CuO within three months, and CuS was partly oxidized to Cu(II) in 60% water-holding capacity within nine months and adsorbed to the organic phase (Lin, Xu, Chen, et al., 2017).

EXAFS spectra identified 62.7% of Pb sorbed on kaolinite and 23.6% as a Pb-phosphate after the addition of oak wood biochars into a shooting-range soil (Ahmad, Lee, et al., 2014). The soybean stover biochar effectively immobilized Pb in a shooting-range soil by formation of $Pb_5(PO_4)_3Cl$ and $Pb_3(PO_4)_2$, which was confirmed by EXAFS analysis (Moon et al., 2013). Increasing pyrolysis temperature of buffalo weed biochars induced the formation of Pb-gibbsite but decreased the formation of hydrocerussite and chloromorphite (Rajapaksha et al., 2015). The EXAFS analysis revealed that tsumebite [$(Pb_2Cu(PO_4)(SO_4)(OH)$] was the dominant precipitate when buffalo weed and its biochar were added to the shooting-range soil (Rajapaksha et al., 2015). The EXAFS spectra revealed that the biochar derived from switchgrass at 600ºC mainly exist as metacinnabar while the biochars produced at 300ºC exist as cinnabar in a Hg-contaminated sediment (Liu, Ptacek, et al., 2016). Wu et al. (2019) conducted a number of batch-type Zn sorption experiments using the mixture of γ-Al_2O_3 and rice-straw biochar as a model binary geosorbent systems. EXAFS spectroscopy analysis indicated that over 60% of Zn existed as Zn-Al layered double hydroxide on γ-Al_2O_3 at pH 7.5. The Zn in biochar-treated soil mainly existed as Zn-OM and Zn_2SiO_4, whereas the proportion of Zn_2SiO_4 was negligible compared with Zn-Al silicate (26–48%) in the mixture of γ-Al_2O_3 and rice-straw biochar.

6.8. Sequential fractionation

Sequential fractionation methods are used to evaluate the distribution of various chemical forms of PTEs among the solid phases in soils or sediments (Adriano, Wenzel, Vangronsveld, & Bolan, 2004). These methods can be used to identify PTEs bound to various fractions including soluble, exchangeable, precipitated, organic matter bound and occluded (Rajapaksha, Vithanage, Oze,

Bandara, & Weerasooriya, 2012; Yang, Lu, et al., 2017). However, the efficiency of the methods depends on the reagents, nature of the sample, duration of extraction, temperature, pH and solid/solution ratio (Bolan et al., 2014). The chemical fractionation methods have been used to correlate the plant-available PTEs in soils and plant uptake of PTEs (Adriano et al., 2004).

Yang, Lu, et al. (2017) found that exchangeable Cd was redistributed to carbonate and the faction of Fe-Mn oxides while Zn was redistributed to Fe-Mn oxides fraction upon biochar addition. Similarly, Park, Choppala, Bolan, Chung, and Chuasavathi (2011) observed that the addition of biochars decreased the concentration of exchangeable Cd while increased the organic-matter-bound fraction. The Cd bound to the Fe-Mn oxides fraction increased with increasing biochar addition rates (Jiang, Xu, Jiang, & Li, 2012). The biochar-induced redistribution of exchangeable Cd into carbonate-bound fraction was attributed to the enhancement of soil pH due to alkaline biochar input (Houben and Sonnet, 2015).

The bioavailability of PTEs in soils has also been determined using the Potentially Bioavailable Sequential Extraction (PBASE), Physiologically-Based Extraction Test (PBET), and Gastrointestinal (GI) Test (Bolan et al., 2014). For instance, Qi et al. (2018) showed that aging of chicken litter biochar decreased the Cd bioaccessibility to the human gastric phase while acidic-wood-shaving biochar showed no effect. Similarly, Ahmad, Lee, Yang, et al. (2012) observed that addition of oak-wood biochar into the shooting-range soil decreased Pb bioaccessibility by 12% compared to the control. Sequential extraction procedure, PBET and PBASE have been widely used due to their analytical simplicity for the estimation of the bioavailable PTEs in soil.

7. Efficiency enhancement through modification

The sorption capacity of pristine biochars for PTEs is inferior due to their inadequate surface functional groups and mineral component (Zuo, Chen, Cui, & Fu, 2017). Recently, a number of studies have focused on modification of biochars to enhance their surface area, functional groups, porosity, and point of zero charge (pH_{pzc}) (Shu, Lu & He, 2013; Sikarwar et al., 2016; Tan, Sun, Xu, Wang, & Xu, 2016; Zama et al., 2018; Zhao, Zhao, et al., 2017). However, most of the studies have mainly focused on the removal of PTEs in aqueous systems, the use of modified biochars in soil systems is not fully studied.

Various advanced methods have been developed to enhance the efficiency of pristine biochar. The modification includes physical, chemical and magnetic modifications, and impregnation with mineral compounds (Table 4) (Rajapaksha et al., 2016).

7.1. Physical modification

Physical modifications are usually a low-cost and less technological-involved process. Nevertheless, the efficiency in PTE immobilization due to physical modification is lower than that to be achieved by chemical modification methods. On the other hand, physical activation is better than chemical activation for soil application because chemical activation may have adverse consequences in the soil system. The physical modification involves two steps (Cheng, Zeng, & Jiang, 2017; Rajapaksha et al., 2016). The first step is that initial pyrolysis reactions in the oxygen-free environment produce biochar. The resulting biochar is then subjected to the partial gasification with steam, CO_2, air, O_3 or NH_3. During the biomass pyrolysis, most of the impurities such as products of incomplete combustion are retained within the biochar and subsequent steam activation process could help to remove impurities and increase the porosity (Sizmur, Fresno, Akgül, Frost, & Moreno-Jiménez, 2017). It can potentially modify the surface functional groups (Sikarwar et al., 2016). The addition of Eucalyptus-wood-derived biochar with steam activation could help to suppress emission of CH_4 and N_2O from the soil (Fungo et al., 2014). In contrast, the addition of steam-activated stover biochar increased CH_4 emission from the soil (Fungo et al., 2014).

The activation with NH_3 introduces amino functional groups into biochar, and was effective for the removal of Pb(II) and Cu(II) in aqueous solutions (Wu, Li, et al., 2017; Yang and Jiang, 2014). During CO_2 activation, C of the biochars reacts with CO_2 to form CO, resulting in hot corrosion of the surface and hence increasing surface area by creating micropores (Rajapaksha et

al., 2016). Zhang et al. (2014) observed that the combination of CO_2 and NH_3 increased surface area and N-containing surface functional groups compared to conventional CO_2 or NH_3 modification. Properties of physically-activated biochars depend on precursors, activation temperature, oxidizing agent and degree of activation (Cheng, Zeng, et al., 2017).

Recently, Sajjadi et al. (2019) reported that combined physical and chemical activation enhanced the capacity of softwood-pine biochar to adsorb Ni(II). They observed that > 99% of Ni(II) from solution was removed by biochars after physical activation via ultrasound irradiation for 20 s, chemical activation using 50% H_3PO_4 and functionalized with 6 M urea solution. A combination of different activation methods appears to be more effective than single activation, and therefore future research is needed to focus on the effectiveness of modified biochars with combined methods.

7.2. Chemical modification

Chemical modification involves acid/base treatment, organic solvent treatment, and coating with graphene/nanotube/metal oxides. In terms of PTE removal efficiency, chemically-modified biochars are more effective than physically-modified ones. The major disadvantages of chemical activation are high cost and risk of chemical changes in the soil matrix.

The common chemical activating acids are HNO_3, H_2SO_4, H_3PO_4, and HCl. The acid activation leads to degradation of micropores due to erosive nature, resulting in a decreased surface area (Mandal et al., 2016; Rajapaksha et al., 2016). The mineral acids are capable of introducing acidic functional groups such as carboxylic, amine groups onto biochar surface and thus high possibility to remove PTEs through PTE-functional group interaction (Wu et al., 2016; Wu, Li, et al., 2017). The activation of sewage sludge biochars with HNO_3 (4 h at 90^{o}C) enhances Cu, Zn, and Al removal by 98%, 42% and 34% from the natural acid rock drainage because of increased surface carboxylic groups compared to the unmodified biochar (Li, Gong, & Abida, 2019). Biomass pre-treatment with H_3PO_4 introduces P-O-P crosslink with C and resulting structure shows an enhanced sorption affinity for Pb (Zhao, Zheng, et al., 2017). Also, H_3PO_4-treated corn-straw biochar increased Cr(VI) adsorption capacity due to increases in surface groups and aromatic compounds (Zhao, Zhao, et al., 2017). Soil type significantly affects the immobilization of PTEs with biochar. Especially, much more attention is needed when contaminated soils are low in clay and organic matter contents. Un-activated biochars significantly mobilize Pb and Cu in soils low in clay and organic matter because of the formation of soluble ion complexes with dissolved organic carbon originated from biochar (Uchimiya & Bannon, 2013). The activation of biochars with strong acids can be very expensive and the use of these modified biochars will lead to other environmental issues such as disposal of the activation media and potential toxicity to the microorganisms. Nevertheless, activation with H_2O_2 has been considered an environmentally- and economically-friendly activation method to modify biochars. Activation with H_2O_2 obviously increases oxygen-rich functional groups on the biochar surface and facilitates the formation of binding sites for the heavy metals (Zuo, Chen, Fu, & Li, 2016). For instance, the activation of biochars with H_2O_2 showed 91.7% higher Cu(II) removal efficiency compared to the un-modified biochar in aqueous solution because of higher number of carboxylic functional groups (Zuo, Liu, & Chen, 2016).

The mineral component of biochar matrix plays an important role in PTE removal by precipitation (Qi, Kuppusamy, et al., 2017). Biochar modification with strong acids or oxidizing agents, subsequently dissolves the mineral component, which may reduce sorption of PTEs via precipitation (Sizmur et al., 2017). Activation or modification with an alkali solution such as KOH or NaOH can also increase biochar's sorption capacity of heavy metals by increasing surface area, porosity, and surface functional groups. KOH is an effective oxidant and its activation process stimulates the formation of pore structure on carbon surface. The use of biochar modified with KOH increased Cu removal efficiency by 3.4 times through increased surface complexation with the oxygen-containing functional groups (Jin et al., 2016). KOH converts Cu(II) to $Cu(OH)^+$ which has a higher affinity for sorption than Cu(II). Similarly, biochar with NaOH modification increased the sorption capacity of heavy metals 2.6-5.8 times via increasing surface area, oxygen-containing functional groups and cation-exchange capacity (Ding, Hu, Wan, Wang, & Gao, 2016). Recently, An, Jiang, Nan, Yu, and Jiang (2019) showed that the biochar modified by KOH

followed by $KMnO_4$ enhanced the removal capacity of Ni(II) from the aqueous solution. The FTIR and XPS analyses revealed that the $–NH_2$ and –OH groups present in the modified biochar could form surface complexation and co-precipitation with Ni(II).

The use of biochar coated with iron-phosphate nanoparticles increased Cd(II) immobilization efficiency by 81% and decreased bioaccessibility by up to 80% (Qiao et al., 2017). The study revealed that the composite promoted the growth of plants via providing available P. In the same way, the biochar modified with Fe-Mn oxides reduced As(V) concentration in contaminated paddy soils (Lin, Gao, et al., 2017). The Fe-oxides present on the biochar particles enhanced As adsorption and Mn-oxides oxidize soluble As(III) to less soluble As(V). Wheat-straw biochar modified with 0.05 M $Bi(NO_3)_3$ promoted the co-precipitation of Fe(II) and As(III) ions (Zhu et al., 2019). Thus Bi-impregnated biochar regulated ferrolysis, which contributed to immobilization of As in paddy soils. Recently, biochars coated with graphene oxide have received much attention due to their strong affinity of pollutants for remediation (Shang et al., 2016).

7.3. Magnetic modification

The surface of biochars is typically rich in negative charges. Thus, with biochar application, anionic contaminants are leached out or mobilized from the soil solutions (Beesley & Marmiroli, 2011). Magnetic biochars have been recognized as an effective solution for remediation of anionic contaminants (Chen, Chen, & Lv, 2011). The magnetic modification is either pre- or post-pyrolysis process (Šafařík et al., 2016). For instance, biomass was modified with $FeCl_3$ as a pre-pyrolysis treatment and Fe(III)/Fe(II) precipitated on biochar surfaces as a post-pyrolysis process (Wang et al., 2015b). The surface area of magnetically-modified biochars decreases because Fe oxide has a small specific surface area compared to the unmodified biochar (Rajapaksha et al., 2016). Cation exchange and surface complexation are the primary mechanisms which are involved in remediation of PTEs by magnetically-modified biochar (Trakal et al., 2016). The removal efficiency of As(V) and Sb(III) depends on the method of magnetization. Fe-loaded biochar produced via evaporation displays three- and five-fold increases in As(V) and Sb(III) sorption capacity, respectively, compared to the pristine biochar (Calugaru, Neculita, Genty, & Zaguru, 2019). In comparison, Fe-loaded biochar produced via precipitation shows a two-fold increase in sorption capacity for both metals. The Cd(II) adsorption onto magnetically-modified biochars decreases because of the presence of a large number of protons after modification (Li, Yang, et al., 2017). Iron oxide on the surface of the magnetically-modified biochar competes with Cd, and the number of Cd fixed on the modified biochar decreases (Tan et al., 2017). However, magnetic chlorinated biochar (Fe-Cl/biochar) shows a higher adsorption capacity for Hg^o compared to the commercial activated carbon (Xu, Luo, et al., 2019). Chemisorption is the main mechanism of Hg^o removal because Fe_3O_4, C=O and Cl-Cl provide active sorption sites. Compared to a regular magnetic biochar, a novel CeO_2-MoS_2 hybrid magnetic biochar has been shown to have a higher Pb(II)-removal capacity and removes >99% Pb(II) within 6 h, predominantly via electrostatic interaction, Cπ-Pb(II) interaction, surface adsorption and complexation (Li, Deng, et al., 2019). Similarly, $KMnO_4$-treated magnetic biochar has nearly 7 times more Pb(II) and Cd(II) adsorption capacity than the untreated magnetic biochar (Sun et al., 2019). The XPS and FTIR analyses confirmed the formation of manganese oxides and O-containing functional groups on $KMnO_4$-treated magnetic biochar. From the above literature, it is evident that the PTE immobilization capacity of magnetic biochar is enhanced with further modifications with various compounds. Future research should focus on the immobilization of PTEs by these hybridized biochar materials in soil.

7.4. Impregnation with minerals

The significant disadvantage of biochars is their weak affinity with oxyanions. Due to net negative surface charges, biochars build electrostatic repulsion with oxyanions. Impregnation with clay minerals or metal oxides increases the net positive charges on the biochar surface, which facilitates adsorption of oxyanions. Most common impregnation agents are clay minerals such as montmorillonite, bentonite, $MgCl_2$, and MnO_x (Rajapaksha et al., 2016). Modification of biochars with clay minerals is considered as pre-pyrolysis modification process (Sizmur et al., 2017). The

impregnation of bamboo biochars with montmorillonite significantly increased specific surface area, pore diameter, pore volume and mineral components such as Ca(II), Mg(II), Al(III) and Fe(III) (Chen, Chen, et al., 2017). The impregnation of bamboo biomass with iron-kaolinite or iron-bentonite significantly prevented cellulose degradation and increased pore volume at 250^{o}C while it increased the concentration of aromatic, phenolic and acidic carbons and reduced pore volume at 350-550^{o}C (Rawal et al., 2016). Bionanocomposite developed from chitosan, montmorillonite nanoclay and biochar decreased leaching of Pb(II), Cu(II) and Zn(II) from the acidic mine soil by 52%, 100% and 100%, respectively (Arabyarmohammadi et al., 2018). The FTIR analysis confirmed $–NH_2$ group being involved in the immobilization of heavy metals. The $MgCl_2$ impregnation significantly increased the surface area, ash and Mg content of biochars (Cui et al., 2016). Pre-modification with $MgCl_2$ showed a higher number of nano-MgO particles and a larger number of oxygen-containing surface functional groups compared to the post-modified biochar (Yu et al., 2016). The impregnation of biochars derived from corn straw at 600^{o}C with $KMnO_4$, significantly increased surface micro/nano-MnO_x, polarity, oxygen-containing functional groups, and average pore width but decreased surface area (Song et al., 2014). Similarly, the impregnation of corn-straw biochars with Mn-oxides, significantly decreased the bioavailability and mobility of As(III) and As(V) in contaminated paddy soils (Yu et al., 2017). Wang, Zhao, et al. (2019) critically reviewed the production, properties and contaminant removal from soil and water using biochar-supported nanoscale zero-valent iron which exhibited excellent reactions with PTEs due to increased electron transfer capacity, catalytic capacity and conductivity. The impregnation of biochars with clay minerals or metal oxides possesses an excellent potential to remove PTEs in an environmentally-friendly manner. On the other hand, modification of biochars with clay minerals is a highly economical and feasible technique.

8. Conclusions and future perspectives

Biochars have been recognised as carbon-rich materials with an excellent potential to remediate soil and water systems polluted by PTEs. However, as a soil amendment, many aspects need to be exploited due to contrasting observations in relation to the immobilization of PTEs. The variations in feedstock, production condition, application rate, soil and environmental conditions, and PTE behaviour contribute to such contrasting observations. The present review also highlights the interactive mechanisms of biochars and microbes in the immobilization of PTEs in contaminated soils to make some guidance for future biochar application.

The characteristics of biochar products are mainly governed by the feedstock material, and production conditions which are primary factors determining the success of PTE immobilization. Different feedstock materials have various unique properties, and hence depending on production method, pyrolysis temperature and holding time for biochar production need to be optimized for immobilization of PTEs. Biochars with high dissolved organic C are effective in immobilization of cations such as Cd, Pb and Hg, but are not suitable for the immobilization of anions such as As and Sb.

The chemical behaviours of anion PTEs are entirely different from the cationic ones. Biochars possess net negative charges on their particle surfaces and therefore anions bound to the soil colloids are easily mobilized. Moreover, the addition of biochar increases soil pH and thus promotes the retention of cationic PTEs while mobilizing anionic PTEs due to increases of negative charges in soil. Through some modifications, biochars can be effective to immobilize anion contaminants. Especially, a combination of various modification methods is more efficient than single modification. Therefore, identification of efficient modification methods for remediation of both cations and anions is essential because most of the soils are contaminated with multiple PTEs. However, the remediation mechanisms of modified biochars in soils contaminated with PTEs are still not fully understood. Furthermore, it would be necessary to understand the immobilization mechanisms based on the soil types, and climatic zones due to variability of immobilization reactions. New advanced techniques, such as synchrotron-based techniques can be exploited to study the mechanisms behind the biochar-PTE interactions.

Other than the direct mechanisms of biochar-PTE interactions, some indirect mechanisms are also involved. For instance, the enhancement of soil pH and cation exchange capacity, change of soil redox potential, and facilitation of soil microorganisms could indirectly promote

immobilization of PTEs in soil. Soil biological components play a vital role in the remediation of PTEs. Biochar addition would facilitate microbial growth in contaminated soils by decreasing PTE toxicity and providing nutrients and habitats. Soil microorganisms further participate in immobilization of PTEs by stimulating redox reactions, biosorption, and physical-chemical interactions with extracellular polymeric substances. However, there is no clear evidence of microbial immobilization mechanisms upon biochar addition and future research is needed on the synergistic effects of biochar and microbes on PTE immobilization. Specially, combined application of PTE-tolerant microbes and biochar would be an effective strategy to enhance the efficiency of PTE immobilization.

Finally, it is important to summarize more acceptable guidelines for biochar application with production conditions and methods, feedstock materials, application dosage, soil type and environmental conditions to achieve optimum immobilization capacity for development of environmentally-friendly remediation strategies.

Acknowledgments

We thank anonymous reviewers, Dr Zhongmin Dai and Dr Yu Luo for their constructive comments. JMX was financially supported by the National Natural Science Foundation of China (41520104001).

References

Abbas, T., Rizwan, M., Ali, S., Zia-ur-Rehman, M., Qayyum, M.F., Abbas, F., Hannan, F., … Ok, Y.S. (2017). Effect of biochar on cadmium bioavailability and uptake in wheat (*Triticum aestivum* L.) grown in a soil with aged contamination. *Ecotoxicology and Environmental Safety*, *140*, 37-47.

Abdu, N., Abdullahi, A., & Abdulkadir, A. (2017). Heavy metals and soil microbes. *Environmental Chemistry Letters*, *15*, 65-84.

Abiven, S., Schmidt, M.W.I., & Lehmann, J. (2014). Biochar by design. *Nature Geoscience*, *7*, 326-327.

Adriano, D.C., Wenzel, W.W., Vangronsveld, J., & Bolan, N.S. (2004). Role of assisted natural remediation in environmental cleanup. *Geoderma*,*122*, 121-142.

Ahmad, M., Lee, S., Lee, S., Al-Wabel, M., Tsang, D., & Ok, Y. (2017). Biochar-induced changes in soil properties affected immobilization/mobilization of metals/metalloids in contaminated soils. *Journal of soils and sediments*,*17*, 717-730.

Ahmad, M., Lee, S.S., Lim, J.E., Lee, S.-E., Cho, J.S., Moon, D.H., … Ok, Y.S. (2014). Speciation and phytoavailability of lead and antimony in a small arms range soil amended with mussel shell, cow bone and biochar: EXAFS spectroscopy and chemical extractions. *Chemosphere*, *95*, 433-441.

Ahmad, M., Lee, S.S., Yang, J.E., Ro, H.-M., Lee, Y.H., & Ok, Y.S. (2012). Effects of soil dilution and amendments (mussel shell, cow bone, and biochar) on Pb availability and phytotoxicity in military shooting range soil. *Ecotoxicology and Environmental Safety*,*79*, 225-231.

Ahmad, M., Ok, Y.S., Kim, B.-Y., Ahn, J.-H., Lee, Y.H., Zhang, M., … Lee, S.S. (2016). Impact of soybean stover- and pine needle-derived biochars on Pb and As mobility, microbial community, and carbon stability in a contaminated agricultural soil. *Journal of Environmental Management*,*166*, 131-139.

Ahmad, M., Ok, Y.S., Rajapaksha, A.U., Lim, J.E., Kim, B.-Y., Ahn, J.-H., … Lee, S.S. (2016). Lead and copper immobilization in a shooting range soil using soybean stover- and pine needle-derived biochars: Chemical, microbial and spectroscopic assessments. *Journal of Hazardous Materials*, *301*, 179-186.

Ahmad, M., Rajapaksha, A.U., Lim, J.E., Zhang, M., Bolan, N., Mohan, D., … Ok, Y.S. (2014). Biochar as a sorbent for contaminant management in soil and water: A review. *Chemosphere*, *99*, 19-33.

Al-Wabel, M.I., Al-Omran, A., El-Naggar, A.H., Nadeem, M., & Usman, A.R.A. (2013). Pyrolysis temperature induced changes in characteristics and chemical composition of biochar produced from conocarpus wastes. *Bioresource Technology*, *131*, 374-379.

Ali, A., Guo, D., Zhang, Y., Sun, X., Jiang, S., Guo, Z., … Zhang, Z. (2017). Using bamboo biochar with compost for the stabilization and phytotoxicity reduction of heavy metals in mine-contaminated soils of China. *Scientific Reports*, 7,

Alkurdi, S.S.A., Herath, I., Bundschuh, J., Al-Juboori, R.A., Vithanage, M., & Mohan, D. (2019). Biochar versus bone char for a sustainable inorganic arsenic mitigation in water: What needs to be done in future research? *Environment international*, *127*, 52-69.

Ameloot, N., De Neve, E.R., Graber, F.G.A., & Verheijen, S. (2013). Interactions between biochar stability and soil organisms: Review and research needs. *European Journal of Soil Science*, *64*, 379-390.

Amin, F., Huang, Y., He, Y., Zhang, R., Liu, G., & Chen, C. (2016). Biochar applications and modern techniques for characterization. *Clean Technologies and Environmental policy*, *18*, 1457-1473.

An, Q., Jiang, Y.-Q., Nan, H.-Y., Yu, Y., & Jiang, J.-N. (2019). Unraveling sorption of nickel from aqueous solution by $KMnO_4$ and KOH-modified peanut shell biochar: Implicit mechanism. *Chemosphere*, *214*, 846-854.

Antal, M., & Gronli, M. (2003). The art, science, and technology of charcoal production *Industrial & Engineering Chemistry Research*, *42*(8), 1619-1640.

Arabyarmohammadi, H., Darban, A.K., Abdollahy, M., Yong, R., Ayati, B., Zirakjou, A., & van der Zee, S.E. (2018). Utilization of a novel chitosan/clay/Biochar Nanobiocomposite for immobilization of heavy metals in acid soil environment. *Journal of Polymers and the Environment*, *26*, 2107-2119.

Arán, D., Antelo, J., Fiol, S., & Macías, F. (2016). Influence of feedstock on the copper removal capacity of waste-derived biochars. *Bioresource Technology*, *212*, 199-206.

Arshad, M., Khan, A.H.A., Hussain, I., Anees, M., Iqbal, M., Soja, G., … Yousaf, S. (2017). The reduction of chromium (VI) phytotoxicity and phytoavailability to wheat (*Triticum aestivum* L.) using biochar and bacteria. *Applied Soil Ecology*, *114*, 90-98.

Awad, Y.M., Ok, Y.S., Abrigata, J., Beiyuan, J., Beckers, F., Tsang, D.C.W., & Rinklebe, J. (2018). Pine sawdust biomass and biochars at different pyrolysis temperatures change soil redox processes. *Science of the Total Environment*, *625*, 147-154.

Azargohar, R., Nanda, S., Dalai, A.K., & Rao, A.K. (2013). Slow pyrolysis of deoiled canola meal: Product yields and characterization. *Energy and Fuels*, *27*, 5268-5279.

Bachmann, H.J., Bucheli, T.D., Dieguez-Alonso, A., Fabbri, D., Knicker, H., Schmidt, H.-P., … Zehetner, F. (2016). Toward the Standardization of Biochar Analysis: The COST Action TD1107 Interlaboratory Comparison. *Journal of Agricultural and Food Chemistry* 64, 513-527.

Bakshi, S., He, Z.L., & Harris, W.G. (2014). Biochar amendment affects leaching potential of copper and nutrient release behavior in contaminated sandy soils. *Journal of Environmental Quality*, *43*, 1894-1902.

Bamminger, C., Poll, C., Sixt, C., Hogy, P., Wust, D., Kandeler, E., & Marhan, S. (2016). Short-term response of soil microorganisms to biochar addition in a temperate agroecosystem under soil warming. *Agriculture, Ecosystems & Environment*, *233*, 308-317.

Bandara, T., Herath, I., Kumarathilaka, P., Hseu, Z.-Y., Ok, Y., & Vithanage, M. (2017). Efficacy of woody biomass and biochar for alleviating heavy metal bioavailability in serpentine soil. *Environmental Geochemistry and Health*, *39*, 391-401.

Bandara, T., Herath, I., Kumarathilaka, P., Seneviratne, M., Seneviratne, G., Rajakaruna, N., … Ok, Y. (2017). Role of woody biochar and fungal-bacterial co-inoculation on enzyme activity and metal immobilization in serpentine soil. *Journal of soils and sediments* 17, 665-673.

Banik, C., Lawrinenko, M., Bakshi, S., & Laird, D.A. (2018). Impact of Pyrolysis Temperature and Feedstock on Surface Charge and Functional Group Chemistry of Biochars. *Journal of Environmental Quality*, *47*, 452-461.

Bashir, S., Hussain, Q., Akmal, M., Riaz, M., Hu, H., Ijaz, S.S., Iqbal, M., … Ahmad, M. (2017). Sugarcane bagasse-derived biochar reduces the cadmium and chromium bioavailability to mash bean and enhances the microbial activity in contaminated soil. *Journal of soils and sediments*, *18*, 874-886.

Bashir, S., Hussain, Q., Shaaban, M., & Hu, H. (2018). Efficiency and surface characterization of different plant derived biochar for cadmium (Cd) mobility, bioaccessibility and bioavailability to Chinese cabbage in highly contaminated soil. *Chemosphere*, *211*, 632-639.

Beckers, F., Mothes, S., Abrigata, J., Zhao, J., Gao, Y., & Rinklebe, J. (2019). Mobilization of mercury species under dynamic laboratory redox conditions in a contaminated floodplain soil as affected by biochar and sugar beet factory lime. *Science of the Total Environment*, *672*, 604-617.

Beesley, L., Inneh, O.S., Norton, G.J., Moreno-Jimenez, E., Pardo, T., Clemente, R., & Dawson, J.J.C. (2014). Assessing the influence of compost and biochar amendments on the mobility and toxicity of metals and arsenic in a naturally contaminated mine soil. *Environmental pollution*, *186*, 195-202.

Beesley, L. & Marmiroli, M. (2011). The immobilisation and retention of soluble arsenic, cadmium and zinc by biochar. *Environmental pollution*, *159*, 474-480.

Beesley, L., Marmiroli, M., Pagano, L., Pigoni, V., Fellet, G., Fresno, T., … Marmiroli, N. (2013). Biochar addition to an arsenic contaminated soil increases arsenic concentrations in the pore water but reduces uptake to tomato plants (*Solanum lycopersicum* L.). *Science of the total environment*, *454-455*, 598-603.

Beiyuan, J., Awad, Y.M., Beckers, F., Tsang, D.C.W., Ok, Y.S., & Rinklebe, J. (2017). Mobility and phytoavailability of As and Pb in a contaminated soil using pine sawdust biochar under systematic change of redox conditions. *Chemosphere*, *178*, 110-118.

Bolan, N., Kunhikrishnan, A., Thangarajan, R., Kumpiene, J., Park, J., Makino, T., … Scheckel, K. (2014). Remediation of heavy metal(loid)s contaminated soils – To mobilize or to immobilize? *Journal of Hazardous Materials*, *266*, 141-166.

Bolan, N.S., Choppala, G., Kunhikrishnan, A., Park, J., & Naidu, R. (2013). Microbial Transformation of Trace Elements in Soils in Relation to Bioavailability and Remediation. In D. M. Whitacre (ed.) *Reviews of Environmental Contamination and Toxicology* (pp. 1-56). New York, NY: Springer New York.

Boostani, H.R., Najafi-Ghiri, M., Hardie, A.G., & Khalili, D. (2019). Comparison of Pb stabilization in a contaminated calcareous soil by application of vermicompost and sheep manure and their biochars produced at two temperatures. *Applied Geochemistry*, *102*, 121-128.

Bruun, E.W., Ambus, P., Egsgaard, H., & Hauggaard-Nielsen, H. (2012). Effects of slow and fast pyrolysis biochar on soil C and N turnover dynamics. *Soil Biology and Biochemistry*, *46*, 73-79.

Bussan, D.D., Sessums, R.F., & Cizdziel, J.V. (2016). Activated Carbon and Biochar Reduce Mercury Methylation Potentials in Aquatic Sediments. *Bulletin of environmental contamination and toxicology*, *96*, 536-539.

Calugaru, I.L., Neculita, C.M., Genty, T., & Zagury, G.J. (2019). Removal efficiency of As(V) and Sb(III) in contaminated neutral drainage by Fe-loaded biochar. *Environmental Science and Pollution Research*, *26*, 9322-9332.

Cao, X., Ma, L., Gao, B., & Harris, W. (2009). Dairy-Manure Derived Biochar Effectively Sorbs Lead and Atrazine. *Environmental Science & Technology*, *43*, 3285-3291.

Cao, X., Ma, L., Liang, Y., Gao, B., & Harris, W. (2011). Simultaneous immobilization of lead and atrazine in contaminated soils using dairy-manure biochar. *Environmental Science & Technology*, *45*, 4884-4889.

Cely, P., Tarquis, A.M., Paz-Ferreiro, J., Méndez, A., & Gascó, G. (2014). Factors driving the carbon mineralization priming effect in a sandy loam soil amended with different types of biochar. *Solid Earth*, *5*, 585-594.

Cha, J.S., Park, S.H., Jung, S.-C., Ryu, C., Jeon, J.-K., Shin, M.-C., & Park, Y.-K. (2016). Production and utilization of biochar: A review. *Journal of Industrial and Engineering Chemistry*, 40, 1-15.

Chang, J., Duan, Y., Dong, J., Shen, S., Si, G., He, F., Yang, Q., & Chen, J. (2019). Bioremediation of Hg-contaminated soil by combining a novel Hg-volatilizing Lecythophora sp. fungus, DC-F1, with biochar: Performance and the response of soil fungal community. *Science of the Total Environment*, *671*, 676-684.

Chen, B., Chen, Z., & Lv, S. (2011). A novel magnetic biochar efficiently sorbs organic pollutants and phosphate. *Bioresource Technology*, *102*, 716-723.

Chen, D., Guo, H., Li, R., Li, L., Pan, G., Chang, A., & Joseph, S. (2016). Low uptake affinity cultivars with biochar to tackle Cd-tainted rice — A field study over four rice seasons in Hunan, China. *Science of the Total Environment*, *541*, 1489-1498.

Chen, D., Liu, X., Bian, R., Cheng, K., Zhang, X., Zheng, J., … Li, L. (2018). Effects of biochar on availability and plant uptake of heavy metals – A meta-analysis. *Journal of Environmental Management*, *222*, 76-85.

Chen, G., Zhang, Z., Zhang, Z., & Zhang, R. (2017). Influence of Biochar Addition on the Denitrification Process and N_2O Emission in Cd-Contaminated Soil. *Water, Air, & Soil Pollution*, *228*, 47.

Chen, H., Yang, X., Gielen, G., Mandal, S., Xu, S., Guo, J., … Wang, H. (2019). Effect of biochars on the bioavailability of cadmium and di-(2-ethylhexyl) phthalate to Brassica chinensis L. in contaminated soils. *Science of The Total Environment 678,* 43-52.

Chen, H., Zhang, J., Tang, L., Su, M., Tian, D., Zhang, L., … Hu, S. (2019). Enhanced Pb immobilization via the combination of biochar and phosphate solubilizing bacteria. *Environment International*, *127*, 395-401.

Chen, L., Chen, X.L., Zhou, C.H., Yang, H.M., Ji, S.F., Tong, D.S., … Chu, M.Q. (2017). Environmental-friendly montmorillonite-biochar composites: Facile production and tunable adsorption-release of ammonium and phosphate. *Journal of Cleaner Production*, *156*, 648-659.

Chen, Z., Wang, Y., Xia, D., Jiang, X., Fu, D., Shen, L., … Li, Q.B. (2016). Enhanced bioreduction of iron and arsenic in sediment by biochar amendment influencing microbial community composition and dissolved organic matter content and composition. *Journal of Hazardous Materials*, *311*, 20-29.

Chen, Z., Zhang, J., Liu, M., Wu, Y., & Yuan, Z. (2018). Immobilization of metals in contaminated soil from E-waste recycling site by dairy-manure-derived biochar. *Environmental Technology*, *39*, 2801-2809.

Cheng, B.-H., Zeng, R.J., & Jiang, H. (2017). Recent developments of post-modification of biochar for electrochemical energy storage. *Bioresource Technology*, *246*, 224-233.

Cheng, C.-H., Lehmann, J., Thies, J.E., Burton, S.D., & Engelhard, M.H. (2006). Oxidation of black carbon by biotic and abiotic processes. *Organic Geochemistry*, *37*, 1477-1488.

Chibuike, G.U., & Obiora, S.C. (2014). Heavy Metal Polluted Soils: Effect on Plants and Bioremediation Methods. *Applied and Environmental Soil Science*, *2014*.

Choppala, G., Bolan, N., Kunhikrishnan, A., & Bush, R. (2016). Differential effect of biochar upon reduction-induced mobility and bioavailability of arsenate and chromate. *Chemosphere*, *144*, 374-381.

Choppala, G., Bolan, N., Kunhikrishnan, A., Skinner, W., & Seshadri, B. (2015). Concomitant reduction and immobilization of chromium in relation to its bioavailability in soils. *Environmental Science and Pollution Research*, *22*, 8969-8978.

Choppala, G.K., Bolan, N.S., Megharaj, M., Chen, Z., & Naidu, R. (2012). The influence of biochar and black carbon on reduction and bioavailability of chromate in soils. *Journal of Environmental Quality*, *41*, 1175-1184.

Cui, L., Noerpel, M.R., Scheckel, K.G., & Ippolito, J.A. (2019). Wheat straw biochar reduces environmental cadmium bioavailability. *Environment international*, *126*, 69-75.

Cui, L., Yan, J., Yang, Y., Ding, C., Chen, T., Fu, Q., … Chang, A. (2013). Influence of biochar on microbial activities of heavy metals contaminated paddy fields. *BioResources*, *8*, 5536-5548.

Cui, X., Dai, X., Khan, K.Y., Li, T., Yang, X., & He, Z. (2016). Removal of phosphate from aqueous solution using magnesium-alginate/chitosan modified biochar microspheres derived from Thalia dealbata. *Bioresource Technology*, *218*, 1123-1132.

Dai, Z., Barberán, A., Li, Y., Brookes, P.C., & Xu, J. (2017). Bacterial Community Composition Associated with Pyrogenic Organic Matter (Biochar) Varies with Pyrolysis Temperature and Colonization Environment. *mSphere*, *2*.

Dai, Z., Zhang, X., Tang, C., Muhammad, N., Wu, J., Brookes, P.C., & Xu, J. (2017). Potential role of biochars in decreasing soil acidification - A critical review. *Science of the Total Environment*, *581-582*, 601-611.

DeCiucies, S., Whitman, T., Woolf, D., Enders, A., & Lehmann, J. (2018). Priming mechanisms with additions of pyrogenic organic matter to soil. *Geochimica et Cosmochimica Acta*, *238*, 329-342.

Deng, J., Liu, Y., Liu, S., Zeng, G., Tan, X., Huang, B., … Yan, Z. (2017). Competitive adsorption of Pb(II), Cd(II) and Cu(II) onto chitosan-pyromellitic dianhydride modified biochar. *Journal of Colloid And Interface Science*, *506*, 355-364.

Diao, Z.-H., Du, J.-J., Jiang, D., Kong, L.-J., Huo, W.-Y., Liu, C.-M., … Xu, X.-R. (2018). Insights into the simultaneous removal of Cr^{6+} and Pb^{2+} by a novel sewage sludge-derived biochar immobilized nanoscale zero valent iron: Coexistence effect and mechanism. *Science of the Total Environment*, *642*, 505-515.

Ding, W., Zeng, X., Wang, Y., Du, Y., & Zhu, Q. (2011). Characteristics and performances of biofilm carrier prepared from agro-based biochar. *China Environmental Science*, *31*, 1451-1455.

Ding, Z., Hu, X., Wan, Y., Wang, S., & Gao, B. (2016). Removal of lead, copper, cadmium, zinc, and nickel from aqueous solutions by alkali-modified biochar: Batch and column tests. *Journal of Industrial and Engineering Chemistry*, *33*, 239-245.

Dixit, R., Wasiullah, Malaviya, D., Pandiyan, K., Singh, U., Sahu, A., … Paul, D. (2015). Bioremediation of Heavy Metals from Soil and Aquatic Environment: An Overview of Principles and Criteria of Fundamental Processes. *Sustainability*, *7*, 2189-2212.

Dong, D., Feng, Q., McGrouther, K., Yang, M., Wang, H., & Wu, W. (2015). Effects of biochar amendment on rice growth and nitrogen retention in a waterlogged paddy field. *Journal of soils and sediments*, *15*, 153-162.

Egene, C.E., Van Poucke, R., Ok, Y.S., Meers, E., & Tack, F.M.G. (2018). Impact of organic amendments (biochar, compost and peat) on Cd and Zn mobility and solubility in contaminated soil of the Campine region after three years. *Science of the Total Environment*, *626*, 195-202.

El-Naggar, A., Lee, S.S., Rinklebe, J., Farooq, M., Song, H., Sarmah, A.K., … Ok, Y.S. (2019). Biochar application to low fertility soils: A review of current status, and future prospects. *Geoderma*, *337*, 536-554.

El-Naggar, A., Shaheen, S.M., Hseu, Z.-Y., Wang, S.-L., Ok, Y.S., & Rinklebe, J. (2019). Release dynamics of As, Co, and Mo in a biochar treated soil under pre-definite redox conditions. *Science of the Total Environment*, *657*, 686-695.

El-Naggar, A., Shaheen, S.M., Ok, Y.S., & Rinklebe, J. (2018). Biochar affects the dissolved and colloidal concentrations of Cd, Cu, Ni, and Zn and their phytoavailability and potential mobility in a mining soil under dynamic redox-conditions. *Science of the Total Environment*, *624*, 1059-1071.

Fang, J., Zhan, L., Ok, Y.S., & Gao, B. (2018). Minireview of potential applications of hydrochar derived from hydrothermal carbonization of biomass. *Journal of Industrial and Engineering Chemistry*, *57*, 15-21.

Fang, S.En, Tsang, D.C.W., Zhou, F., Zhang, W., & Qiu, R. (2016). Stabilization of cationic and anionic metal species in contaminated soils using sludge-derived biochar. *Chemosphere*, *149*, 263-271.

Frankel, M.L., Bhuiyan, T.I., Veksha, A., Demeter, M.A., Layzell, D.B., Helleur, R.J., … Turner, R.J. (2016). Removal and biodegradation of naphthenic acids by biochar and attached environmental biofilms in the presence of co-contaminating metals. *Bioresource Technology*, *216*, 352-361.

Fungo, B., Thiongo, M., Neufeldt, H., Guerena, D., Lehmann, J., & Kalbi, B. (2014). N_2O and CH_4 emission from soil amended with steam-activated biochar. *Journal of Plant Nutrition and Soil Science*, *177*, 34-38.

Gadd, G.M., Rhee, Y.J., Stephenson, K., & Wei, Z. (2012). Geomycology: metals, actinides and biominerals. *Environmental Microbiology Reports*, *4*, 270-296.

Gan, C., Liu, Y., Tan, X., Wang, S., Zeng, G., Zheng, B., … Liu, W. (2015). Effect of porous zinc–biochar nanocomposites on Cr(VI) adsorption from aqueous solution. *RSC Advances, 5*, 35107-35115.

Gao, B., Han, L., Hao, H., & Zhou, H. (2016). Pollution characteristics of mercury (Hg) in surface sediments of major basins, China. *Ecological Indicators*, *67*, 577-585.

Gong, X., Huang, D., Liu, Y., Zeng, G., Chen, S., Wang, R., … Xue, W. (2019). Biochar facilitated the phytoremediation of cadmium contaminated sediments: Metal behavior, plant toxicity, and microbial activity. *Science of the Total Environment*, *666*, 1126-1133.

González-Chávez, M.D.C.A., Carrillo-González, R., Hernández Godínez, M.I., & Evangelista Lozano, S. (2017). *Jatropha curcas* and assisted phytoremediation of a mine tailing with biochar and a mycorrhizal fungus. *International Journal of Phytoremediation*, *19*, 174-182.

Gregory, S.J., Anderson, C.W.N., Camps Arbestain, M., & McManus, M.T. (2014). Response of plant and soil microbes to biochar amendment of an arsenic-contaminated soil. *Agriculture, ecosystems & environment*, *191*, 133-141.

Gurtler, J.B., Boateng, A.A., Han, Y., & Douds, D.D. (2014). Inactivation of *E. coli* O157:H7 in Cultivable Soil by Fast and Slow Pyrolysis-Generated Biochar. *Foodborne Pathogens and Disease*, *11*, 215-223.

Hafeez, F., Rizwan, M., Saqib, M., Yasmeen, T., Ali, S., Abbas, T., … Qayyum, M.F. (2019). Residual effect of biochar on growth, antioxidant defence and cadmium (Cd) accumulation in rice in a cd contaminated saline soil. *Pakistan Journal of Agricultural Sciences*, *56*, 197-204.

Hamer, U., Marschner, B., Brodowski, S., & Amelung, W. (2004). Interactive priming of black carbon and glucose mineralisation. *Organic Geochemistry*, *35*, 823-830.

Han, L., Sun, H., Ro, K.S., Sun, K., Libra, J.A., & Xing, B. (2017). Removal of antimony(III) and cadmium(II) from aqueous solution using animal manure-derived hydrochars and pyrochars. *Bioresource Technology*, *234*, 77-85.

Harms, H., Schlosser, D., & Wick, L.Y. (2011). Untapped potential: exploiting fungi in bioremediation of hazardous chemicals. *Nature Reviews Microbiology*, *9*, 177-192.

Hartley, W., Dickinson, N.M., Riby, P., & Lepp, N.W. (2009). Arsenic mobility in brownfield soils amended with green waste compost or biochar and planted with *Miscanthus*. *Environmental pollution*, *157*, 2654-2662.

He, L., Fan, S., Müller, K., Wang, H., Che, L., Xu, S., … Tsang, D.C. (2018). Comparative analysis biochar and compost-induced degradation of di-(2-ethylhexyl) phthalate in soils. *Science of the Total Environment*, *625*, 987-993.

He, L., Gielen, G., Bolan, N.S., Zhang, X., Qin, H., Huang, H., & Wang, H. (2015). Contamination and remediation of phthalic acid esters in agricultural soils in China: a review. *Agronomy for Sustainable Development*, *35*, 519-534.

Herath, I., Iqbal, M., Al-Wabel, M., Abduljabbar, A., Ahmad, M., Usman, A., …Vithanage, M. (2017). Bioenergy-derived waste biochar for reducing mobility, bioavailability, and phytotoxicity of chromium in anthropized tannery soil. *Journal of soils and sediments*, *17*, 731-740.

Hernandez-Soriano, M.C., Kerré, B., Kopittke, P.M., Horemans, B., & Smolders, E. (2016). Biochar affects carbon composition and stability in soil: a combined spectroscopy-microscopy study. *Scientific Reports*, *6*, 25127.

Houben, D., Evrard, L., & Sonnet, P. (2013). Mobility, bioavailability and pH-dependent leaching of cadmium, zinc and lead in a contaminated soil amended with biochar. *Chemosphere*, *92*, 1450-1457.

Houben, D., & Sonnet, P. (2015). Impact of biochar and root-induced changes on metal dynamics in the rhizosphere of *Agrostis capillaris* and *Lupinus albus*. *Chemosphere*,*139*, 644-651.

Hua, L., Zhang, H., Wei, T., Yang, C., & Guo, J. (2019). Effect of biochar on fraction and species of antimony in contaminated soil. *Journal of soils and sediments*, 1-14.

Huang, D., Liu, L., Zeng, G., Xu, P., Huang, C., Deng, L., … Wan, J. (2017). The effects of rice straw biochar on indigenous microbial community and enzymes activity in heavy metal-contaminated sediment. *Chemosphere*,*174*, 545-553.

Huang, S., Bao, J., Shan, M., Qin, H., Wang, H., Yu, X., … Xu, Q. (2018). Dynamic changes of polychlorinated biphenyls (PCBs) degradation and adsorption to biochar as affected by soil organic carbon content. *Chemosphere*, *211*, 120-127.

Huang, X., Liu, Y., Liu, S., Tan, X., Ding, Y., Zeng, G., … Zheng, B. (2015). Effective removal of Cr(VI) using β-cyclodextrinchitosan modified biochars with adsorption/reduction bifuctional roles. *RSC Advances*, *6*, 94-104.

Hussain, M., Farooq, M., Nawaz, A., Al-Sadi, A., Solaiman, Z., Alghamdi, S., … Siddique, K. (2017). Biochar for crop production: potential benefits and risks. *Journal of soils and sediments*,*17*, 685-716.

Hyväluoma, J., Hannula, M., Arstila, K., Wang, H., Kulju, S., & Rasa, K. (2018). Effects of pyrolysis temperature on the hydrologically relevant porosity of willow biochar. *Journal of Analytical and Applied Pyrolysis*,*134*, 446-453.

Ibrahim, M., Khan, S., Hao, X., & Li, G. (2016). Biochar effects on metal bioaccumulation and arsenic speciation in alfalfa (*Medicago sativa* L .) grown in contaminated soil. *International Journal of Environmental Science and Technology*,*13*, 2467-2474.

Ibrahim, M., Li, G., Khan, S., Chi, Q., & Xu, Y. (2017). Biochars mitigate greenhouse gas emissions and bioaccumulation of potentially toxic elements and arsenic speciation in *Phaseolus vulgaris* L. *Environmental Science and Pollution Research*, *24*, 19524-19534.

Igalavithana, A.D., Kim, K.-H., Jung, J.-M., Heo, H.-S., Kwon, E.E., Tack, F.M., … Ok, Y.S. (2019). Effect of biochars pyrolyzed in N_2 and CO_2, and feedstock on microbial community in metal(loid)s contaminated soils. *Environment international*, *126*, 791-801.

Igalavithana, A.D., Kwon, E.E., Vithanage, M., Rinklebe, J., Moon, D.H., Meers, E., … Ok, Y.S. (2019). Soil lead immobilization by biochars in short-term laboratory incubation studies. *Environment international*, *127*, 190-198.

Igalavithana, A.D., Lee, S.E., Lee, Y.H., Tsang, D.C.W., Rinklebe, J., Kwon, E.E., & Ok, Y.S. (2017). Heavy metal immobilization and microbial community abundance by vegetable waste and pine cone biochar of agricultural soils. *Chemosphere*, *174*, 593-603.

Igalavithana, A.D., Mandal, S., Niazi, N.K., Vithanage, M., Parikh, S.J., Mukome, F.N., … Ok, Y.S. (2017). Advances and future directions of biochar characterization methods and applications. *Critical Reviews in Environmental Science and Technology*, *47*, 2275-2330.

Igalavithana, A.D., Park, J., Ryu, C., Lee, Y.H., Hashimoto, Y., Huang, L., … Lee, S.S. (2017). Slow pyrolyzed biochars from crop residues for soil metal (loid) immobilization and microbial community abundance in contaminated agricultural soils. *Chemosphere*, *177*, 157-166.

Igalavithana, A.D., Yang, X., Zahra, H.R., Tack, F.M., Tsang, D.C., Kwon, E.E., & Ok, Y.S. (2018). Metal (loid) immobilization in soils with biochars pyrolyzed in N_2 and CO_2 environments. *Science of the Total Environment*, *630*, 1103-1114.

Intani, K., Latif, S., Islam, M. and Müller, J., 2019. Phytotoxicity of Corncob Biochar before and after Heat Treatment and Washing. *Sustainability*, *11*, 30.

Jia, Y., Zhang, Y., Fu, J., Yuan, L., Li, Z., Liu, C., … Wang, X. (2019). A novel magnetic biochar/MgFe-layered double hydroxides composite removing Pb^{2+} from aqueous solution: Isotherms, kinetics and thermodynamics. *Colloids and Surfaces A: Physicochemical and Engineering Aspects*, *567*, 278-287.

Jiang, J., Xu, R.-k., Jiang, T.-y., & Li, Z. (2012). Immobilization of Cu(II), Pb(II) and Cd(II) by the addition of rice straw derived biochar to a simulated polluted Ultisol. *Journal of Hazardous Materials*, *229-230*, 145-150.

Jiang, T.-Y., Jiang, J., Xu, R.-K., & Li, Z. (2012). Adsorption of Pb(II) on variable charge soils amended with rice-straw derived biochar. *Chemosphere*, *89*, 249-256.

Jiang, T.-Y., Xu, R.-K., Gu, T.-X., & Jiang, J. (2014). Effect of Crop-Straw Derived Biochars on Pb(II) Adsorption in Two Variable Charge Soils. *Journal of Integrative Agriculture*, *13*, 507-516.

Jiang, X., Denef, K., Stewart, C., & Cotrufo, M. (2016). Controls and dynamics of biochar decomposition and soil microbial abundance, composition, and carbon use efficiency during long-term biochar-amended soil incubations. *Biology and Fertility of Soils*, *52*, 1-14.

Jin, H., Hanif, M.U., Capareda, S., Chang, Z., Huang, H., & Ai, Y. (2016). Copper(II) removal potential from aqueous solution by pyrolysis biochar derived from anaerobically digested algae-dairy-manure and effect of KOH activation. *Journal of Environmental Chemical Engineering*, *4*, 365-372.

Jin, Y., O'Connor, D., Ok, Y.S., Tsang, D.C.W., Liu, A., & Hou, D. (2019). Assessment of sources of heavy metals in soil and dust at children's playgrounds in Beijing using GIS and multivariate statistical analysis. *Environment international*, *124*, 320-328.

Jindo, K., Mizumoto, H., Sawada, Y., Sanchez-Monedero, M.A., & Sonoki, T. (2014). Physical and chemical characterization of biochars derived from different agricultural residues. *Biogeosciences*, *11*, 6613-6621.

Jing, R., & Kjellerup, B.V. (2016). Biogeochemical cycling of metals impacting by microbial mobilization and immobilization. *Journal of Environmental Sciences*, *66*, 146-154.

Joseph, S., Camps-Arbestain, M., Lin, Y., Munroe, P., Chia, C., Hook, J., … Singh, B. (2010). An investigation into the reactions of biochar in soil. *Soil Research*, *48*, 501-515.

Kambo, H.S., & Dutta, A. (2015). A comparative review of biochar and hydrochar in terms of production, physico-chemical properties and applications. *Renewable and Sustainable Energy Reviews*, *45*, 359-378.

Kappler, A., Wuestner, M.L., Ruecker, A., Harter, J., Halama, M., & Behrens, S. (2014). Biochar as an electron shuttle between bacteria and Fe(III) minerals. *Environmental Science & Technology Letters*, *1*, 339-344.

Kim, H.-B., Kim, S.-H., Jeon, E.-K., Kim, D.-H., Tsang, D.C.W., Alessi, D.S., … Baek, K. (2018). Effect of dissolved organic carbon from sludge, Rice straw and spent coffee ground biochar on the mobility of arsenic in soil. *Science of the Total Environment*, *636*, 1241-1248.

Kookana, R.S., Sarmah, A.K., Van Zwieten, L., Krull, E., & Singh, B. (2011). Biochar application to soil: agronomic and environmental benefits and unintended consequences. *Advances in agronomy*, *112*, 103-143.

Kopittke, P.M., Wang, P., Lombi, E., & Donner, E. (2017). Synchrotron-based X-Ray Approaches for Examining Toxic Trace Metal(loid)s in Soil–Plant Systems. *Journal of Environmental Quality*, *46*, 1175-1189.

Kumarathilaka, P., Ahmad, M., Herath, I., Mahatantila, K., Athapattu, B.C.L., Rinklebe, J., … Vithanage, M. (2018). Influence of bioenergy waste biochar on proton- and ligand-promoted release of Pb and Cu in a shooting range soil. *Science of the Total Environment*, *625*, 547-554.

Kuppusamy, S., Thavamani, P., Megharaj, M., Venkateswarlu, K., & Naidu, R. (2016). Agronomic and remedial benefits and risks of applying biochar to soil: Current knowledge and future research directions. *Environment international*, *87*, 1-12.

Lehmann, J., Rillig, M.C., Thies, J., Masiello, C.A., Hockaday, W.C., & Crowley, D. (2011). Biochar effects on soil biota – A review. *Soil Biology and Biochemistry*, *43*, 1812-1836.

Li, B., Yang, L., Wang, C.-q., Zhang, Q.-p., Liu, Q.-c., Li, Y.-d., & Xiao, R. (2017). Adsorption of Cd(II) from aqueous solutions by rape straw biochar derived from different modification processes. *Chemosphere*,*175*, 332-340.

Li, G., Khan, S., Ibrahim, M., Sun, T.-R., Tang, J.-F., Cotner, J.B., & Xu, Y.-Y. (2018). Biochars induced modification of dissolved organic matter (DOM) in soil and its impact on mobility and bioaccumulation of arsenic and cadmium. *Journal of Hazardous Materials*, *348*, 100-108.

Li, H., Dong, X., Da Silva, E.B., de Oliveira, L.M., Chen, Y., & Ma, L.Q. (2017). Mechanisms of metal sorption by biochars: Biochar characteristics and modifications. *Chemosphere*, *178*, 466-478.

Li, H., Ye, X., Geng, Z., Zhou, H., Guo, X., Zhang, Y., … Wang, G. (2016). The influence of biochar type on long-term stabilization for Cd and Cu in contaminated paddy soils. *Journal of Hazardous Materials*, *304*, 40-48.

Li, J., Dai, J., Liu, G., Zhang, H., Gao, Z., Fu, J., … Huang, Y. (2016). Biochar from microwave pyrolysis of biomass: A review. *Biomass and Bioenergy*, *94*, 228-244.

Li, J., Wang, S.-L., Zheng, L., Chen, D., Wu, Z., Xie, Y., … Wang, H. (2019). Sorption of lead in soil amended with coconut fiber biochar: Geochemical and spectroscopic investigations. *Geoderma 350*, 52-60.

Li, J., Zheng, L., Wang, S.-L., Wu, Z., Wu, W., Niazi, N.K.,… Wang, H. 2019. Sorption mechanisms of lead on silicon-rich biochar in aqueous solution: Spectroscopic investigation. *Science of The Total Environment*, *672*, 572-582.

Li, L.Y., Gong, X. and Abida, O., 2019. Waste-to-resources: Exploratory surface modification of sludge-based activated carbon by nitric acid for heavy metal adsorption. *Waste Management*, *87*, pp.375-386.

Li, R., Deng, H., Zhang, X., Wang, J.J., Awasthi, M.K., Wang, Q., … Zhang, Z. (2019). High-efficiency removal of Pb(II) and humate by a CeO_2–MoS_2 hybrid magnetic biochar. *Bioresource Technology*, *273*, 335-340.

Li, Y., Shen, F., Guo, H., Wang, Z., Yang, G., Wang, L., … Deng, S. (2015). Phytotoxicity assessment on corn stover biochar, derived from fast pyrolysis, based on seed germination, early growth, and potential plant cell damage. *Environmental Science and Pollution Research*, *22*, 9534-9543.

Li, Z., Song, Z., Singh, B.P., & Wang, H. (2018). The impact of crop residue biochars on silicon and nutrient cycles in croplands. *Science of the Total Environment*, *659*, 673-680.

Lin, L., Gao, M., Qiu, W., Wang, D., Huang, Q., & Song, Z. (2017). Reduced arsenic accumulation in indica rice (*Oryza sativa* L.) cultivar with ferromanganese oxide impregnated biochar composites amendments. *Environmental Pollution*, *231*, 479-486.

Lin, Q., Xu, X., Chen, Q., Fang, J., Shen, X., & Zhang, L. (2017). Changes in structural characteristics and metal speciation for biochar exposure in typic udic ferrisols. *Environmental Science and Pollution Research*, *25*, 153-162.

Lin, Q., Xu, X., Wang, L., Chen, Q., Fang, J., Shen, X., … Tian, G. (2017). The speciation, leachability and bioaccessibility of Cu and Zn in animal manure-derived biochar: effect of feedstock and pyrolysis temperature. *Fronties of Environmental Science & Engineering*, *11*, 1-12.

Liu, H., Xu, F., Xie, Y., Wang, C., Zhang, A., Li, L., & Xu, H. (2018). Effect of modified coconut shell biochar on availability of heavy metals and biochemical characteristics of soil in multiple heavy metals contaminated soil. *Science of the Total Environment*, *645*, 702-709.

Liu, P., Ptacek, C.J., Blowes, D.W., & Finfrock, Y.Z. (2019). Mercury distribution and speciation in biochar particles reacted with contaminated sediment up to 1030 days: A synchrotron-based study. *Science of the Total Environment*, *662*, 915-922.

Liu, P., Ptacek, C.J., Blowes, D.W., Finfrock, Y.Z., & Gordon, R.A. (2016). Stabilization of mercury in sediment by using biochars under reducing conditions. *Journal of Hazardous Materials*, *325*, 120-128.

Liu, P., Ptacek, C.J., Blowes, D.W., & Gould, W.D. (2018). Control of mercury and methylmercury in contaminated sediments using biochars: A long-term microcosm study. *Applied Geochemistry*, *92*, 30-44.

Liu, Q., Wu, L., Gorring, M., & Deng, Y. (2019). Aluminum-Impregnated Biochar for Adsorption of Arsenic(V) in Urban Stormwater Runoff. *Journal of Environmental Engineering*, *145*, 04019008.

Liu, S.-j., Liu, Y.-g., Tan, X.-f., Zeng, G.-m., Zhou, Y.-h., Liu, S.-b., … Wen, J. (2018). The effect of several activated biochars on Cd immobilization and microbial community composition during in-situ remediation of heavy metal contaminated sediment. *Chemosphere*, *208*, 655-664.

Liu, W., Wang, S., Lin, P., Sun, H., Hou, J., Zuo, Q., & Huo, R. (2016). Response of $CaCl_2$-extractable heavy metals, polychlorinated biphenyls, and microbial communities to biochar amendment in naturally contaminated soils. *Journal of soils and sediments*, *16*, 476-485.

Lomaglio, T., Hattab-Hambli, N., Bret, A., Miard, F., Trupiano, D., Scippa, G.S., … Morabito, D. (2017). Effect of biochar amendments on the mobility and (bio) availability of As, Sb and Pb in a contaminated mine technosol. *Journal of Geochemical Exploration*, *182*, 138-148.

Lombi, E., & Susini, J. (2009). Synchrotron-based techniques for plant and soil science: opportunities, challenges and future perspectives. *Plant and Soil*, *320*, 1-35.

Lu, H., Li, Z., Fu, S., Méndez, A., Gascó, G., & Paz-Ferreiro, J. (2015). Combining phytoextraction and biochar addition improves soil biochemical properties in a soil contaminated with Cd. *Chemosphere*, *119*, 209-216.

Lu, K., Yang, X., Gielen, G., Bolan, N., Ok, Y.S., Niazi, N.K., … Wang, H. (2017). Effect of bamboo and rice straw biochars on the mobility and redistribution of heavy metals (Cd, Cu, Pb and Zn) in contaminated soil. *Journal of Environmental Management*, *186*, 285-292.

Lu, K., Yang, X., Shen, J., Robinson, B., Huang, H., Liu, D., … Wang, H. (2014). Effect of bamboo and rice straw biochars on the bioavailability of Cd, Cu, Pb and Zn to *Sedum plumbizincicola*. *Agriculture, ecosystems & environment*, *191*, 124-132.

Luo, Y., Durenkamp, M., De Nobili, M., Lin, Q., & Brookes, P.C. (2011). Short term soil priming effects and the mineralisation of biochar following its incorporation to soils of different pH. *Soil Biology and Biochemistry*, *43*, 2304-2314.

Luo, Y., Lin, Q., Durenkamp, M., & Kuzyakov, Y. (2017). Does repeated biochar incorporation induce further soil priming effect? *Journal of soils and sediments*, *18*, 128-135.

Mandal, S., Sarkar, B., Bolan, N., Novak, J., Ok, Y.S., Van Zwieten, L., … Spokas, K. (2016). Designing advanced biochar products for maximizing greenhouse gas mitigation potential. *Critical Reviews in Environmental Science and Technology*, *46*, 1367-1401.

Mandal, S., Sarkar, B., Bolan, N., Ok, Y.S., & Naidu, R. (2017). Enhancement of chromate reduction in soils by surface modified biochar. *Journal of Environmental Management*, *186*, 277-284.

Mao, X., Kang, Q., Liu, Y., Siyal, A.A., Ao, W., Ran, C., … Dai, J. (2019). Microwave-assisted pyrolysis of furfural residue in a continuously operated auger reactor: Biochar characterization and analysis. *Energy*, *168*, 573-584.

Melo, T.M., Bottlinger, M., Schulz, E., Leandro, W.M., Botelho de Oliveira, S., Menezes de Aguiar Filho, A., … Rinklebe, J. (2019). Management of biosolids-derived hydrochar (Sewchar): Effect on plant germination, and farmers' acceptance. *Journal of Environmental Management*, *237*, 200-214.

Meng, F., Yuan, G., Wei, J., Bi, D., Ok, Y.S., & Wang, H. (2017). Humic substances as a washing agent for Cd-contaminated soils. *Chemosphere*, *181*, 461-467.

Meng, J., Tao, M., Wang, L., Liu, X., & Xu, J. (2018). Changes in heavy metal bioavailability and speciation from a Pb-Zn mining soil amended with biochars from co-pyrolysis of rice straw and swine manure. *Science of the Total Environment*, 633, 300-307.

Mian, M. M., Liu, G., Yousaf, B., Fu, B., Ullah, H., Ali, M, U., … Ruijia, L. (2018). 'Simultaneous functionalization and magnetization of biochar via NH_3 ambiance pyrolysis for efficient removal of Cr (VI)', *Chemosphere*, *208*, 712-21.

Mohamed, I., Zhang, G.-s., Li, Z.-g., Liu, Y., Chen, F., & Dai, K. (2015). Ecological restoration of an acidic Cd contaminated soil using bamboo biochar application. *Ecological Engineering*, *84*, 67-76.

Moon, D.H., Park, J.-W., Chang, Y.-Y., Ok, Y.S., Lee, S.S., Ahmad, M., … Baek, K. (2013). Immobilization of lead in contaminated firing range soil using biochar. *Environmental Science and Pollution Research*, *20*, 8464-8471.

Moore, F., González, M.-E., Khan, N., Curaqueo, G., Sanchez-Monedero, M., Rilling, J., … Meier, S. (2018). Copper immobilization by biochar and microbial community abundance in metal-contaminated soils. *Science of the Total Environment*, *616-617*, 960-969.

Mueller, C.W., Weber, P.K., Kilburn, M.R., Hoeschen, C., Kleber, M., & Pett-Ridge, J. (2013). Advances in the analysis of biogeochemical interfaces: NanoSIMS to investigate soil microenvironments. *Advances in agronomy*, *121*, 1-46.

Nagodavithane, C.L., Singh, B., & Fang, Y. (2014). Effect of ageing on surface charge characteristics and adsorption behaviour of cadmium and arsenate in two contrasting soils amended with biochar. *Soil Research*, *52*, 155-163.

Newsome, L., Lopez Adams, R., Downie, H.F., Moore, K.L., & Lloyd, J.R. (2018). NanoSIMS imaging of extracellular electron transport processes during microbial iron(III) reduction. *FEMS Microbiology Ecology*, *94*, fiy104.

Nie, C., Yang, X., Niazi, N.K., Xu, X., Wen, Y., Rinklebe, J., … Wang, H. (2018). Impact of sugarcane bagasse-derived biochar on heavy metal availability and microbial activity: A field study. *Chemosphere*, *200*, 274-282.

Norini, M.-P., Thouin, H., Miard, F., Battaglia-Brunet, F., Gautret, P., Guégan, R., … Motelica-Heino, M. (2019). Mobility of Pb, Zn, Ba, As and Cd toward soil pore water and plants (willow and ryegrass) from a mine soil amended with biochar. *Journal of Environmental Management*, *232*, 117-130.

O'Connor, D., Peng, T., Li, G., Wang, S., Duan, L., Mulder, J., … Hou, D. (2018). Sulfur-modified rice husk biochar: A green method for the remediation of mercury contaminated soil. *Science of the Total Environment*, *621*, 819-826.

Oh, S.-Y., & Yoon, H.-S. (2016). Biochar Amendment for Reducing Leachability of Nitro Explosives and Metals from Contaminated Soils and Mine Tailings. *Journal of Environmental Quality*, *45*, 993-1002.

Ok, Y.S., Oh, S.-E., Ahmad, M., Hyun, S., Kim, K.-R., Moon, D.H., … Yang, J.E. (2010). Effects of natural and calcined oyster shells on Cd and Pb immobilization in contaminated soils. *Environmental Earth Sciences*, *61*, 1301-1308.

Padhye, Lokesh P. (2017). Influence of surface chemistry of carbon materials on their interactions with inorganic nitrogen contaminants in soil and water. *Chemosphere 184*, 532-547.

Palansooriya, K. N., Wong, J. T. F., Hashimoto, Y., Huang, L., Rinklebe, J., Chang, S. X., . . . Ok, Y. S. (2019). Response of microbial communities to biochar-amended soils: a critical review. *Biochar, 1*, 3-22.

Pal, D., & Maiti, S.K. (2019). Abatement of cadmium (Cd) contamination in sediment using tea waste biochar through meso-microcosm study. *Journal of Cleaner Production*, *212*, 986-996.

Park, J.H., Choppala, G.K., Bolan, N.S., Chung, J.W., & Chuasavathi, T. (2011). Biochar reduces the bioavailability and phytotoxicity of heavy metals. *Plant and soil*, *348*, 439-451.

Pellera, F.-M., & Gidarakos, E. (2015). Effect of dried olive pomace – derived biochar on the mobility of cadmium and nickel in soil. *Journal of Environmental Chemical Engineering*, *3*, 1163-1176.

Penen, F., Malherbe, J., Isaure, M.-P., Dobritzsch, D., Bertalan, I., Gontier, E., … Schaumlöffel, D. (2016). Chemical bioimaging for the subcellular localization of trace elements by high contrast TEM, TEM/X-EDS, and NanoSIMS. *Journal of Trace Elements in Medicine and Biology*, *37*, 62-68.

Peng, X., Deng, Y., Peng, Y., & Yue, K. (2018). Effects of biochar addition on toxic element concentrations in plants: A meta-analysis. *Science of the Total Environment*, *616*, 970-977.

Purakayastha, T.J., Kumari, S., & Pathak, H. (2015). Characterisation, stability, and microbial effects of four biochars produced from crop residues. *Geoderma*, *239*, 293-303.

Qi, F., Dong, Z., Lamb, D., Naidu, R., Bolan, N.S., Ok, Y.S., … Semple, K.T. (2017). Effects of acidic and neutral biochars on properties and cadmium retention of soils. *Chemosphere*, *180*, 564-573.

Qi, F., Kuppusamy, S., Naidu, R., Bolan, N.S., Ok, Y.S., Lamb, D., … Wang, H. (2017). Pyrogenic carbon and its role in contaminant immobilization in soils. *Critical Reviews in Environmental Science and Technology*, *47*, 795-876.

Qi, F., Lamb, D., Naidu, R., Bolan, N.S., Yan, Y., Ok, Y.S., … Choppala, G. (2018). Cadmium solubility and bioavailability in soils amended with acidic and neutral biochar. *Science of the Total Environment*, *610-611*, 1457-1466.

Qian, T.-T., Wu, P., Qin, Q.-Y., Huang, Y.-N., Wang, Y.-J., & Zhou, D.-M. (2019). Screening of wheat straw biochars for the remediation of soils polluted with Zn(II) and Cd(II). *Journal of Hazardous Materials*, *362*, 311-317.

Qiao, J.-t., Li, X.-m., & Li, F.-b. (2018). Roles of different active metal-reducing bacteria in arsenic release from arsenic-contaminated paddy soil amended with biochar. *Journal of Hazardous Materials*, *344*, 958-967.

Qiao, Y., Crowley, D., Wang, K., Zhang, H., & Li, H. (2015). Effects of biochar and *Arbuscular mycorrhizae* on bioavailability of potentially toxic elements in an aged contaminated soil. *Environmental pollution*, *206*, 636-643.

Qiao, Y., Wu, J., Xu, Y., Fang, Z., Zheng, L., Cheng, W., … Zhao, D. (2017). Remediation of cadmium in soil by biochar-supported iron phosphate nanoparticles. *Ecological Engineering*, *106*, 515-522.

Qiu, G., Feng, X., Wang, S., & Shang, L. (2006). Environmental contamination of mercury from Hg-mining areas in Wuchuan, northeastern Guizhou, China. *Environmental Pollution*, *142*, 549-558.

Que, W., Zhou, Y.-h., Liu, Y.-g., Wen, J., Tan, X.-f., Liu, S.-j., & Jiang, L.-h. (2018). Appraising the effect of in-situ remediation of heavy metal contaminated sediment by biochar and activated carbon on Cu immobilization and microbial community. *Ecological Engineering*, *127*, 519-526.

Quilliam, R.S., Rangecroft, S., Emmett, B.A., Deluca, T.H., & Jones, D.L. (2013). Is biochar a source or sink for polycyclic aromatic hydrocarbon (PAH) compounds in agricultural soils? *Gcb Bioenergy*, *5*, 96-103.

Rajapaksha, A., Ahmad, M., Vithanage, M., Kim, K.-R., Chang, J., Lee, S., & Ok, Y. (2015). The role of biochar, natural iron oxides, and nanomaterials as soil amendments for immobilizing metals in shooting range soil. *Environmental Geochemistry and Health*, *37*, 931-942.

Rajapaksha, A.U., Chen, S.S., Tsang, D.C.W., Zhang, M., Vithanage, M., Mandal, S., … Ok, Y.S. (2016). Engineered/designer biochar for contaminant removal/immobilization from soil and water: Potential and implication of biochar modification. *Chemosphere*, *148*, 276-291.

Rajapaksha, A.U., Vithanage, M., Oze, C., Bandara, W.M.A.T., & Weerasooriya, R. (2012). Nickel and manganese release in serpentine soil from the Ussangoda Ultramafic Complex, Sri Lanka. *Geoderma*, *189-190*, 1-9.

Rangabhashiyam, S., & Balasubramanian, P. (2019). The potential of lignocellulosic biomass precursors for biochar production: Performance, mechanism and wastewater application-A review. *Industrial Crops and Products*, *128*, 405-423.

Rao, D.V., Gigante, G.E., Cesareo, R., Brunetti, A., Schiavon, N., Akatsuka, T., … Takeda, T. (2017). Synchrotron-based XRD from rat bone of different age groups. *Materials Science and Engineering: C*, *74*, 207-218.

Rawal, A., Joseph, S.D., Hook, J.M., Chia, C.H., Munroe, P.R., Donne, S., … Webber, J.B.W. (2016). Mineral–Biochar Composites: Molecular Structure and Porosity. *Environmental Science & Technology*, *50*, 7706-7714.

Rechberger, M.V., Kloss, S., Wang, S.-L., Lehmann, J., Rennhofer, H., Ottner, F., … Soja, G. (2019). Enhanced Cu and Cd sorption after soil aging of woodchip-derived biochar: What were the driving factors? *Chemosphere*, *216*, 463-471.

Rees, F., Watteau, F., Mathieu, S., Turpault, M.-P., Le Brech, Y., Qiu, R., & Morel, J.L. (2017). Metal Immobilization on Wood-Derived Biochars: Distribution and Reactivity of Carbonate Phases. *Journal of Environmental Quality*, *46*, 845-854.

Rinklebe, J., Antoniadis, V., Shaheen, S.M., Rosche, O., & Altermann, M. (2019). Health risk assessment of potentially toxic elements in soils along the Central Elbe River, Germany. *Environment international*, *126*, 76-88.

Rittl, T.F., Hoffland, E.H., Kuyper, F.C., Novotny, E., Balieiro, B.J.R., & Alves, T.W. (2015). Negative priming of native soil organic carbon mineralization by oilseed biochars of contrasting quality. *European Journal of Soil Science*, *66*, 714-721.

Ruan, X., Sun, Y., Du, W., Tang, Y., Liu, Q., Zhang, Z., … Tsang, D.C. (2019). Formation, Characteristics, and Applications of Environmentally Persistent Free Radicals in Biochars: A Review. *Bioresource Technology*, *281*, 457-468.

Šafařík, I., Maděrová, Z., Pospíšková, K., Schmidt, H.P., Baldíková, E., Filip, J., … Šafaříková, M. (2016). Magnetically modified biochar for organic xenobiotics removal. *Water Science and Technology*, *74*, 1706-1715.

Sajjadi, B., Broome, J.W., Chen, W.Y., Mattern, D.L., Egiebor, N.O., Hammer, N., & Smith, C.L. (2019). Urea functionalization of ultrasound-treated biochar: A feasible strategy for enhancing heavy metal adsorption capacity. *Ultrasonics Sonochemistry*, *51*, 20-30.

Salam, A., Shaheen, S.M., Bashir, S., Khan, I., Wang, J., Rinklebe, J., … Hu, H. (2019). Rice straw- and rapeseed residue-derived biochars affect the geochemical fractions and phytoavailability of Cu and Pb to maize in a contaminated soil under different moisture content. *Journal of Environmental Management*, *237*, 5-14.

Sanchez-Hernandez, J.C., Ríos, J.M., Attademo, A.M., Malcevschi, A., & Andrade Cares, X. (2019). Assessing biochar impact on earthworms: Implications for soil quality promotion. *Journal of Hazardous Materials*, *366*, 582-591.

Saquing, J.M., Yu, Y.-H., & Chiu, P.C. (2016). Wood-derived black carbon (biochar) as a microbial electron donor and acceptor. *Environmental Science & Technology Letters*, *3*, 62-66.

Seneviratne, M., Gunaratne, S., Bandara, T., Weerasundara, L., Rajakaruna, N., Seneviratne, G., & Vithanage, M. (2016). Plant growth promotion by Bradyrhizobium japonicum under heavy metal stress. *South African Journal of Botany*, *105*, 19-24.

Seneviratne, M., Vithanage, M., Madawala, H.M.S.P., & Seneviratne, G. (2015). A Novel Microbial Biofilm for Bioremoval of Nickel from Aqueous Media. *Bioremediation Journal*, *19*, 239-248.

Shaheen, S.M., El-Naggar, A., Wang, J., Hassan, N.E.E., Niazi, N.K., Wang, H., … Rinklebe, J. (2019). Chapter 14 - Biochar as an (Im)mobilizing Agent for the Potentially Toxic Elements in Contaminated Soils In Y. S. Ok, D. C. W. Tsang, N. Bolan and J. M. Novak (eds.) *Biochar from Biomass and Waste*, 255-274: Elsevier

Shaheen, S.M., Niazi, N.K., Hassan, N.E., Bibi, I., Wang, H., Tsang, D.C., … Rinklebe, J. (2019). Wood-based biochar for the removal of potentially toxic elements in water and wastewater: a critical review. *International Materials Reviews*, *64*, 216-247.

Shang, M.-R., Liu, Y.-G., Liu, S.-B., Zeng, G.-M., Tan, X.-F., Jiang, L.-H., …Wang, S.-F. (2016). A novel graphene oxide coated biochar composite: synthesis, characterization and application for Cr(VI) removal. *RSC Advances, 6*, 85202-85212.

Shen, Z., McMillan, O., Jin, F., & Al-Tabbaa, A. (2016). Salisbury biochar did not affect the mobility or speciation of lead in kaolin in a short-term laboratory study. *Journal of Hazardous Materials*, *316*, 214-220.

Shen, Z., Zhang, Y., Jin, F., McMillan, O., & Al-Tabbaa, A. (2017). Qualitative and quantitative characterisation of adsorption mechanisms of lead on four biochars. *Science of the Total Environment*, *609*, 1401-1410.

Shu, R., Wang, Y., & Zhong, H. (2016). Biochar amendment reduced methylmercury accumulation in rice plants. *Journal of Hazardous Materials*, *313*, 1-8.

Shu, T., Lu, P., & He, N. (2013). Mercury adsorption of modified mulberry twig chars in a simulated flue gas. *Bioresource Technology*, *136*, 182-187.

Sikarwar, V.S., Zhao, M., Clough, P., Yao, J., Zhong, X., Memon, M.Z., … Fennell, P.S. (2016). An overview of advances in biomass gasification. *Energy & Environmental Science*, *9*, 2939-2977.

Sizmur, T., Fresno, T., Akgül, G., Frost, H., & Moreno-Jiménez, E. (2017). Biochar modification to enhance sorption of inorganics from water. *Bioresource Technology*, *246*, 34-47.

Song, C., Shan, S., Müller, K., Wu, S., Niazi, N.K., Xu, S., … Wang, H. (2018). Characterization of pig manure-derived hydrochars for their potential application as fertilizer. *Environmental Science and Pollution Research*, *25*, 25772-25779.

Song, Z., Lian, F., Yu, Z., Zhu, L., Xing, B., & Qiu, W. (2014). Synthesis and characterization of a novel MnOx-loaded biochar and its adsorption properties for Cu^{2+} in aqueous solution. *Chemical Engineering Journal*, *242*, 36-42.

Strawn, D.G., Rigby, A.C., Baker, L.L., Coleman, M.D., & Koch, I. (2016). Biochar Soil Amendment Effects on Arsenic Availability to Mountain Brome (*Bromus marginatus*). *Journal of Environmental Quality*, *44*, 1315-1320.

Su, P., Lou, J., Brookes, P., Luo, Y., He, Y., & Xu, J. (2017). Taxon-specific responses of soil microbial communities to different soil priming effects induced by addition of plant residues and their biochars. *Journal of soils and sediments*, *17,* 674-684.

Suksabye, P., Pimthong, A., Dhurakit, P., Mekvichitsaeng, P., & Thiravetyan, P. (2016). Effect of biochars and microorganisms on cadmium accumulation in rice grains grown in Cd-contaminated soil. *Environmental Science and Pollution Research*, *23*, 962-973.

Suman, S., & Gautam, S. (2017). Effect of pyrolysis time and temperature on the characterization of biochars derived from biomass. *Energy Sources, Part A: Recovery, Utilization and Environmental Effects*, *39*, 933-940.

Sun, C., Chen, T., Huang, Q., Wang, J., Lu, S., & Yan, J. (2019). Enhanced adsorption for Pb(II) and Cd(II) of magnetic rice husk biochar by $KMnO_4$ modification. *Environmental Science and Pollution Research*, *26*, 8902-8913.

Sun, D., Meng, J., Liang, H., Yang, E., Huang, Y., Chen, W., … Gao, J. (2015). Effect of volatile organic compounds absorbed to fresh biochar on survival of *Bacillus mucilaginosus* and structure of soil microbial communities. *Journal of soils and sediments*, *15*, 271-281.

Sun, J., He, F., Zhang, Z., Shao, H., & Xu, G. (2016). Temperature and moisture responses to carbon mineralization in the biochar-amended saline soil. *Science of the Total Environment*, *569*, 390-394.

Sun, J., Lian, F., Liu, Z., Zhu, L., & Song, Z. (2014). Biochars derived from various crop straws: Characterization and Cd(II) removal potential. *Ecotoxicology and Environmental Safety*, *106*, 226-231.

Tack, F.M.G., Rinklebe, J., & Ok, Y.S. (2019). Interactions between biochar and trace elements in the environment. *Science of the Total Environment*, *649*, 792.

Tan, G., Sun, W., Xu, Y., Wang, H., & Xu, N. (2016). Sorption of mercury (II) and atrazine by biochar, modified biochars and biochar based activated carbon in aqueous solution. *Bioresource Technology*, *211*, 727-735.

Tan, Z., Wang, Y., Zhang, L., & Huang, Q. (2017). Study of the mechanism of remediation of Cd-contaminated soil by novel biochars. *Environmental science and pollution research*, *24*, 24844-24855.

Tang, C., Weligama, C., & Sale, P. (2013). Subsurface Soil Acidification in Farming Systems: Its Possible Causes and Management Options In J. Xu and D. L. Sparks (eds.) *Molecular Environmental Soil Science* (pp. 389-412). Dordrecht: Springer Netherlands.

Thangarajan, R., Bolan, N.S., Kunhikrishnan, A., Wijesekara, H., Xu, Y., Tsang, D.C., … Hou, D. (2018). The potential value of biochar in the mitigation of gaseous emission of nitrogen. *Science of the Total Environment*, *612*, 257-268.

Thangarajan, R., Chowdhury, S., Kunhikrishnan, A., & Bolan, N. (2014). Interactions of soluble and solid organic amendments with priming effects induced by glucose. *Vadose Zone Journal*, *13*.

Trakal, L., Veselská, V., Šafařík, I., Vítková, M., Číhalová, S., & Komárek, M. (2016). Lead and cadmium sorption mechanisms on magnetically modified biochars. *Bioresource Technology*, *203*, 318-324.

Tripathi, M., Sahu, J.N., & Ganesan, P. (2016). Effect of process parameters on production of biochar from biomass waste through pyrolysis: A review. *Renewable and Sustainable Energy Reviews*, *55*, 467-481.

Tsai, W.-T., Liu, S.-C., Chen, H.-R., Chang, Y.-M., & Tsai, Y.-L. (2012). Textural and chemical properties of swine-manure-derived biochar pertinent to its potential use as a soil amendment. *Chemosphere*, *89*, 198-203.

Uchimiya, M., & Bannon, D.I. (2013). Solubility of lead and copper in biochar-amended small arms range soils: influence of soil organic carbon and pH. *Journal of Agricultural and Food Chemistry*, *61*, 7679-7688.

Uchimiya, M., Bannon, D.I., & Wartelle, L.H. (2012). Retention of heavy metals by carboxyl functional groups of biochars in small arms range soil. *Journal of Agricultural and Food Chemistry*, *60*, 1798-1809.

Uchimiya, M., Bannon, D.I., Wartelle, L.H., Lima, I.M., & Klasson, K.T. (2012). Lead retention by broiler litter biochars in small arms range soil: impact of pyrolysis temperature. *Journal of Agricultural and Food Chemistry*, *60*, 5035-5044.

Van Poucke, R., Ainsworth, J., Maeseele, M., Ok, Y.S., Meers, E., & Tack, F.M.G. (2018). Chemical stabilization of Cd-contaminated soil using biochar. *Applied Geochemistry*, *88,* 122-130.

Vithanage, M., Bandara, T., Al-Wabel, M.I., Abduljabbar, A., Usman, A.R.A., Ahmad, M., & Ok, Y.S. (2018). Soil Enzyme Activities in Waste Biochar Amended Multi-Metal Contaminated Soil; Effect of Different Pyrolysis Temperatures and Application Rates. *Communications in Soil Science and Plant Analysis*, *49*, 635-643.

Vithanage, M., Herath, I., Almaroai, Y.A., Rajapaksha, A.U., Huang, L., Sung, J.-K., … Ok, Y.S. (2017). Effects of carbon nanotube and biochar on bioavailability of Pb, Cu and Sb in multi-metal contaminated soil. *Environmental Geochemistry and Health*, *39*, 1409-1420.

Vithanage, M., Herath, I., Joseph, S., Bundschuh, J., Bolan, N., Ok, Y.S., … Rinklebe, J. (2017). Interaction of arsenic with biochar in soil and water: a critical review. *Carbon*, *113*, 219-230.

Wagner, A., Kaupenjohann, M., Hu, Y., Kruse, J., & Leinweber, P. (2015). Biochar-induced formation of Zn-P-phases in former sewage field soils studied by P K-edge XANES spectroscopy. *Journal of Plant Nutrition and Soil Science*, *178*, 582-585.

Wahi, R., Zuhaidi, N.F.Q.a., Yusof, Y., Jamel, J., Kanakaraju, D., & Ngaini, Z. (2017). Chemically treated microwave-derived biochar: An overview. *Biomass and Bioenergy*, *107*, 411-421.

Wang, A.O., Ptacek, C.J., Blowes, D.W., Gibson, B.D., Landis, R.C., Dyer, J.A., & Ma, J. (2019). Application of hardwood biochar as a reactive capping mat to stabilize mercury derived from contaminated floodplain soil and riverbank sediments. *Science of the Total Environment*, *652*, 549-561.

Wang, C., Alidoust, D., Yang, X., & Isoda, A. (2018). Effects of bamboo biochar on soybean root nodulation in multi-elements contaminated soils. *Ecotoxicology and Environmental Safety*, *150*, 62-69.

Wang, H.-Y., Chen, P., Zhu, Y.-G., Cen, K., & Sun, G.-X. (2019). Simultaneous adsorption and immobilization of As and Cd by birnessite-loaded biochar in water and soil. *Environmental Science and Pollution Research*, *26*, 8575-8584.

Wang, J., Dokohely, M., Xiong, Z., & Kuzyakov, Y. (2016). Contrasting effects of aged and fresh biochars on glucose-induced priming and microbial activities in paddy soil. *Journal of soils and sediments*, *16*, 191-203.

Wang, J., Xia, K., Waigi, M.G., Gao, Y., Odinga, E.S., Ling, W., & Liu, J. (2018). Application of biochar to soils may result in plant contamination and human cancer risk due to exposure of polycyclic aromatic hydrocarbons. *Environment international*, *121*, 169-177.

Wang, J., Xiong, Z., & Kuzyakov, Y. (2016). Biochar stability in soil: meta-analysis of decomposition and priming effects. *Gcb Bioenergy*, *8*, 512-523.

Wang, L., Wang, J., Wang, Z., He, C., Lyu, W., Yan, W., & Yang, L. (2018). Enhanced antimonate (Sb(V)) removal from aqueous solution by La-doped magnetic biochars. *Chemical Engineering Journal*, *354*, 623-632.

Wang, M., Wu, S., Guo, J., Zhang, X., Yang, Y., Chen, F., & Zhu, R. (2019). Immobilization of cadmium by hydroxyapatite converted from microbial precipitated calcite. *Journal of Hazardous Materials*, *366*, 684-693.

Wang, N., Xue, X.-M., Juhasz, A.L., Chang, Z.-Z., & Li, H.-B. (2017). Biochar increases arsenic release from an anaerobic paddy soil due to enhanced microbial reduction of iron and arsenic. *Environmental pollution*, *220*, 514-522.

Wang, Q., Chen, L., He, L., & Sheng, X. (2016). Increased biomass and reduced heavy metal accumulation of edible tissues of vegetable crops in the presence of plant growth-promoting *Neorhizobium huautlense* T1-17 and biochar. *Agriculture, Ecosystems & Environment*, *228*, 9-18.

Wang, S., Gao, B., Li, Y., Mosa, A., Zimmerman, A.R., Ma, L.Q., … Migliaccio, K.W. (2015). Manganese oxide-modified biochars: Preparation, characterization, and sorption of arsenate and lead. *Bioresource Technology*, *181*, 13-17.

Wang, S., Gao, B., Zimmerman, A.R., Li, Y., Ma, L., Harris, W.G., & Migliaccio, K.W. (2015a). Physicochemical and sorptive properties of biochars derived from woody and herbaceous biomass. *Chemosphere*, *134*, 257-262.

Wang, S., Gao, B., Zimmerman, A.R., Li, Y., Ma, L., Harris, W.G., & Migliaccio, K.W. (2015b). Removal of arsenic by magnetic biochar prepared from pinewood and natural hematite. *Bioresource Technology*, *175*, 391-395.

Wang, S., Zhao, M., Zhou, M., Li, Y.C., Wang, J., Gao, B., … Ok, Y.S. (2019). Biochar-Supported nZVI (nZVI/BC) for Contaminant Removal from Soil and Water: A Critical Review. *Journal of Hazardous Materials*, *373*, 820-834.

Wang, T., Sun, H., Ren, X., Li, B., & Mao, H. (2017). Evaluation of biochars from different stock materials as carriers of bacterial strain for remediation of heavy metal-contaminated soil. *Scientific Reports*, *7*, 12114.

Wang, Y., Dang, F., Zheng, X., & Zhong, H. (2019). Biochar amendment to further reduce methylmercury accumulation in rice grown in selenium-amended paddy soil. *Journal of Hazardous Materials*, *365*, 590-596.

Wei, J., Tu, C., Yuan, G., Bi, D., Wang, H., Zhang, L., & Theng, B.K. (2018). Pyrolysis Temperature-Dependent Changes in the Characteristics of Biochar-Borne Dissolved Organic Matter and Its Copper Binding Properties. *Bulletin of environmental contamination and toxicology*, 1-6.

Weng, Z., Van Zwieten, L., Singh, B.P., Tavakkoli, E., Joseph, S., Macdonald, L.M., … Cowie, A. (2017). Biochar built soil carbon over a decade by stabilizing rhizodeposits. *Nature Climate Change*, *7*, 371-376.

Wijayawardena, M., Megharaj, M., & Naidu, R. (2016). Exposure, toxicity, health impacts, and bioavailability of heavy metal mixtures. In *Advances in Agronomy* (pp.175-234). Elsevier.

Wood, J.L., Tang, C. and Franks, A.E. (2016). Microbial associated plant growth and heavy metal accumulation to improve phytoextraction of contaminated soils. *Soil Biology and Biochemistry*, *103*, 131-137.

Wood, J.L., Tang, C., Franks, A.E., & Liu, C. (2016). Microorganisms in heavy metal bioremediation: strategies for applying microbial-community engineering to remediate soils. *AIMS Bioengineering*, *3*, 211-229.

Wood, J.M., & Wang, H.-K. (1983). Microbial resistance to heavy metals. *Environmental Science & Technology*, *17*, 582A-590A.

Wu, C., Huang, L., Xue, S.G., Huang, Y.Y., Hartley, W., Cui, M.Q., & Wong, M.H. (2017). Arsenic sorption by red mud-modified biochar produced from rice straw. *Environmental Science and Pollution Research*, *24*, 18168-18178.

Wu, P., Cui, P., Alves, M.E., Peijnenburg, W.J.G.M., Liu, C., … Wang, Y. (2019). Interactive effects of rice straw biochar and γ-Al_2O_3 on immobilization of Zn. *Journal of Hazardous Materials*, *373*, 250-257.

Wu, S., Fang, G., Wang, D., Jaisi, D.P., Cui, P., Wang, R., … Zhou, D. (2018). Fate of As(III) and As(V) during Microbial Reduction of Arsenic-Bearing Ferrihydrite Facilitated by Activated Carbon. *ACS Earth and Space Chemistry*, *2*, 878-887.

Wu, W., Li, J., Lan, T., Müller, K., Niazi, N.K., Chen, X., … Wang, H. (2017). Unraveling sorption of lead in aqueous solutions by chemically modified biochar derived from coconut fiber: A microscopic and spectroscopic investigation. *Science of the Total Environment*, *576*, 766-774.

Wu, W., Li, J., Niazi, N.K., Müller, K., Chu, Y., Zhang, L., … Wang, H. (2016). Influence of pyrolysis temperature on lead immobilization by chemically modified coconut fiber-derived biochars in aqueous environments. *Environmental Science and Pollution Research*, *23*, 22890-22896.

Xia, S., Song, Z., Jeyakumar, P., Shaheen, S.M., Rinklebe, J., Ok, Y.S., … Wang, H. (2019). A critical review on bioremediation technologies for Cr(VI)-contaminated soils and wastewater. *Critical Reviews in Environmental Science and Technology*, 1-52.

Xiao, F., Cheng, J., Cao, W., Yang, C., Chen, J., & Luo, Z. (2019). Removal of heavy metals from aqueous solution using chitosan-combined magnetic biochars. *Journal of Colloid And Interface Science*, *540*, 579-584.

Xiao, X., Chen, B., Chen, Z., Zhu, L., & Schnoor, J.L. (2018). Insight into Multiple and Multilevel Structures of Biochars and Their Potential Environmental Applications: A Critical Review. *Environmental Science & Technology*, *52*, 5027-5047.

Xing, Y., Wang, J., Xia, J., Liu, Z., Zhang, Y., Du, Y., & Wei, W. (2019). A pilot study on using biochars as sustainable amendments to inhibit rice uptake of Hg from a historically polluted soil in a Karst region of China. *Ecotoxicology and Environmental Safety*, *170*, 18-24.

Xiong, Z., Shihong, Z., Haiping, Y., Tao, S., Yingquan, C., & Hanping, C. (2013). Influence of NH_3/CO_2 Modification on the Characteristic of Biochar and the CO_2 Capture. *BioEnergy Research, 6*, 1147-1153.

Xu, M., Xia, H., Wu, J., Yang, G., Zhang, X., Peng, H., … Qi, H. (2017). Shifts in the relative abundance of bacteria after wine-lees-derived biochar intervention in multi metal-contaminated paddy soil. *Science of the Total Environment*, *599-600*, 1297-1307.

Xu, Y., Luo, G., He, S., Deng, F., Pang, Q., Xu, Y., & Yao, H. (2019). Efficient removal of elemental mercury by magnetic chlorinated biochars derived from co-pyrolysis of $Fe(NO_3)_3$-laden wood and polyvinyl chloride waste. *Fuel*, *239*, 982-990.

Xu, Y., Seshadri, B., Sarkar, B., Wang, H., Rumpel, C., Sparks, D., … Bolan, N. (2018). Biochar modulates heavy metal toxicity and improves microbial carbon use efficiency in soil. *Science of the Total Environment*, *621*, 148-159.

Xu, Y., Yan, Y., Obadamudalige, N.L., Ok, Y.S., Bolan, N., & Li, Q. (2019). Redox-Mediated Biochar-Contaminant Interactions in Soil. In *Biochar from Biomass and Waste* (pp. 409-419). Elsevier.

Xu, Z., Xu, X., Tsang, D.C., & Cao, X. (2018). Contrasting impacts of pre-and post-application aging of biochar on the immobilization of Cd in contaminated soils. *Environmental Pollution*, *242*, 1362-1370.

Yang, G.-X., & Jiang, H. (2014). Amino modification of biochar for enhanced adsorption of copper ions from synthetic wastewater. *Water Research*, *48*, 396-405.

Yang, X., Liu, J., McGrouther, K., Huang, H., Lu, K., Guo, X., … Wang, H. (2016). Effect of biochar on the extractability of heavy metals (Cd, Cu, Pb, and Zn) and enzyme activity in soil. *Environmental Science and Pollution Research*, *23*, 974-984.

Yang, X., Lu, K., McGrouther, K., Che, L., Hu, G., Wang, Q., … Ye, Z. (2017). Bioavailability of Cd and Zn in soils treated with biochars derived from tobacco stalk and dead pigs. *Journal of soils and sediments*, *17*, 751-762.

Yasmin, K.K., Ali, B., Cui, X., Feng, Y., Yang, X., & Joseph, S.P. (2017). Impact of different feedstocks derived biochar amendment with cadmium low uptake affinity cultivar of pak choi (*Brassica rapa ssb. chinensis* L.) on phytoavoidation of Cd to reduce potential dietary toxicity. *Ecotoxicology and Environmental Safety*, *141*, 129-138.

Yin, D., Wang, X., Chen, C., Peng, B., Tan, C., & Li, H. (2016). Varying effect of biochar on Cd, Pb and As mobility in a multi-metal contaminated paddy soil. *Chemosphere*, *152*, 196-206.

Yousaf, B., Liu, G., Abbas, Q., Ali, M.U., Wang, R., Ahmed, R., Wang, C., … Usman, A.R. (2018). Operational control on environmental safety of potentially toxic elements during thermal conversion of metal-accumulator invasive ragweed to biochar. *Journal of Cleaner Production*, *195*, 458-469.

Yu, P., Xue, Y., Gao, F., Liu, Z., Cheng, X., & Yang, K. (2016). Phosphorus Removal from Aqueous Solution by Pre- or Post-Modified Biochars Derived from Agricultural Residues. *Water, Air, & Soil Pollution*, *227*, 370.

Yu, Z., Qiu, W., Wang, F., Lei, M., Wang, D., & Song, Z. (2017). Effects of manganese oxide-modified biochar composites on arsenic speciation and accumulation in an indica rice (*Oryza sativa* L.) cultivar. *Chemosphere*, *168*, 341-349.

Yu, Z., Zhou, L., Huang, Y., Song, Z., & Qiu, W. (2015). Effects of a manganese oxide-modified biochar composite on adsorption of arsenic in red soil. *Journal of Environmental Management*,*163*, 155-162.

Yuan, J.H., & Xu, R.K. (2011). The amelioration effects of low temperature biochar generated from nine crop residues on an acidic Ultisol. *Soil Use and Management*, *27*, 110-115.

Yuan, P., Wang, J., Pan, Y., Shen, B., & Wu, C. (2018). Review of biochar for the management of contaminated soil: Preparation, application and prospect. *Science of the Total Environment*, *659*, 473-490.

Yuan, Y., Bolan, N., Prévoteau, A., Vithanage, M., Biswas, J.K., Ok, Y.S., & Wang, H. (2017). Applications of biochar in redox-mediated reactions. *Bioresource Technology*, *246*, 271-281.

Zama, E.F., Reid, B.J., Sun, G.-X., Yuan, H.-Y., Li, X.-M., & Zhu, Y.-G. (2018). Silicon (Si) biochar for the mitigation of arsenic (As) bioaccumulation in spinach (*Spinacia oleracean*) and improvement in the plant growth. *Journal of Cleaner Production*, *189*, 386-395.

Zhang, F., Wang, X., Yin, D., Peng, B., Tan, C., Liu, Y., … Wu, S. (2015). Efficiency and mechanisms of Cd removal from aqueous solution by biochar derived from water hyacinth (*Eichornia crassipes*). *Journal of Environmental Management*, *153*, 68-73.

Zhang, G., Guo, X., Zhu, Y., Liu, X., Han, Z., Sun, K., … Han, L. (2018). The effects of different biochars on microbial quantity, microbial community shift, enzyme activity, and biodegradation of polycyclic aromatic hydrocarbons in soil. *Geoderma*, *328*, 100-108.

Zhang, J., Huang, B., Chen, L., Li, Y., Li, W., & Luo, Z. (2018). Characteristics of biochar produced from yak manure at different pyrolysis temperatures and its effects on the yield and growth of highland barley. *Chemical Speciation & Bioavailability*, *30*, 57-67.

Zhang, J., Kumari, D., Fang, C., & Achal, V. (2019). Combining the microbial calcite precipitation process with biochar in order to improve nickel remediation. *Applied Geochemistry*, *103*, 68-71.

Zhang, J., Wu, S., Xu, Z., Wang, M., Man, Y.B., Christie, P., … Wong, M.H. (2019). The role of sewage sludge biochar in methylmercury formation and accumulation in rice. *Chemosphere*, *218*, 527-533.

Zhang, J., Zhang, J., Wang, M., Wu, S., Wang, H., Niazi, N.K., … Wong, M.H. (2019). Effect of tobacco stem-derived biochar on soil metal immobilization and the cultivation of tobacco plant. *Journal of soils and sediments*, *19*, 2313-2321.

Zhang, S., Yang, X., Ju, M., Liu, L., & Zheng, K. (2019). Mercury adsorption to aged biochar and its management in China. *Environmental Science and Pollution Research*, *26*, 4867-4877.

Zhang, T.a., Chen, H.Y.H., & Ruan, H. (2018). Global negative effects of nitrogen deposition on soil microbes. *The ISME Journal*,*12*, 1817-1825.

Zhang, X., Wang, H., He, L., Lu, K., Sarmah, A., Li, J., Bolan, N.S., … Huang, H. (2013). Using biochar for remediation of soils contaminated with heavy metals and organic pollutants. *Environmental Science and Pollution Research*, *20*, 8472-8483.

Zhang, X., Zhang, S., Yang, H., Feng, Y., Chen, Y., Wang, X., & Chen, H. (2014). Nitrogen enriched biochar modified by high temperature CO_2–ammonia treatment: Characterization and adsorption of CO_2. *Chemical Engineering Journal*, *257*, 20-27.

Zhang, Y., Cao, B., Zhao, L., Sun, L., Gao, Y., Li, J., & Yang, F. (2018). Biochar-supported reduced graphene oxide composite for adsorption and coadsorption of atrazine and lead ions. *Applied Surface Science*, *427*, 147-155.

Zhang, Y., Liu, Y.R., Lei, P., Wang, Y.J., & Zhong, H. (2018). Biochar and nitrate reduce risk of methylmercury in soils under straw amendment. *Science of the Total Environment*, *619-620*, 384-390.

Zhang, Z., Zhu, Z., Shen, B., & Liu, L. (2019). Insights into biochar and hydrochar production and applications: A review. *Energy*, *171*, 581-598.

Zhao, L., Zheng, W., Mašek, O., Chen, X., Gu, B., Sharma, B.K., & Cao, X. (2017). Roles of phosphoric acid in biochar formation: Synchronously improving carbon retention and sorption capacity. *Journal of Environmental Quality*, *46*, 393-401.

Zhao, N., Zhao, C., Lv, Y., Zhang, W., Du, Y., Hao, Z., & Zhang, J. (2017). Adsorption and coadsorption mechanisms of Cr(VI) and organic contaminants on H_3PO_4 treated biochar. *Chemosphere*, *186*, 422-429.

Zheng, H., Wang, X., Luo, X., Wang, Z., & Xing, B. (2018). Biochar-induced negative carbon mineralization priming effects in a coastal wetland soil: Roles of soil aggregation and microbial modulation. *Science of the Total Environment*, *610-611*, 951-960.

Zhou, H., Wang, P., Chen, D., Shi, G., Cheng, K., Bian, R., … Pan, G. (2018). Short-term biochar manipulation of microbial nitrogen transformation in wheat rhizosphere of a metal contaminated Inceptisol from North China plain. *Science of the Total Environment*, *640-641*, 1287-1296.

Zhu, N., Qiao, J., & Yan, T. (2019). Arsenic immobilization through regulated ferrolysis in paddy field amendment with bismuth impregnated biochar. *Science of the Total Environment*, *648*, 993-1001.

Zhu, N., Zhang, J., Tang, J., Zhu, Y., & Wu, Y. (2018). Arsenic removal by periphytic biofilm and its application combined with biochar. *Bioresource Technology*, *248*, 49-55.

Zhu, X., Chen, B., Zhu, L., & Xing, B. (2017). Effects and mechanisms of biochar-microbe interactions in soil improvement and pollution remediation: A review. *Environmental Pollution*, *227*, 98-115.

Zimmerman, A.R., Gao, B., & Ahn, M.Y. (2011). Positive and negative carbon mineralization priming effects among a variety of biochar-amended soils. *Soil Biology and Biochemistry*, *43*, 1169-1179.

Zuo, W.Q., Chen, C., Cui, H.J., & Fu, M.L. (2017). Enhanced removal of Cd(II) from aqueous solution using $CaCO_3$ nanoparticle modified sewage sludge biochar. *RSC Advances, 7*, 16238-16243.

Zuo, X., Chen, M., Fu, D., & Li, H. (2016). The formation of alpha-FeOOH onto hydrothermal biochar through H_2O_2 and its photocatalytic disinfection. *Chemical Engineering Journal*, *294*, 202-209.

Zuo, X., Liu, Z., & Chen, M. (2016). Effect of H_2O_2 concentrations on copper removal using the modified hydrothermal biochar. *Bioresource Technology*, *207*, 262-267.

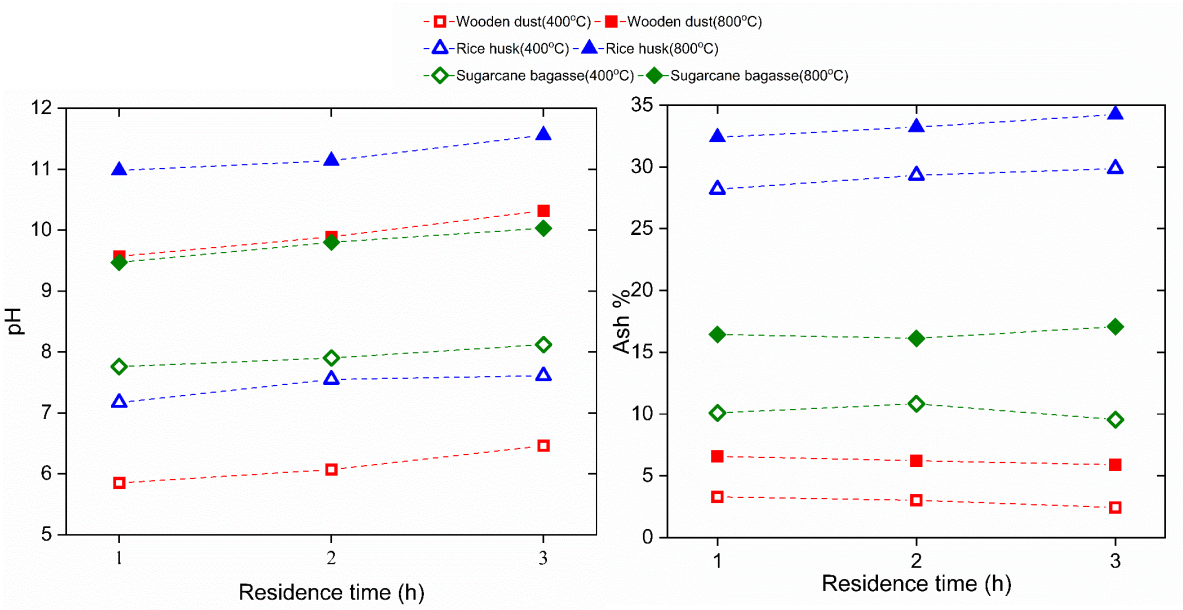

Figure 1. The pH and ash percentage of biochars produced from various types of feedstock at different residence time of pyrolysis (1, 2, and 3 h) and temperatures (400 and 800 °C). Data obtained from Suman and Gautam (2017).

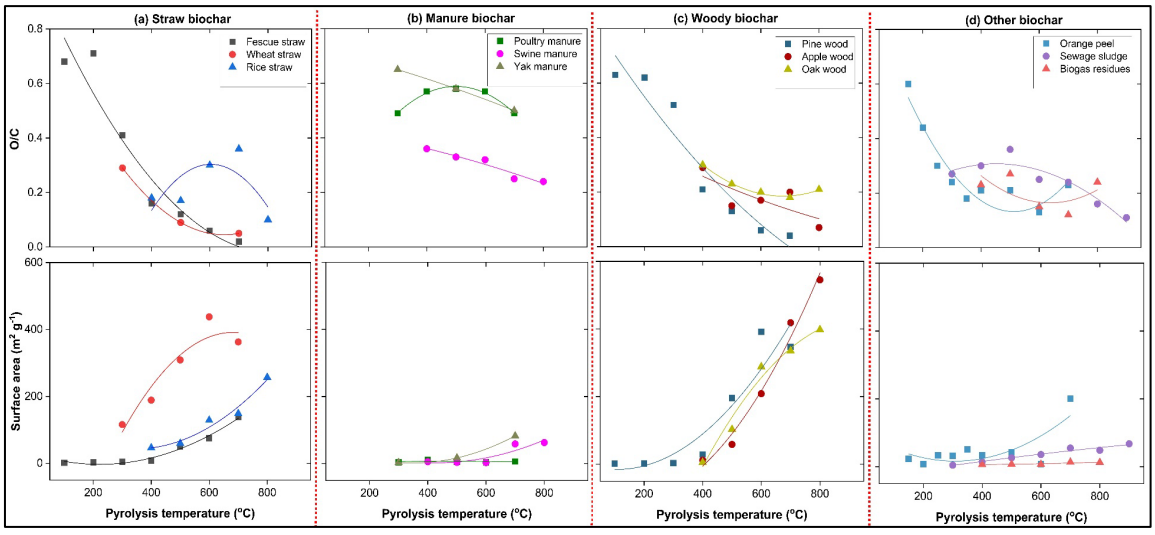

Figure 2. The effects of pyrolysis temperatures on the O/C atomic ratio and surface area of biochars produced from various feedstocks. Data obtained from Ahmad, Rajapaksha, et al. (2014), Jindo, Mizumoto, Sawada, Sanchez-Monedero, and Sonoki (2014), Li, Dong, et al. (2017), Tsai, Liu, Chen, Chang, and Tsai (2012), and Zhang, Huang, et al. (2018)

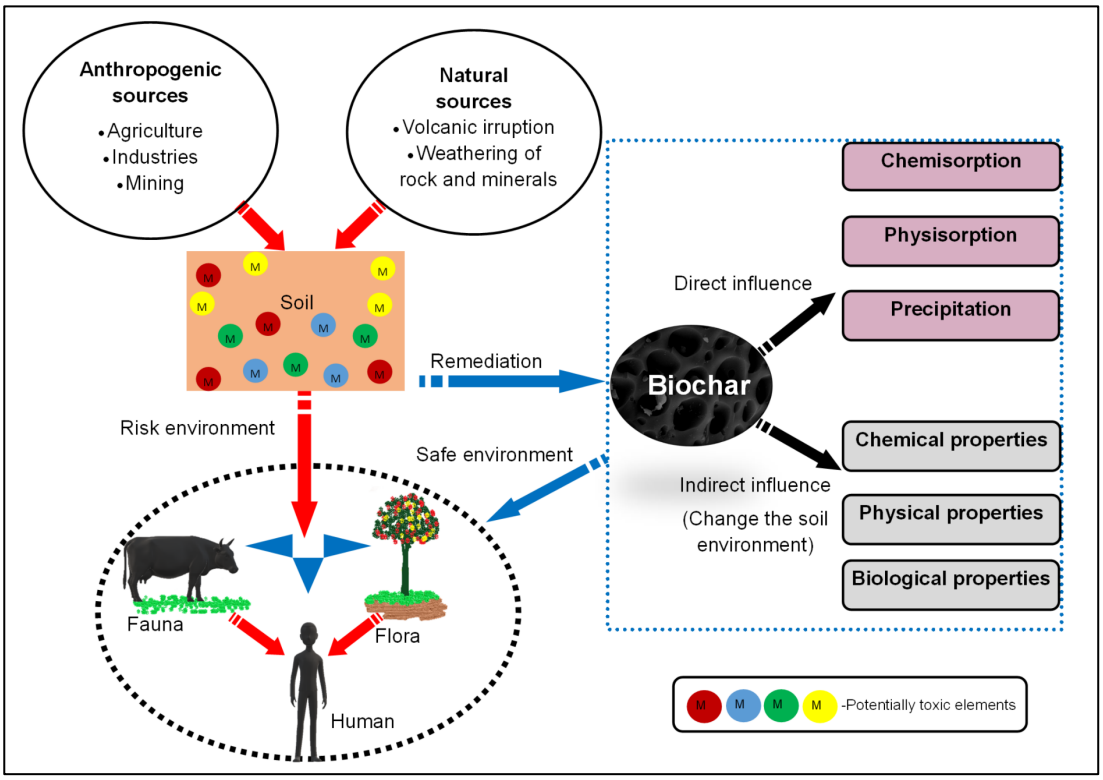

Figure 3. Overall concept of biochar in environmental remediation.

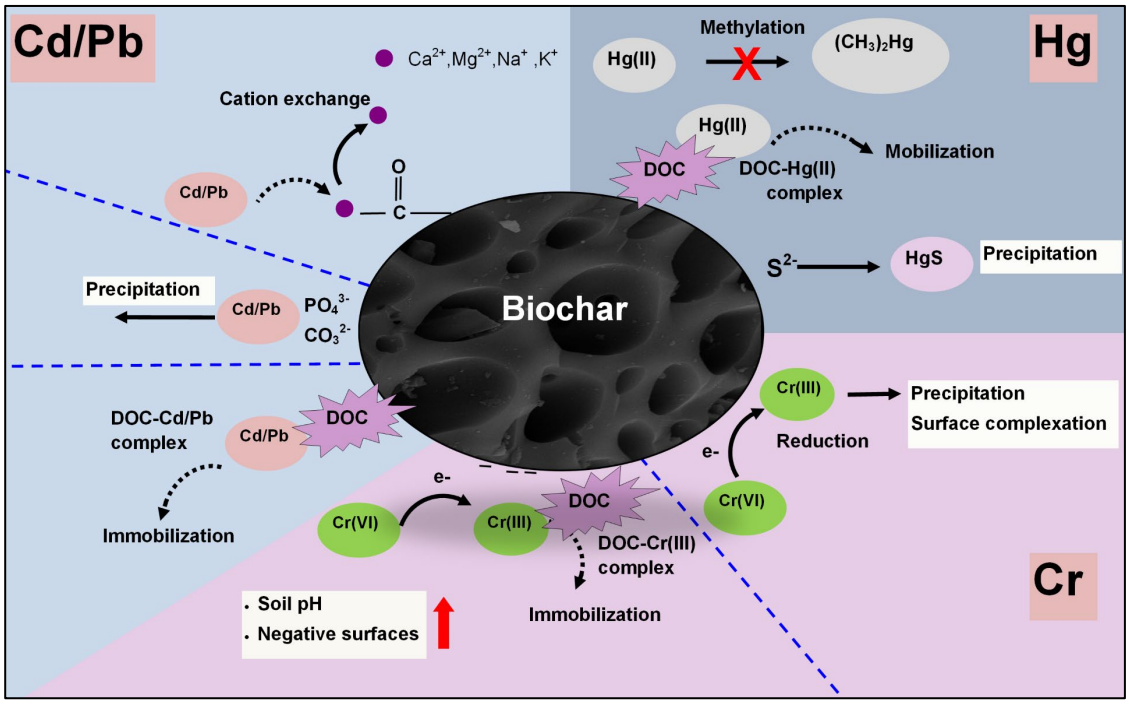

Figure 4. Mechanistic illustration of Cd, Pb, Hg and Cr sorption by biochars in soil. (DOC, Dissolved organic carbon)

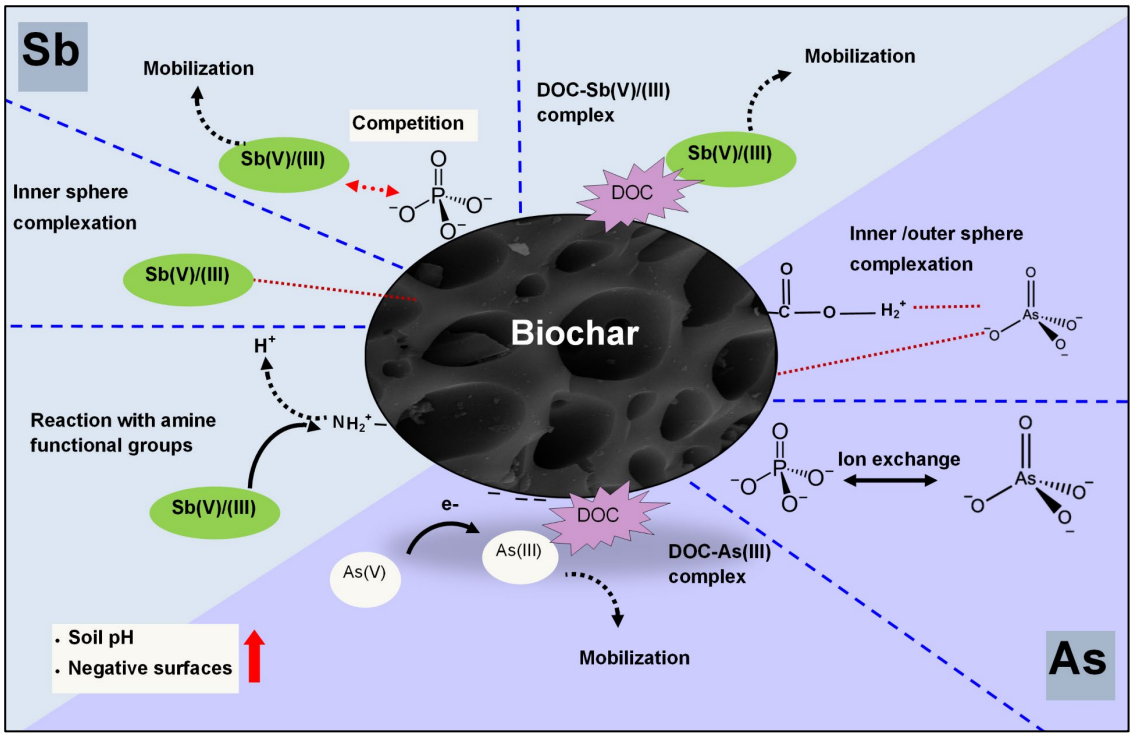

Figure 5. Graphical illustration of Sb and As sorption by biochars in soil. (DOC, Dissolved organic carbon)

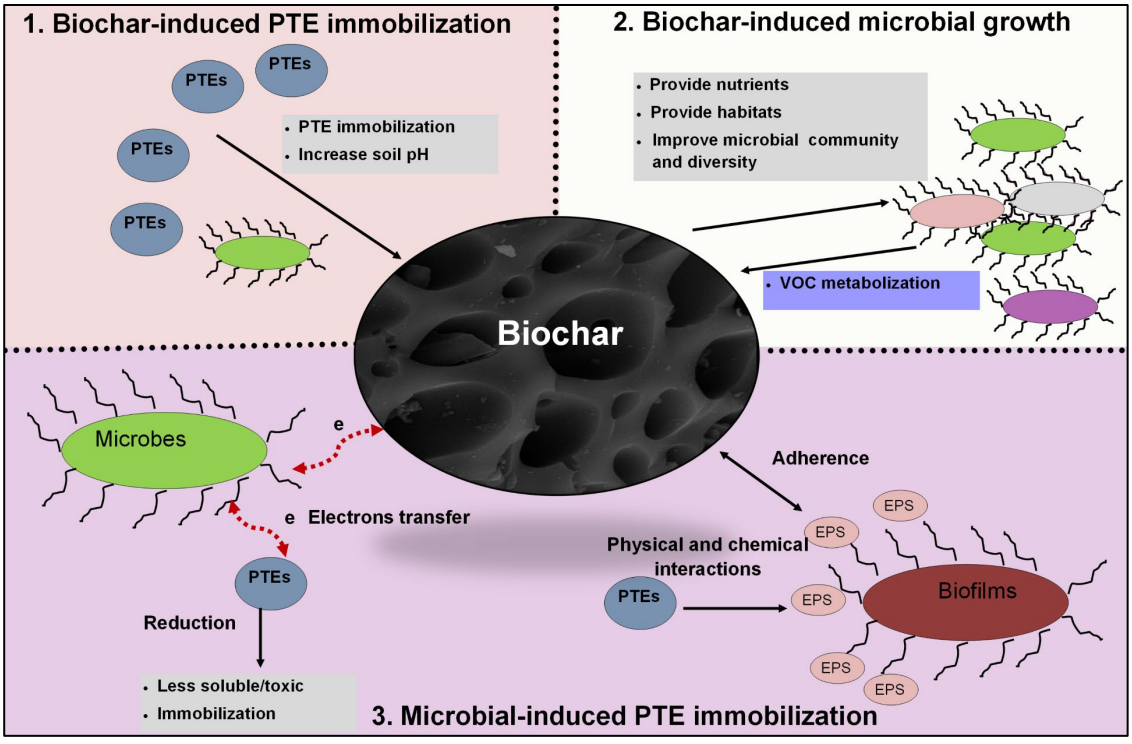

Figure 6. Proposed immobilization mechanisms of potentially toxic elements (PTEs) by soil microorganisms in biochar-amended soil. Step 1, Immobilization of PTEs by biochars; Step 2, Growth and reproduction of microbes; Step 3, Microbial immobilization of PTEs. (PTE, Potential toxic elements; VOC, Volatile organic compounds; EPS, Extracellular polymeric substances)

Table captions:

Table 1. Effects of biochar properties and application rates on mobility and bioavailability of potentially toxic elements (PTEs) in contaminated soils.

Table 2. Microbial responses to biochar addition in soils contaminated with potentially toxic elements (PTEs).

Table 3. The effects of biochar on behaviours of soil enzymes in soils contaminated with potentially toxic elements (PTEs).

Table 4. The enhanced removal efficiency of potentially toxic elements (PTEs), associated mechanisms, advantages and disadvantages of different biochar modification methodologies.

Table 1. Effects of biochar properties and application rates on mobility and bioavailability of potentially toxic elements (PTEs) in contaminated soils.

Biochar type	PTEs	Pyrolysis temp. (ºC)	Application rate (% w/w)	Soil type (texture)	Immobilization mechanisms / effects	References
Chicken litter Wood shaving	Cd	550 650	5	Entisol Inceptisol Andisol Vertisol	• Both biochars effective for redistribution of Cd to less bioavailable soil fractions • pH controlled Cd solubility in soils amended with wood-shaving biochar • Chicken-litter biochar form surface complexation with Cd • Both biochars effectively decreased Cd bioavailability in Entisol and Vertisol with lower sorption capacity	Qi et al. (2018)
Chicken litter Wood shaving	Cd	550 650	5	Ferrosol Dermosol	• Acidic wood-shaving biochar did not change Cd sorption capacity of both soils • Chicken-litter biochar increased Cd sorption in acidic Ferrosol	Qi, Dong, et al. (2017)
Rice straw Rice hull Maize stover	Cd	500	1.5 and 3	Ultisol (silty clay loam)	• Cd immobilized due to surface complexation with surface functional groups, and precipitation with minerals (KCl, calcite, quartz, dolomite and kaolinite)	Bashir, Hussain, Shaaban, and Hu (2018)
Barley straw Tomato green waste Chicken manure Duck manure Swine manure	Cd	500	2.5 and 5	Mollisol	• Addition of 5% biochar derived from chicken manure and tomato green waste immobilized more Cd due to higher pH, surface area and O-containing functional groups	Yasmin et al. (2017)
Rice straw	Cd	450	1.5, 3 and 5	Sandy clay loam	• Biochar addition decreased bioavailable Cd and increased soil pH and Si in soil • Biochar increased plant Zn and Mn concentrations	Abbas et al. (2017)

Bamboo	Cd	400	0.5, 1 and 1.5	Silty loam	• Biochar increased soil pH, electrical conductivity, organic carbon and cation exchange capacity (CEC) • 1.5% application rate was more effective than lower application rates	Mohamed et al. (2015)
Soybean straw	Pb	700	1, 2, 3, 4, 5, 10 and 20	Shooting-range soil (sandy loam)	• Increasing biochar application rate decreased Pb leachability • The formation of chloropyromorphite and Pb-phosphate are the main responsible immobilization process	Moon et al. (2013)
Dairy manure	Pb	450	2.5 and 5	Shooting-range site (sandy soil) Battery recycling site (sandy soil)	• Pb precipitated as hydroxypyromorphite with phosphate of biochar	Cao et al. (2011)
Rice straw	Pb	300	3 and 5	Ultisosl Oxisol	• Biochar increased non-electrostatic adsorption of Pb at relatively low pH	Jiang, Jiang, Xu and Li (2012)
Peanut straw Soybean straw Canola straw Rice straw	Pb	400	5	Ultisosl Oxisol	• All the biochars increased soil pH and CEC • Legume-straw biochar increased Pb adsorption via non-electrostatic mechanism (surface complexation with functional groups) • Biochars derived from non-legume straw showed electrostatic adsorption mechanism by increasing soil CEC	Jiang et al. (2014)
Salibury wood	Pb	600	1	Kaolin	• Pb-immobilising ability of biochar was mainly related to soil properties • Biochar may not be effective in soil with high clay	Shen, McMillan, Jin, and Al-Tabbaa (2016)
Chicken manure *Solanum elaeagnifolium*	Cr	550 300		Calcic red clay Sodosol Calcic red sandy loam Sodosol	• Biochar derived from dissolved organic matter (DOM) enhanced reduction of Cr(VI) to Cr(III) • Addition of biochar significantly enhanced reduction of Cr(VI) in alkaline Chromosol soil	Choppala et al. (2012)

				Tannery waste soil		
Gliricidia sepium wood	Cr	900	1, 2.5 and 5	Tannery waste soil	• 5% biochar amendment was more effective than other rates • Cr immobilized by pore diffusion and adsorption via π-π electron donor-acceptor interactions	Herath et al. (2017)
Rice straw	Hg	600	1 and 4	Paddy soil	• Methylmercury immobilization facilitated by high surface area and organosulfur content of biochar • Biodilution of methylmercury in rice grain due to the increased of grain biomass by biochar	Shu et al. (2016)
Switchgrass	Hg	300 600	5	Sediment	• Hg co- occurred with S, Fe, Cu and other elements within the plant structure of low-temperature-derived biochar	Liu, Ptacek, et al. (2016)
Hardwood	Hg	700	50 (v/v)	River bank sediment Floodplain soil	• Hg immobilization via complexation with surface functional groups • Biochar did not promote methylation	Wang, Ptacek, et al. (2019)
Bamboo	Hg	600	0.5	Paddy soil	• Biochar decreased methylmercury via the complexation of Hg with organosulfur groups • Biochar increased methylmercury partitioning into soil solids by adsorption and complexation	Wang, Dang, et al. (2019)
Sewage sludge	Hg	600	5	Paddy soil (acidic and calcareous)	• Sewage-sludge biochar increased soil organic matter content and hence methylmercury production • Biochar inhibited methylmercury accumulation in rice plants in acidic soil • Biochar did not influence the accumulation of methylmercury in rice plants in calcareous soil	Zhang, Wu, et al. (2019)
Rice straw	As	500	3	Paddy soil	• Biochar increased As mobilization under anaerobic condition • Biochar enhanced dissolution of Fe oxides by promoting Fe-reducing bacteria	Wang, Xue, et al. (2017)
Oil palm fiber	As	700	3	Paddy soil	• Biochar enhanced microbial reduction of As(V) and Fe(III) and released As(III) into soil solution	Qiao, Li and Li (2018)
Granular sludge	As	300	10	Paddy soil	• Biochar produced at low temperature released more dissolved organic C (DOC) than biochar produced at high temperature	Kim et al. (2018)

Rice straw Coffee grounds		550 700			• DOC enhanced reductive dissolution and ligand-enhanced dissolution of Fe(II) and As release • DOC competed with As for adsorption onto soil • Biochar increased P in soil solution and further competed with As adsorption	
Wheat straw Apple tree branch	Sb	500	0.5, 5 and 10	Paddy soil (sandy soil)	• Sb mobilized by wheat-straw biochar and apple-tree biochar during first 20 and 50 days of incubation, respectively • Sb mobilized due to electrostatic repulsion of organic matter and functional groups of biochar • Sb immobilized by wheat-straw biochar and apple-tree biochar after 20 and 50 days of incubation due to secondary mineral precipitation, organic complex between Sb and humic acid and complex between Sb and organic matter and Fe (hydr)oxide of biochar	Hua, Zhang, Wei, Yang, and Guo (2019)
Mushroom waste Sewage sludge Soybean straw Rice straw Peanut shells	As Cd	200 350	3	Sandy loam	• Biochar modified the composition of DOC in soil • Sewage-sludge biochar was effective in decreasing DOM-Cd and DOM-As concentrations • Biochar derived at 350 °C significantly decreased As/Cd uptake in rice • All biochars decreased uptake of As(III)	Li, Khan, et al. (2018)
Umbrella tree wood bark Cocopeat Palm kernel shell	Pb As	500	5	Paddy soil Upland agriculture soil	• Pb immobilized in the upland agriculture soil by all biochars • Umbrella tree wood bark and cocopeat effectively immobilized Pb in the paddy soil • As mobilized in the upland agriculture soil by Umbrella tree wood bark and cocopeat • High pH, P content and Si content of biochar controlled Pb immobilization and As mobilization	Igalavithana, Park, et al. (2017)
Rice hull	As Co Mo	500	5	Mining soil	• Biochar stimulated the mobility and phytoavailability of As, Mo and Co under oxic-acidic conditions	El-Naggar, Shaheen, et al. (2019)
Hard wood	Pb Zn	500	2 and 5	Mining soil	• Biochar decreased Pb and Zn in soil pore water but had no effects on As and Cd	Norini et al. (2019)

	Ba As Cd				• Pb immobilized via surface complexation and adsorption	
Gliricidia sepium wood	Pb Cu	900	10	Shooting-range soil (silty loam)	• Biochar increased soil pH but decreased Pb and Cu dissolution • Electrostatic attractions, surface diffusion, ion exchange, precipitation and complexation could immobilize Pb and Cu	Kumarathilaka et al. (2018)
Red pepper stalks	As Pb Cd Zn	650 (with N_2 gas) 650 (with CO_2 gas)	2.5	Sandy loam Sandy	• Biochar produced under CO_2 immobilized Pb compared to the biochar produced under N_2 due to high surface area, surface functional groups and atomicity • Both biochars effectively decreased the mobility of Cd and Zn • Biochar produced under N_2 significantly decreased As mobility due to low pH compared to biochar produced under CO_2	Igalavithana et al. (2018)
Soybean stover	Pb Cu Sb	300	0.5, 1 and 2.5	Shooting-range soil	• Pb and Cu immobilized via adsorption of DOC-metal complexes, electrostatic and π-π electron donor-acceptor interaction and precipitation • Sb mobilized due to repulsive electrostatic forces of biochar	Vithanage, Herath, Almaroai, et al. (2017)
Dairy manure NaOH modified dairy manure biochar	Cu Zn Pb Cd	300	2.5 and 5	E-waste recycling site (sandy soil)	• Both non-modified and modified biochar decreased the bioavailability and mobility of PTEs by transforming more stable species and soil fraction	Chen, Zhang, Liu, Wu, and Yuan (2018)

Table 2. Microbial responses to biochar addition in soils contaminated with potentially toxic elements (PTEs).

Biochar type	Pyrolysis temp. (°C)	Application rate	PTEs	Soil type	Microbial response to biochar addition	Impact of biochar	Reference
Red pepper stalk (produced under N_2 or CO_2)	650	2.5 %	Pb As Cd Zn	Sandy loam Sandy soil	• Addition of biochar to contaminated soil restore the bacterial community similar to non-contaminated soil	• Biochar decreased PTE toxicity, neutralized soil pH, provided C, minerals and surface area	Igalavithana, Kim, et al. (2019)
Macadamia nutshell	465	5%	Cd Pb	Sodosol (silty loam)	• Total microbial PLFA concentration increased by 26, 25 and 26% in Cd, Pb and Cd+Pb treated soils, respectively, compared to the control. • Microbial carbon-use efficiency increased by 0.05, 0.09 and 0.12 units in Cd, Pb and Cd+Pb treated soils, respectively	• Biochar increased soil C and nutrients and decreased PTE toxicity	Xu et al. (2018)
Coconut shell Coconut-shell biochar modified with 1 M HCl and ultrasonication	800	2.5 and 5%	Cd Ni Zn	Paddy soil	• 5% modified biochar had higher number of bacteria and fungi than the non-modified biochar amended soil and control	• Biochar modification significantly increased surface area, functional groups and microcosmic pore structure • Modified biochar increased soil CEC and Olsen-P	Liu, Xu, et al. (2018)
Wheat straw	350-550	20 and 40 t/ha	Cd Pb	Inceptisol	• 40 t/ha significantly increased microbial abundance and N transformation by decreasing mobility of heavy metals	• 40 t/ha addition significantly increased rhizosphere pH, heavy metal bioavailability compared to the 20 t/ha amendment and control soil	Zhou et al. (2018)
Wine-lees	600	0.5, 1 and 2%	Cr Ni Cu Zn As Cd Pb Hg	Paddy soil	• Increasing application rate increased the relative abundance of *Actinobacteria*, *Firmicutes*, *Proteobactreia*, *Planctomycetes* and *Cyanobacteria* but decreased that of *Gemmatimonadetes*	• Biochar decreased PTE toxicity and increased soil fertility	Xu, Xia, et al. (2017)

Rice husk Modified with H_3PO_4, HNO_3, H_2SO_4, H_2O_2 and $ZnCl_2$	500	2%	Cd	River sediment	• Activated biochar negatively affected indigenous microbes and induced new microbial community • Control treatment showed the higher abundance and diversity of bacteria	• Activated biochar reduced Cd bioavailability due to increased surface area, and functional groups • Changes of sediment physicochemical properties negatively affected native microbes	Liu, Liu, et al. (2018)
Chicken manure Oat hull	500 300	1 and 5%	Cu	Alfisol (sandy loam)	• Biochar produced at low temperature increased fungal and bacterial richness	• Biochar produced at low temperature provided more labile C, N, and P	Moore et al. (2018)
Rice husk	500	2, 5 and 10%	Cu	River sediment	• New microbial community immerged due to biochar addition	• Biochar increased soil total organic C and N • Less pH variation could enhanced bacterial abundance	Que et al. (2018)
Rice straw	600	1 and 5%	Cd Zn	River sediment	• 5% biochar decreased bacterial 16S RNA and fungal 18S rNA gene copies by 74 and 25%, respectively • 5% biochar decreased relative intensity of dominant species • 1% biochar increased bacterial and fungal abundance	• 5% biochar increased soil pH and inhibited growth of some bacteria and fungi • 92% variation of total microbial community due to changes of pH, organic matter and PTEs • 45% variation due to organic matter changes with biochar addition	Huang et al. (2017)
Vegetable waste Pine cone Vegetable waste + Pine cone (1:1)	200 500	5%	Pb As	Paddy soil (sandy loam) Upland agriculture soil (sandy loam)	• Biochar derived from vegetable waste at 200 °C increased microbial activity and abundance compared to other biochars	• Biochar derived from vegetable waste at low temperature supplied more labile C to microbial growth	Igalavithana, Lee, et al. (2017)
Rice straw	500	3%	As	Paddy soil	• Biochar increased the relative abundance of *Clostridum*, *Bacillus*, *Caloramator*, *Desulfitobacterium*, *Desulfosporosinus* and *Geobacter*	• Biochar increased dissolved organic C, NH_4^+ and EC	Wang, Xue, et al. (2017)

Soybean stover Pine needle	300 700	10%	Pb As	Agriculture soil (sandy loam)	• Low-temperature-derived biochar increased the abundance of Gram-positive and negative bacteria, fungi , arbuscular mycorrhizal fungi and actinomycetes • *Actinobacteria* substantially increased while *Acidobacteria* and *Chloroflexi* decreased with biochar addition	• Low temperature derived biochar provide more dissolved organic and active carbon • High temperature derived biochar may cause the physical disconnection between microbes and organic carbon	Ahmad, Ok, et al. (2016)
Soybean stover Pine needle	300 700		Pb Cu Sb	Shooting-range soil (sandy loam)	• Low-temperature-derived biochar significantly increased soil microbial concentration	• Low temperature derived biochar provide more mobile matter and nutrients	Ahmad, Ok, Rajapaksha, et al. (2016)
Fresh biogas slurry and residue	550	3%	Fe As	Sediment	• Biochar shifted soil microbial community and increased the relative abundance of *Geobacter*, *Anaeromyxobacter*, *Desulfosporosinus* and *Pedobacter*	• Biochar application favoured the utilization of electron donor	Chen, Wang, et al. (2016)
Wheat straw	450	10, 20 and 40 t/ha	Cd Pb	Paddy soil	• Increasing biochar rate increased the population of fungi and actinomycetes	• Biochar decreased PTEs toxicity and modulate soil pH • Biochar increased soil organic C	Cui et al. (2013)

Table 3. The effects of biochar on behaviours of soil enzymes in soils contaminated with potentially toxic elements (PTEs).

Biochar type	Production temperature (°C)	PTEs	Enzymes	Study duration	Effects	Reference
Bamboo Rice straw	750 500	Cd Cu Pb Zn	Urease Catalase Acid phosphatase	1 year	• Addition of 5% rice-straw biochar increased urease activity by 143%. • Both bamboo and rice-straw biochars increased catalase activity but did not affect the activity of acid phosphatase.	Yang et al. (2016)
Wheat straw	350-550	Cd Cu Pb Zn	Catalase Urease Phosphatase	112 days	• 3% biochar increased the activity of catalase and phosphatase by 57% and 27% while 6% amendment rate increase d by up to 65% and 35%, respectively. • Urease activity decreased by 23% and 26% in 3% and 6% amendment rate, respectively.	Liu, Wang, et al. (2016)
Vegetable waste Pine cone	200 500	Pb	Dehydrogenase	45 days	• Low-temperature-derived biochar enhanced the activity compared to high-temperature-derived biochar.	Igalavithana, Lee, et al. (2017)
Rice straw	600	Cu Zn Pb Cd	Invertase Urease Alkaline phosphatase	90 days	• 5% application rate increased urease activity by 1.9 times. • Biochar decreased activities of invertase and alkaline phosphatase, depending on biochar application rate.	Huang et al. (2017)
Dairy manure Rice straw	350 550	Cd	Denitrifying reductase	56 days	• Cd decreased the activity of denitrifying reductase enzymes in soil. • Biochar increased the activity of denitrifying reductase and abundance of functional genes.	Chen, Zhang, et al. (2017)
Wheat straw	450	Cd Pb	Neutral phosphatase Cellulase Urease Sucrase	1.5 years	• Biochars enhanced the activity of all the enzymes. • Cellulase displayed the highest activity which was 117, 123 and 178% higher at biochar rates of 10, 20 and 40 t/ha, respectively, than in the control.	Cui et al. (2013)
Willow	350 550	As	Dehydrogenase	180 days	• Biochar decreased As toxicity and hence increased soil dehydrogenase activity. • No significant difference in enzyme activity between application rates. • Low-temperature-derived biochar had higher enzyme activity because of its higher concentration of labile carbon.	Gregory et al. (2014)
Gliricidia sepium	300 700	Cr Mn Ni	Dehydrogenase Catalase Polyphenol oxidase	42 days	• Increasing application rate of high-temperature-derived biochar decreased enzymatic activities.	Bandara, Herath, Kumarathilaka, Seneviratne, et al. (2017)
Poulty litter Eucalyptus	400 600	Cd	Invertase β-glucosidase	60 days	• The presence of plants enhanced soil enzymatic activities. • Poultry-litter biochar increased β-glucosidase activity in soil.	Lu et al. (2015)

Tea waste	300	Cd	β-glucosaminidase Urease Phosphomonoesterase Urease Phosphatase Invertase Catalase	60 days	• Tea-waste biochar slightly increased catalase activity compared to the control • The activity of urease and phosphatase significantly increased at an early stage (7 days) of incubation and then levelled off on day 60 • The activity of invertase decreased with increasing incubation time	Gong et al. (2019)

Table 4. The enhanced removal efficiency of potentially toxic elements (PTEs), associated mechanisms, advantages and disadvantages of different biochar modification methodologies.

Modification method	Biochar type	Target PTEs	Mechanisms	Removal efficiency/ Sorption capacity	Advantages	Disadvantages	Reference
Chemical modification with β-cyclodextrin-chitosan	Walnut shell	Cr(VI)	• Electrostatic interaction via amino and carboxylic groups • Cr(VI) reduction to Cr(III) • Cr(III) complexation with functional groups	Removal efficiency increased by 27-93%	• Low cost • Simple synthesis • Enhance surface area, porosity and thermal stability	• Part of the Cr(III) released into solution	Huang et al. (2015)
Impregnation with $Zn(NO_3)_2$	Sugarcane bagasse	Cr(VI)	• Ion exchange • Chelating reaction • Surface adsorption via functional groups	1.2 to 2.0-time higher removal efficiency	• Low cost • Increase surface area and pore volume • Adsorbent could be regenerated and reused	• Surface C% reduced from 84% to 78%	Gan et al. (2015)
Chemical modification with chitosan-pyromellitic	Rice straw	Pb(II) Cd(II) Cu(II)	• Chemisorption on the monolayer surface • N-C=O functional group mainly responsible for Pb(II) removal • Cd-π complexation between Cd and C=C • C=O functional groups responsible for Cu(II) adsorption	Cu(II) removal efficiency was 2.5 times higher than raw biochar Pb(II) and Cd(II) removal efficiency increased by up to 10%	• Greater capacity of Cu removal • Enhanced surface functional groups	• Modification removed KCl and $CaCO_3$ • Surface C% reduced form 75% to 63%	Deng et al. (2017)
Impregnation with $CaCO_3$ nanoparticles	Sewage sludge	Cd(II)	• Surface precipitation	3 times higher removal efficiency	• Simple method • Low cost • Higher efficiency	• Surface area slightly reduced	Zuo et al. (2017)
Chemical modification with H_2O_2	*Cymbopogon schoenanthus* L Spreng	Cu(II)	• Sorption with carboxylic functional groups	92% higher removal efficiency	• Enhanced the number of surface functional groups	• Aromatic C decomposed by H_2O_2	Zuo, Chen, et al. (2016)
Chemical modification with graphene oxide	Water hyacinth	Cr(VI)	• Electrostatic adsorption with functional groups • Complexation • Reduction	Increased from 25-72% to 35-96%	• Facile • Low cost • Higher surface area • More O-containing surface functional groups	• Surface C, N and P% reduced • Lower pore volume	Shang et al. (2016)
Magnetic modification	Nut shield Wheat straw Grape stalk	Pb(II) Cd(II)	• Pb(II) and Cd(II) precipitate with CO_3^{2-}	Cd(II) sorption capacity increase of 2.2-16.9 times	• High efficiency for more mobile metals • More surface functional groups	• Smaller range of pH compared to the pristine biochar	Trakal et al. (2016)

	Grape husk Plum stone		• Metal-chelating complexes with functional groups	Pb(II) sorption capacity increase of 5.63-8.40 times for nut shield and plum stone respectively	• Cation exchange capacity significantly increased	• BET surface area decreased biochar with high surface area	
Physical modification with NH_3	Saw dust	Cu(II)	• Complexation with amino functional groups	5 times higher removal efficiency	• Low cost • Easy method • Enhanced the number of surface functional groups	• C% and surface area • slightly decreased	Yang and Jiang (2014)
Impregnation with manganese oxide and birnessite	Loblolly pine wood	As(V) Pb(II)	• As(V) and Pb(II) sorption into birnessite particles	As(V) sorption capacity increase of 3-4.7 times Pb(II) sorption capacity increase of 2.1-20.0 times	• Increase surface area and pore volume • Higher thermal stability • Low cost	• C, H, N, Mg and Al% decreased	Wang, Gao, et al. (2015)
Chemical modification with NaOH	Hickory wood	Pb(II) Cu(II) Zn(II) Ni(II)	• Adsorption with O-containing functional groups	2.6 to 5.8 times higher heavy metals sorption capacity	• Increased surface area, O-containing surface functional groups and cation exchange capacity	• Ca and Mg mineral contents decreased • C and N% slightly decreased	Ding et al. (2016)
Chemical activation with KOH	Anaerobically digested algae-dairy manure	Cu(II)	• Surface complexation with O-containing functional groups • Form $Cu(OH)^+$ and more effectively adsorb compared to the Cu(II)	3.4 times higher adsorption capacity	• Simple method • Low cost • Can be used in large scale • Increased surface functional groups	• Organic matter and ash contents decreased	Jin et al. (2016)
Chemical modification with H_3PO_4	Corn straw	Cr(VI)	• Inner-sphere complex with the surface O-containing functional groups	Maximum adsorption capacity is 116 mg/g	• Increased surface area • Enhancement of aromatic compounds • Ash content increased	• H, N and O% decreased • O containing functional groups decreased	Zhao, Zhao, et al. (2017)
Chemical oxidation with $KMnO_4$	Corn straw	Cu(II)	• Surface complexation with MnO_x and O-containing functional groups • Cation exchange • Cu(II)-π bonding	Maximum adsorption capacity is 160 mg/g	• Low cost absorbent • Effective in various environmental applications • Ash content increased	• C, H, N, S% and surface area decreased	Song et al. (2014)
Chemical modification with Fe-Mn oxides	Corn straw	As(III)	• Anionic adsorption • Oxidation of As(III) to As(V)	Compared to the control, As(V) concentration decreased by 11-18%	• Fe-oxides enhance As adsorption • Mn-oxides change the speciation of As by oxidation • Ash and K content increased	• C, N and H% decreased	Lin, Gao, et al. (2017)

Chemical modification with chitosan and zerovalent iron	Poultry, cow and sheep manure	Cr(VI)	• Cr(VI) reduced to Cr(III) by O-containing functional groups • Zerovalent particles act as the adsorption site for the Cr(III) • Surface complexation and precipitation	Cr(VI) reduction capacity increase of 40-55% in modified sheep manure biochar and 45-48% in modified poultry-manure biochar	• Cr(VI) converted to less toxic Cr(III) • Enhanced surface functional groups	• C and N% decreased • Surface area and pore volume slightly decreased	Mandal et al. (2017)
Impregnation with Mn-oxides	Corn straw	As(III)	• Anionic adsorption • Oxidation of As(III) to As(V)	Compared to the control, As(III) decreased by 82% and As(V) by 29%	• Oxidation of As(III) to As(V) • Ash % increased from 10 to 13%	• Surface C, N and H% decreased • Surface area decreased from 61 to 3 m^2/g	Yu et al. (2017)
Chemical modification with iron phosphate nanoparticles	Chinese herb medicine residue	Cd(II)	• Cd(II) precipitate as $Cd_3(PO_4)_2$	The immobilization efficiency increased by 81% and bioaccessibility decreased by 80%	• Bioavailable Cd redistributed into less bioavailable species • Promote d plant growth with increased P supply	• Soil pH and organic matter content decreased compared to the pristine biochar	Qiao et al. (2017)
Chemical modification with graphene oxide	Corn straw	Pb(II)	• Electrostatic interaction • Surface adsorption • Pb(II) precipitate with phosphate	Maximum adsorption capacity increase of 1.23 times	• Increased surface area and pore volume • Increased O-containing functional groups	• Surface C% decreased from 88% to 70% • Surface N and P% declined by 79% and 76%, respectively	Zhang, Cao, et al. (2018)
La-doped magnetic modification	*Phragmites australis*	Sb(V)	• Inner-sphere La-O-Sb complex • H-bonding • Electrostatic interaction • Ligand exchange	Compared to the pristine and magnetic-modified biochar adsorption capacity increased by 9 and 4 times in La-doped magnetic biochar	• Increased surface area and pore volume • Increase –OH groups	• Decreased magnetic properties	Wang, Wang, et al. (2018)
Magnetic biochar/MgFe-layered double hydroxides	Oil-tea camellia shells	Pb(II)	• Heterogeneous diffusion and chemisorption	Maximum adsorption capacity is 476 mg/g, 7 times higher than magnetic biochar	• Cyclic utilization • Simple synthesis • Increased surface area and pore volume	• Surface C, and K content decreased	Jia et al. (2019)
Chitosan-combined magnetic modification	Loofah sponges	Cr(VI) Cu(II)	• Ion exchange • Surface complexation	Maximum adsorption capacity for Cr(VI) and Cu(II) is 30 and 55 mg/g, respectively	• Cyclic utilization	• Surface area and pore volume significantly decreased	Xiao et al. (2019)

Biochar supported nanoscale zero-valent iron	Sewage sludge	Cr(VI) Pb(II)	• Adsorption • Reduction • Precipitation	82% and 90% of Pb(II) and Cr(VI) removal, respectively, within 30 min	• Cyclic utilization • Cr(VI) converted to less toxic Cr(III)	• Surface area and pore volume significantly decreased	Diao et al. (2018)
Birnessite-loaded biochar	Rice husk	As(III) As(V) Cd(II)	• Cd formed surface complex with functional groups and O atoms in birnessite structure • As formed surface complex with functional groups • Co-adsorption of As(III)/As(V) and Cd(II)	Maximum adsorption capacities for As(III), As(V) and Cd(II) is 3.5, 2.4 and 9.1 mg/g, respectively (no As adsorption and 4.3 mg/g for non-modified biochar)	• Pore-water Cd concentration reduced soil under un-flooded condition • Pore-water As concentration decreased soil under both un-flooded and flooded condition	• Surface area, C and N content decreased	Wang, Chen, Zhu, Cen, and Sun (2019)
Aluminium-impregnated biochar	Oak tree	As(V)	• Inner-surface complexation with amorphous aluminium hydroxide	Maximum adsorption capacity is 2.6 mg/g	• Cyclic utilization • Simple synthesis	• Surface area slightly decreased	Liu, Wu, Gorring, and Deng (2019)

Supplementary materials

Chemical and biological immobilization mechanisms of potentially toxic elements in biochar-amended soils

Tharanga Bandara, Ashley Franks, Jianming Xu, Nanthi Bolan, Hailong Wang and Caixian Tang

Table S1. Major characteristics of biochars derived from different feedstocks.

Feedstock	Pyrolysis temp. (°C)	Yield %	pH	Ash%	C%	H%	O%	N%	H/C	O/C	CEC ($cmol_+/kg$)	Surface area (m^2/g)	References
Plant materials													
Rice hull	500	-	10.2	39.2	51.0	-	7	-	-	-	50.4	-	El-Naggar, Shaheen, et al. (2019)
Rice straw	300	38.0	7.9	-	44.7	3.06	19.3	1.62	0.07	0.43	-	6.8	Shen et al. (2019)
	500	31.0	10.4	-	44.5	1.88	9.7	1.35	0.04	0.22	-	22.4	
	700	30.0	10.7	-	44.9	1.24	5.9	1.03	0.03	0.13	-	115.5	
Wood pine chip	500	-	10.0	37.7	89.2	2.67	7.9	0.2	0.36	0.07	-	324.6	Rajapaksha et al. (2019)
Garlic stem	300	-	-	-	58.9	4.81	34.6	1.47	0.97	0.44	-	1.5	Rajapaksha et al. (2019)
	700	-	-	43.1	63.9	1.49	32.6	1.32	0.28	0.38	-	201.7	
Alfalfa	350	47.7	-	7.1	68.8	4.8	14.4	4.9	0.8	0.2	-	3.5	Choi and Kan (2019)
	450	30.7	-	9.1	71.1	3.1	12.0	4.7	0.5	0.1	-	4.0	
	550	28.3	-	16.0	69.5	1.8	8.7	4.0	0.3	0.1	-	183.0	
	650	27.5	-	13.6	72.2	1.1	8.5	4.6	0.2	0.1	-	405.0	
Symphytum officinale L.	350	-	10.0	42.9	41.1	2.73	10.7	1.87	0.07	0.26	-	11.5	Du et al. (2019)
	550	-	10.4	47.8	38.5	1.48	9.8	1.73	0.04	0.25	-	34.5	
	750	-	11.3	55.8	33.6	0.93	7.5	1.52	0.03	0.22	-	273.8	
Rice straw	300	43.2	7.8	28.3	47.7	4.31	21.4	1.39	1.08	0.34	-	12.8	Gao et al. (2019)
	500	34.7	10.0	37.7	46.8	2.42	14.5	1.21	0.62	0.23	-	24.6	
	700	29.0	10.7	42.3	43.3	1.45	14.0	0.87	0.40	0.24	-	41.4	
Rice straw	300	45.2	-	26.3	69.6	5.00	24.5	0.91	0.86	0.26	-	-	Wei et al. (2019)
	400	38.0	-	31.6	75.0	4.33	19.7	0.90	0.69	0.20	-	-	
	500	34.2	-	34.4	79.1	3.84	16.3	0.77	0.58	0.15	-	-	
	600	31.8	-	38.5	80.6	2.89	15.8	0.71	0.43	0.15	-	-	
	700	30.6	-	39.5	81.1	2.58	15.6	0.70	0.38	0.14	-	-	
Pine wood	300	45.5	-	0.9	72.2	4.15	23.5	0.16	0.69	0.24	-	-	Wei et al. (2019)

	400	29.9	-	12	76.5	2.92	20.3	0.19	0.46	0.20	-	-	
	500	27.2	-	1.3	83.6	3.01	13.2	0.19	0.43	0.12	-	-	
	600	25.0	-	1.4	88.2	2.45	9.2	0.19	0.33	0.08	-	-	
	700	23.2	-	1.4	90.7	2.19	7.0	0.14	0.29	0.06	-	-	
Tobacco stem	450	-	10.5	25.5	59.7	3.26	-	2.01	-	-	32.4	368.9	Zhang, Zhang, et al. (2019)
Perilla	700	-	10.6	41.9	71.8	0.9	15.3	1.5	-	-	-	473.4	Sethupathi et al. (2017)
Korean oak	400	-	10.2	5.1	88.7	1.2	9.7	0.4	-	-	-	270.8	Sethupathi et al. (2017)
Japanese oak	500	-	9.9	3.3	89.9	2.4	7.5	0.2	-	-	-	475.6	Sethupathi et al. (2017)
Pine cone	500	-	6.8	-	54.7	3.02	17.4	1.20	0.66	0.08	6.1	193.0	Ngigi, Ok and Thiele-Bruhn (2019)
Rice husk	500	-	10.0	-	51.5	1.54	8.8	0.83	0.36	0.11	40.1	24.6	Ngigi et al. (2019)
Micanthus sinensis	850	-	9.2	-	74.3	1.82	14.8	0.43	0.29	0.03	75.6	37.2	Ngigi et al. (2019)
Tea waste	500	39.5	10.9	14.3	70.7	1.13	5.9	2.16	0.20	0.06	-	312.4	Pal and Maiti (2019)
Vegetable waste	200	75.8	5.9	16.6	41.0	5.35	28.0	3.26	1.56	0.51	-	0.4	Yang et al. (2019)
	500	29.3	11.2	36.7	48.2	1.99	10.8	3.49	0.49	0.17	-	1.2	
Pine cone	200	86.5	4.1	0.8	62.5	1.91	24.3	0.93	0.42	0.21	-	0.5	Yang et al. (2019)
	500	35.8	6.8	9.0	73.1	2.56	20.5	1.77	0.37	0.29	-	193.0	
Vegetable waste + pine cone (1:1)	200	79.6	5.3	7.9	49.8	5.38	35.4	0.52	1.30	0.53	-	0.4	Yang et al. (2019)
	500	33.8	10.4	18.1	67.8	2.19	7.9	3.00	0.39	0.09	-	50.3	
Sorgum	500	-	7.4	29.4	46.7	2.98	13.0	0.00	0.76	0.21	-	4.1	Yang et al. (2018)
	600	-	9.7	45.1	47.4	2.31	9.8	0.00	0.58	0.16	-	4.1	
Burcucumber	300	51.8	10.9	13.5	66.0	5.55	23.1	5.08	1.00	0.26	-	0.8	Rajapaksha et al. (2018)
	700	27.5	12.3	43.7	69.4	1.31	24.4	4.61	0.23	0.26	-	2.3	
Soybean	300	37.0	7.3	10.4	68.8	4.29	25.0	1.88	0.74	0.27	-	5.6	Rajapaksha et al. (2018)
	700	21.6	11.3	17.2	82.0	1.27	15.4	1.30	0.14	0.14	-	420.3	
Sugar cane straw	350	59.6	8.8	32.2	60.8	3.3	53.4	1.8	-	-	7.0	-	Novais, Zenero, Tronto, Conz and Cerri (2018)
	650	40.2	9.2	48.8	68.2	0.8	62.3	1.7	-	-	7.0	-	
Mushroom waste	200	-	6.0	-	43.6	6.58	31.7	1.52	0.15	0.72	-	7.2	Li, Khan, et al. (2018)
	350	-	7.0	-	39.4	4.45	17.2	2.0	0.11	0.43	-	6.5	
Soybean straw	200	-	6.3	-	55.6	6.67	37.1	0.58	0.12	0.67	-	4.6	Li, Khan, et al. (2018)

	350	-	7.4	-	43.8	5.31	13.6	0.85	0.11	0.31	-	4.7	
Peanut shells	200	-	5.0	-	48.7	6.58	32.5	0.86	0.13	0.67	-	7.5	Li, Khan, et al. (2018)
	350	-	8.3	-	63.9	4.74	13.8	1.49	0.07	0.22	-	6.9	
Rice straw	200	-	5.3	-	51.5	6.24	34.2	2.06	0.12	0.66	-	5.0	Li, Khan, et al. (2018)
	350	-	8.0	-	38.4	5.33	11.6	0.49	0.14	0.30	-	2.4	
Rice husk	350	-	8.1	27.0	50.8	3.70	17.8	0.73	0.87	0.26	-	0.8	Wang and Liu (2017)
	550	-	11.5	37.1	53.2	2.11	6.9	0.75	0.48	0.10	-	5.2	
Cotton stem	350	-	8.5	8.8	62.4	4.64	22.6	1.65	0.89	0.27	-	0.7	Wang and Liu (2017)
	550	-	10.9	10.8	72.1	2.85	13.0	1.36	0.47	0.13	-	0.2	
Walnut shell	350	-	7.9	3.0	67.9	4.42	24.2	0.53	0.78	0.27	-	0.4	Wang and Liu (2017)
	550	-	10.3	4.0	80.7	2.94	11.8	0.57	0.44	0.11	-	1.6	
Wheat straw	350	-	7.5	12.1	61.8	4.43	20.5	1.13	0.86	0.25	-	1.0	Wang and Liu (2017)
	550	-	11.0	18.7	67.8	2.45	10.0	1.12	0.43	0.11	-	0.7	
Eucalyptus sawdust	350	-	7.6	2.5	68.5	4.60	23.9	0.52	0.81	0.26	-	1.1	Wang and Liu (2017)
	550	-	9.2	2.9	83.8	2.75	9.8	0.82	0.39	0.09	-	23.1	
Corn stem	350	-	7.7	7.3	63.5	4.08	24.2	0.94	0.77	0.29	-	1.0	Wang and Liu (2017)
	550	-	10.5	9.8	74.5	2.33	12.5	0.96	0.37	0.13	-	0.7	
Rice husk	300	52.5	6.2	13.6	47.7	3.19	24.7	1.10	0.75	0.38	-	68.8	Mayakaduwa, Herath, Ok, Mohan, and Vithanage (2017)
	500	34.9	7.2	18.0	49.0	2.09	24.8	0.99	0.51	0.37		169.8	
	700	33.4	9.9	39.2	50.6	1.29	7.7	0.65	0.32	0.12		236.7	
Gliricidia sepium	300	39.6	6.7	6.0	75.5	4.76	19.0	0.72	0.06	0.25	4.4	1.0	Bandara, Herath, Kumarathilaka, Hseu, et al. (2017)
	500	26.2	9.3	14.7	92.7	3.55	2.8	0.84	0.04	0.03	5.0	76.3	
Umbrella tree wood bark	500	-	9.6	12.8	84.8	3.13	10.2	1.83	-	-	-	13.6	Igalavithana, Park, et al. (2017)
Cocopeat	500	-	10.3	15.9	84.4	2.88	11.7	1.02	-	-	-	13.7	Igalavithana, Park, et al. (2017)
Palm kernel shell	500	-	6.9	6.9	87.8	2.91	8.1	1.11	-	-	-	191.0	Igalavithana, Park, et al. (2017)
Buckwheat husk	350	46.3	9.2	4.0	70.1	4.44	24.4	0.92	0.76	0.26	11.2	11.4	Zama, Zhu, Reid and Sun (2017)
	450	42.3	9.7	25.4	76.5	3.63	18.8	0.99	0.57	0.18	11.5	10.7	
	550	34.2	10.0	5.8	82.8	2.75	13.4	0.90	0.40	0.12	10.1	17.0	

	650	28.5	9.1	33.1	83.9	1.81	13.3	0.89	0.26	0.12	11.7	17.8	
Corn cobs	350	38.6	10.0	6.1	69.6	4.50	24.4	1.36	0.78	0.26	19.6	12.4	Zama et al. (2017)
	450	29.6	10.1	8.4	76.3	3.33	18.9	1.39	0.52	0.19	11.6	14.4	
	550	24.1	10.4	8.8	81.7	2.4	14.5	1.22	0.35	0.13	23.8	37.1	
	650	21.9	10.5	13.2	82.1	1.68	14.9	1.20	0.25	0.14	25.4	47.6	
Mulberry wood	350	37.5	10.2	7.5	67.9	4.53	25.2	2.16	0.80	0.28	23.3	16.6	Zama et al. (2017)
	450	32.7	11.1	7.7	70.8	3.32	23.8	1.92	0.56	0.25	22.1	31.4	
	550	26.2	10.6	9.8	77.0	2.41	18.8	1.68	0.38	0.18	19.0	58.0	
	650	22.8	10.6	9.8	80.1	1.63	16.6	1.58	0.24	0.15	21.8	24.5	
Peanut shells	350	45.7	10.4	7.1	64.3	4.32	29.4	1.69	0.81	0.34	26.5	14.0	Zama et al. (2017)
	450	38.1	11.1	17.0	70.8	3.18	24.1	1.65	0.54	0.26	23.7	14.1	
	550	32.5	10.6	7.1	73.7	2.41	21.7	1.58	0.39	0.22	19.7	18.6	
	650	29.4	10.6	24.4	74.6	1.81	21.7	1.66	0.29	0.22	17.4	28.1	
Castor cake	550	30.2	8.7	15.2	68.4	2.1	9.5	4.76	-	-	-	3.0	Hilioti et al. (2017)
Castor stalks	550	28.9	9.2	12.2	78.4	2.18	3.9	3.28	-	-	-	198.0	Hilioti et al. (2017)
Broadleaf hardwood	600	-	7.0	3.0	78.9	3.61	13.8	0.67	0.05	0.18	7.2	5.3	Shen et al. (2017)
Wheat straw	700	-	10.0	23.8	69.0	1.18	5.3	1.32	0.02	0.08	12.5	23.2	Shen et al. (2017)
Rice husk	700	-	9.8	47.9	47.3	0.63	2.1	0.85	0.01	0.04	5.4	42.0	Shen et al. (2017)
Soft wood	550	-	7.9	1.2	85.5	2.77	10.4	<0.10	0.03	0.12	2.5	26.4	Shen et al. (2017)
Gliricidia sepium	700-1000	-	10.1	19.7	50	1	44	0.5	0.24	0.66	-	714.0	Mayakaduwa, Kumarathilaka, et al. (2016)
Date palm wastes	300	50.0	8.3	14.4	58.0	4.08	20.8	0.54	0.84	0.27	-	-	Usman et al. (2016)
	700	28.9	11.5	21.0	73.4	1.14	3.2	0.35	0.19	0.03	-	-	
Eucalyptus wood	300-400	-	5.1	1.9	69.3	5.1	23.2	0.4	0.88	0.25	-	1.6	Arán et al. (2016)
Acacia wood	300-400	-	7.6	3.5	69.7	4.3	22.0	0.6	0.74	0.24	-	1.3	Arán et al. (2016)
Corn cob	300-400	-	10.1	3.9	85.2	2.1	7.9	0.8	0.29	0.07	-	173.0	Arán et al. (2016)
Olive mill waste	300-400	-	9.6	49.5	31.1	2.4	14.8	2.1	0.94	0.35	-	3.8	Arán et al. (2016)
Rice husk	300-400	-	10.5	23.3	49.6	1.5	23.0	2.3	0.35	0.35	-	62.6	Arán et al. (2016)

Maple wood	300		6.9	0.5	58.9	5.22	32.9	-	1.06	0.42	117.2	72.4	Wang, Lehmann, Hanley, Hestrin and Enders (2016)
	400		7.6	1.7	78.8	3.53	17.0	-	0.54	0.16	98.6	182.0	
	500		8.9	2.2	91.5	2.81	9.5	-	0.37	0.08	78.1	250.0	
	600		9.0	2.3	88.9	2.34	5.6	-	0.32	0.05	72.5	298.0	
	700		10.2	2.6	94.9	1.33	3.9	-	0.17	0.03	47.1	337.0	
Bamboo	820	-	10.8	5.5	76.7	1.59	21.1	0.57	0.25	0.37	-	276.0	Zhang et al. (2016)
Tea waste	300	57.0	6.2	3.8	63.5	4.75	27.1	4.50	0.89	0.32	-	2.3	Mayakaduwa, Vithanage, Karunarathna, Mohan and Ok (2016)
	500	34.3	7.1	8.4	68.1	3.35	24.1	4.40	0.58	0.26	-	1.6	
	700	26.9	10.2	12.8	73.6	1.71	7.7	3.39	0.27	0.07	-	342.2	
Pine sawdust	680	-	9.7	1.0	90.9	1.31	6.1	0.11	0.01	0.07	-	795.0	Srinivasan et al. (2015)
Paunch grass	680	-	8.8	28.7	64.8	2.28	12.4	1.8	0.03	0.19	-	2.0	Srinivasan et al. (2015)
Soybean stover	300	37.0	7.3	10.4	68.8	4.29	25.0	1.88	0.74	0.27	-	5.6	Ahmad, Lee, Dou, et al. (2012)
	700	21.6	11.3	17.2	82.0	1.27	15.4	1.30	0.19	0.14	-	420.3	
Peanut shells	300	36.9	7.8	1.2	68.3	3.85	25.9	1.91	0.67	0.29	-	3.1	Ahmad, Lee, Dou, et al. (2012)
	700	21.9	10.6	8.9	83.8	1.75	13.3	1.14	0.25	0.12	-	448.2	
Animal manure													
Pig manure	300	63.0	-	46.3	68.4	5.85	19.7	6.09	1.03	0.22	-	-	Wei et al. (2019)
	400	50.6	-	57.8	71.1	4.23	19.1	5.63	0.71	0.20	-	-	
	500	46.7	-	62.2	71.4	3.85	19.0	5.68	0.65	0.20	-	-	
	600	44.3	-	65.8	73.9	2.99	17.8	5.34	0.49	0.18	-	-	
	700	42.8	-	67.6	75.8	2.64	17.5	4.04	0.42	0.17	-	-	
Chicken manure	300-400	-	7.1	46.4	32.6	3.9	13.7	3.0	1.45	0.32	-	1.8	Arán et al. (2016)
Broiler litter	680	-	10.1	11.2	86.8	1.89	10.8	1.3	0.01	0.12	-	7.0	Srinivasan et al. (2015)
Poultry manure	350	79.8	9.6	71.4	24.1	1.85	71.5	2.09	0.92	2.23	47.9	3.3	Zama et al. (2017)
	450	69.9	10.0	77.8	22.7	1.35	73.8	1.66	0.71	2.43	47.0	5.5	
	550	67.0	10.4	77.8	21.3	0.86	75.9	1.52	0.48	2.67	39.6	9.0	
	650	66.4	9.9	79.6	23.0	0.30	74.9	1.38	0.16	2.44	33.2	7.2	
Dairy manure	600	-	9.8	84.3	11.5	0.93	10.1	0.00	0.96	0.66	-	3.9	Yang et al. (2018)

Cattle manure	500		9.9	29.3	1.5	-	1.0	-	-	-	-	195.1	Lei, Shi, Qiu, Che, and Xue (2019)
Swine Manure	500		8.5	44.0	2.9	-	2.6	-	-	-	-	59.2	Lei et al. (2019)
Poultry manure	500		8.4	41.8	2.6	-	3.7	-	-	-	-	59.0	Lei et al. (2019)
Pig manure	300	83.8	8.0	47.0	29.7	3.33	0.5	1.92	1.35	0.54	10.9	-	Gascó, Paz-Ferreiro, Álvarez, Saa, and Méndez (2018)
	450	76.6	7.8	54.7	29.7	2.98	0.4	1.81	1.21	0.32	11.6	-	
	600	56.1	8.7	68.2	29.0	1.41	0.3	1.36	0.58	0.12	13.4	-	
Yak manure	350	-	-	40.9	40.4	3.55	12.2	2.96	1.06	0.23	-	1.2	Wang and Liu (2018)
Poultry manure	350	41.5	8.3	24.2	36.3	2.5	37.5	2.6	-	-	36.0	-	Novais et al. (2018)
	650	32.8	10.0	13.9	32.6	2.7	26.8	1.4	-	-	20.0	-	
Guinea fowl manure	500	-	7.8	-	45.6	4.0	8.3	4.5	-	-	-	60.0	Idrees et al. (2018)
Cattle manure	500	-	8.7	20.4	79.0	4.26	7.4	10.21	-	-	-	4.0	Idrees et al. (2018)
Farm yard manure	450-650	-	8.2	27.2	47.5	2.64	17.5	2.31	-	-	-	10.1	Batool, Idrees, Hussain, and Kong (2017)
Poultry manure	450-650	-	7.8	31.4	42.4	3.22	14.9	1.98	-	-	-	8.6	Batool et al. (2017)
Swine manure	300	-	7.9	38.0	37.6	3.88	15.9	4.08	-	-	-	-	Wang, Meng, et al. (2017)
	500	-	9.5	50.0	33.9	2.74	9.4	3.39	-	-	-	-	
	700	-	9.9	60.0	30.4	1.20	5.0	2.48	-	-	-	-	
Yak manure	350	-	8.9	40.9	40.4	3.55	12.2	2.96	1.06	0.23	-	1.2	Wang and Liu (2017)
	550	-	10.5	52.2	37.4	1.56	6.5	2.32	0.50	0.13	-	8.7	
Other													
Sewage sludge	300	82.4	7.4	76.7	11.8	1.37	9.3	1.73	1.39	0.59	-	6.1	Gao et al. (2019)
	500	74.2	7.0	83.3	8.6	0.63	8.8	1.16	0.87	0.76	-	8.5	
	700	65.3	6.7	90.7	8.1	0.08	4.1	0.65	0.12	0.38	-	34.8	
Digested sludge	350	70.3	8.6	-	22.0	1.7	14.9	3.1	0.08	0.68	-	-	Tang et al. (2019)
	400	64.4	8.6	-	19.4	1.3	12.7	2.7	0.07	0.65	-	-	
	450	61.3	9.5	-	18.6	1.0	11.9	2.6	0.05	0.64	-	-	
	500	58.4	10.4	-	17.7	0.8	10.9	2.4	0.04	0.62	-	-	
	550	57.2	10.6	-	15.7	0.6	9.2	2.1	0.04	0.59	-	-	
Sewage sludge	300	85.0	-	66.8	70.6	4.04	19.3	6.10	0.69	0.21	-	-	Wei et al. (2019)

	400	77.2	-	72.9	69.9	4.00	20.5	5.63	0.69	0.22	-	-	
	500	74.1	-	75.8	70.6	3.28	21.0	5.07	0.56	0.22	-	-	
	600	71.8	-	78.6	73.4	3.03	19.2	4.43	0.50	0.20	-	-	
	700	66.7	-	85.0	74.4	2.70	20.0	2.90	0.44	0.20	-	-	
Digestate biosolid	550	-	9.4	-	75.6	1.72	14.9	0.98	0.27	0.08	72.9	27.5	Ngigi et al. (2019)
Sewage-sludge	500	-	8.6	-	36.9	2.34	16.4	6.16	0.76	0.43	15.8	26.2	Ngigi et al. (2019)
Textile dyeing sludge	300	80.8	7.4	63.6	17.9	1.85	10.4	1.71	1.24	0.44	-	23.8	Wang, Li, et al. (2019)
	400	73.1	8.7	68.4	15.0	1.10	9.0	1.11	0.88	0.45	-	22.0	
	500	69.0	10.2	71.3	14.2	0.72	7.3	0.83	0.61	0.39	-	27.1	
	600	66.8	11.0	75.0	13.7	0.54	4.4	0.39	0.47	0.24	-	31.4	
	700	61.0	12.3	78.6	12.3	0.42	2.0	0.12	0.41	0.12	-	65.6	
Algae	500	-	10.2	59.7	24.6	1.33	11.4	3.22	0.65	0.35	-	0.5	Yang et al. (2018)
Sewage sludge	200	-	5.5	-	29.2	5.22	16.5	2.43	0.18	0.56	-	0.5	Li, Khan, et al. (2018)
	350	-	5.8	-	31.8	3.42	11.8	1.65	0.11	0.37	-	7.9	
Waste sludge	400	68.5	7.0	66.1	16.3	1.27	13.9	2.14	0.08	0.85	-	-	Ho et al. (2017)
	600	63.7	10.2	78.7	15.4	0.68	7.4	1.62	0.04	0.48	-	-	
	800	62.7	10.2	79.6	14.4	0.41	5.3	0.77	0.03	0.37	-	-	
Anaerobic digestion sludge	400	70.3	7.6	66.4	16.2	1.50	12.7	1.87	0.09	0.79	-	-	Ho et al. (2017)
	600	65.4	10.8	77.4	14.0	0.73	7.3	0.76	0.05	0.52	-	-	
	800	63.4	10.4	77.9	12.9	0.40	5.4	0.50	0.03	0.42	-	-	
Biosolids	600	36.5	8.0	43.7	42.4	1.91	4.8	6.39	0.05	0.11	-	-	Gonzaga et al. (2017)
Municipal solid waste	450	-	9.7	15.6	60.8	2.79	14.6	1.33	0.04	0.24	-	108.5	Jayawardhana, et al. (2017)
Sewage sludge	680	-	7.9	12.6	78.0	2.10	19.3	0.5	0.02	0.25	-	-	Srinivasan et al. (2015)
Dewatered pond sludge	680	-	7.7	4.0	78.7	2.33	18.6	0.3	0.03	0.24	-	-	Srinivasan et al. (2015)
Dissolved air floatation sludge	680	-	8.3	4.6	66.9	1.9	30.5	0.7	0.02	0.22	-	-	Srinivasan et al. (2015)

CEC, cation exchange capacity

References

Ahmad, M., Lee, S.S., Dou, X., Mohan, D., Sung, J.-K., Yang, J.E., & Ok, Y.S. (2012). Effects of pyrolysis temperature on soybean stover- and peanut shell-derived biochar properties and TCE adsorption in water. *Bioresource Technology*,*118*, 536-544.

Al-Wabel, M.I., Al-Omran, A., El-Naggar, A.H., Nadeem, M., & Usman, A.R.A. (2013). Pyrolysis temperature induced changes in characteristics and chemical composition of biochar produced from conocarpus wastes. *Bioresource Technology*, *131*, 374-379.

Antal, M., & Gronli, M. (2003). The art, science, and technology of charcoal production *Industrial & Engineering Chemistry Research*, *42*(8), 1619-1640.

Arán, D., Antelo, J., Fiol, S., & Macías, F. (2016). Influence of feedstock on the copper removal capacity of waste-derived biochars. *Bioresource Technology*, *212*, 199-206.

Bachmann, H.J., Bucheli, T.D., Dieguez-Alonso, A., Fabbri, D., Knicker, H., Schmidt, H.-P., … Zehetner, F. (2016). Toward the Standardization of Biochar Analysis: The COST Action TD1107 Interlaboratory Comparison. *Journal of Agricultural and Food Chemistry* 64, 513-527.

Bandara, T., Herath, I., Kumarathilaka, P., Hseu, Z.-Y., Ok, Y., & Vithanage, M. (2017). Efficacy of woody biomass and biochar for alleviating heavy metal bioavailability in serpentine soil. *Environmental Geochemistry and Health*, *39*, 391-401.

Batool, S., Idrees, M., Hussain, Q., & Kong, J. (2017). Adsorption of copper (II) by using derived-farmyard and poultry manure biochars: Efficiency and mechanism. *Chemical Physics Letters*, *689*, 190-198.

Bruun, E.W., Ambus, P., Egsgaard, H., & Hauggaard-Nielsen, H. (2012). Effects of slow and fast pyrolysis biochar on soil C and N turnover dynamics. *Soil Biology and Biochemistry*, *46*, 73-79.

Cha, J.S., Park, S.H., Jung, S.-C., Ryu, C., Jeon, J.-K., Shin, M.-C., & Park, Y.-K. (2016). Production and utilization of biochar: A review. *Journal of Industrial and Engineering Chemistry*, 40, 1-15.

Choi, Y.-K., & Kan, E. (2019). Effects of pyrolysis temperature on the physicochemical properties of alfalfa-derived biochar for the adsorption of bisphenol A and sulfamethoxazole in water. *Chemosphere*, *218*, 741-748.

Chu, G., Zhao, J., Chen, F., Dong, X., Zhou, D., Liang, N., … Steinberg, C.E.W. (2017). Physi-chemical and sorption properties of biochars prepared from peanut shell using thermal pyrolysis and microwave irradiation. Environmental Pollution, 227, 372-379.

Dai, L., Tan, F., Li, H., Zhu, N., He, M., Zhu, Q., … Zhao, J. (2017). Calcium-rich biochar from the pyrolysis of crab shell for phosphorus removal. *Journal of Environmental Management*, *198*, 70-74.

Deng, J., Liu, Y., Liu, S., Zeng, G., Tan, X., Huang, B., … Yan, Z. (2017). Competitive adsorption of Pb(II), Cd(II) and Cu(II) onto chitosan-pyromellitic dianhydride modified biochar. *Journal of Colloid And Interface Science*, *506*, 355-364.

Du, J., Zhang, L., Liu, T., Xiao, R., Li, R., Guo, D., … Zhang, Z. (2019). Thermal conversion of a promising phytoremediation plant (*Symphytum officinale* L.) into biochar: Dynamic of potentially toxic elements and environmental acceptability assessment of the biochar. *Bioresource Technology*, *274*, 73-82.

El-Naggar, A., Lee, S.S., Rinklebe, J., Farooq, M., Song, H., Sarmah, A.K., … Ok, Y.S. (2019). Biochar application to low fertility soils: A review of current status, and future prospects. *Geoderma*, *337*, 536-554.

El-Naggar, A., Shaheen, S.M., Hseu, Z.-Y., Wang, S.-L., Ok, Y.S., & Rinklebe, J. (2019). Release dynamics of As, Co, and Mo in a biochar treated soil under pre-definite redox conditions. *Science of the Total Environment*, *657*, 686-695.

Fang, J., Zhan, L., Ok, Y.S., & Gao, B. (2018). Minireview of potential applications of hydrochar derived from hydrothermal carbonization of biomass. *Journal of Industrial and Engineering Chemistry*, *57*, 15-21.

Gao, L.-Y., Deng, J.-H., Huang, G.-F., Li, K., Cai, K.-Z., Liu, Y., & Huang, F. (2019). Relative distribution of Cd^{2+} adsorption mechanisms on biochars derived from rice straw and sewage sludge. *Bioresource Technology*, *272*, 114-122.

Gascó, G., Paz-Ferreiro, J., Álvarez, M.L., Saa, A., & Méndez, A. (2018). Biochars and hydrochars prepared by pyrolysis and hydrothermal carbonisation of pig manure. *Waste Management*, *79*, 395-403.

Gonzaga, M.I.S., Mackowiak, C.L., Comerford, N.B., Moline, E.F.d.V., Shirley, J.P., & Guimaraes, D.V. (2017). Pyrolysis methods impact biosolids-derived biochar composition, maize growth and nutrition. *Soil and Tillage Research*, *165*, 59-65.

Haeldermans, T., Claesen, J., Maggen, J., Carleer, R., Yperman, J., Adriaensens, P., … Vanreppelen, K. (2019). Microwave assisted and conventional pyrolysis of MDF–characterization of the produced biochars. *Journal of Analytical and Applied Pyrolysis*, *138*, 218-230.

Han, L., Sun, H., Ro, K.S., Sun, K., Libra, J.A., & Xing, B. (2017). Removal of antimony(III) and cadmium(II) from aqueous solution using animal manure-derived hydrochars and pyrochars. *Bioresource Technology*, *234*, 77-85.

He, L., Fan, S., Müller, K., Wang, H., Che, L., Xu, S., … Tsang, D.C. (2018). Comparative analysis biochar and compost-induced degradation of di-(2-ethylhexyl) phthalate in soils. *Science of the Total Environment*, *625*, 987-993.

Hilioti, Z., Michailof, C.M., Valasiadis, D., Iliopoulou, E.F., Koidou, V., & Lappas, A.A. (2017). Characterization of castor plant-derived biochars and their effects as soil amendments on seedlings. *Biomass and Bioenergy*, *105*, 96-106.

Ho, S.-H., Chen, Y.-d., Yang, Z.-k., Nagarajan, D., Chang, J.-S., & Ren, N.-q. (2017). High-efficiency removal of lead from wastewater by biochar derived from anaerobic digestion sludge. *Bioresource Technology*, *246,* 142-149.

Idrees, M., Batool, S., Kalsoom, T., Yasmeen, S., Kalsoom, A., Raina, S., … Kong, J. (2018). Animal manure-derived biochars produced via fast pyrolysis for the removal of divalent copper from aqueous media. *Journal of Environmental Management*, *213*, 109-118.

Igalavithana, A.D., Park, J., Ryu, C., Lee, Y.H., Hashimoto, Y., Huang, L., … Lee, S.S. (2017). Slow pyrolyzed biochars from crop residues for soil metal (loid) immobilization and microbial community abundance in contaminated agricultural soils. *Chemosphere*, *177*, 157-166.

Jayawardhana, Y., Mayakaduwa, S., Kumarathilaka, P., Gamage, S., & Vithanage, M. (2017). Municipal solid waste-derived biochar for the removal of benzene from landfill leachate. *Environmental Geochemistry and Health*, 1-15.

Jones, K., Ramakrishnan, G., Uchimiya, M., & Orlov, A. (2015). New applications of X-ray tomography in pyrolysis of biomass: Biochar imaging. *Energy and Fuels*, *29*, 1628-1634.

Kambo, H.S., & Dutta, A. (2015). A comparative review of biochar and hydrochar in terms of production, physico-chemical properties and applications. *Renewable and Sustainable Energy Reviews*, *45*, 359-378.

Lan, R., & Tao, S. (2016). A simple high-performance matrix-free biomass molten carbonate fuel cell without CO_2 recirculation. *Science Advances*, *2*,

Lei, S., Shi, Y., Qiu, Y., Che, L., & Xue, C. (2019). Performance and mechanisms of emerging animal-derived biochars for immobilization of heavy metals. *Science of the Total Environment*, *646*, 1281-1289.

Li, G., Khan, S., Ibrahim, M., Sun, T.-R., Tang, J.-F., Cotner, J.B., & Xu, Y.-Y. (2018). Biochars induced modification of dissolved organic matter (DOM) in soil and its impact on mobility and bioaccumulation of arsenic and cadmium. *Journal of Hazardous Materials*, *348*, 100-108.

Li, H., Dong, X., Da Silva, E.B., de Oliveira, L.M., Chen, Y., & Ma, L.Q. (2017). Mechanisms of metal sorption by biochars: Biochar characteristics and modifications. *Chemosphere*, *178*, 466-478.

Li, J., Dai, J., Liu, G., Zhang, H., Gao, Z., Fu, J., … Huang, Y. (2016). Biochar from microwave pyrolysis of biomass: A review. *Biomass and Bioenergy*, *94*, 228-244.

Mao, X., Kang, Q., Liu, Y., Siyal, A.A., Ao, W., Ran, C., … Dai, J. (2019). Microwave-assisted pyrolysis of furfural residue in a continuously operated auger reactor: Biochar characterization and analysis. *Energy*, *168*, 573-584.

Mayakaduwa, S.S., Herath, I., Ok, Y.S., Mohan, D., & Vithanage, M. (2017). Insights into aqueous carbofuran removal by modified and non-modified rice husk biochars. *Environmental Science and Pollution Research*, *24*, 22755-22763.

Mayakaduwa, S.S., Kumarathilaka, P., Herath, I., Ahmad, M., Al-Wabel, M., Ok, Y.S., … Vithanage, M. (2016). Equilibrium and kinetic mechanisms of woody biochar on aqueous glyphosate removal. *Chemosphere*, *144*, 2516-2521.

Mayakaduwa, S.S., Vithanage, M., Karunarathna, A., Mohan, D., & Ok, Y.S. (2016). Interface interactions between insecticide carbofuran and tea waste biochars produced at different pyrolysis temperatures. *Chemical Speciation & Bioavailability*, *28*, 110-118.

Melo, T.M., Bottlinger, M., Schulz, E., Leandro, W.M., Botelho de Oliveira, S., Menezes de Aguiar Filho, A., … Rinklebe, J. (2019). Management of biosolids-derived hydrochar (Sewchar): Effect on plant germination, and farmers' acceptance. *Journal of Environmental Management*, *237*, 200-214.

Melo, T.M., Bottlinger, M., Schulz, E., Leandro, W.M., de Aguiar Filho, A.M., Wang, H., … Rinklebe, J. (2018). Plant and soil responses to hydrothermally converted sewage sludge (sewchar). *Chemosphere*, *206*, 338-348.

Ngigi, A., Ok, Y.S., & Thiele-Bruhn, S. (2019). Biochar-mediated sorption of antibiotics in pig manure. *Journal of Hazardous Materials*, *364*, 663-670.

Novais, S.V., Zenero, M.D.O., Tronto, J., Conz, R.F., & Cerri, C.E.P. (2018). Poultry manure and sugarcane straw biochars modified with $MgCl_2$ for phosphorus adsorption. *Journal of Environmental Management*, *214*, 36-44.

Pal, D., & Maiti, S.K. (2019). Abatement of cadmium (Cd) contamination in sediment using tea waste biochar through meso-microcosm study. *Journal of Cleaner Production*, *212*, 986-996.

Qin, P., Wang, H., Yang, X., He, L., Müller, K., Shaheen, S.M., … Ok, Y.S. (2018). Bamboo-and pig-derived biochars reduce leaching losses of dibutyl phthalate, cadmium, and lead from co-contaminated soils. *Chemosphere*, *198*, 450-459.

Rajapaksha, A.U., Alam, M.S., Chen, N., Alessi, D.S., Igalavithana, A.D., Tsang, D.C.W., & Ok, Y.S. (2018). Removal of hexavalent chromium in aqueous solutions using biochar: Chemical and spectroscopic investigations. *Science of the Total Environment*, *625*, 1567-1573.

Rajapaksha, A.U., Ok, Y.S., El-Naggar, A., Kim, H., Song, F., Kang, S., & Tsang, Y.F. (2019). Dissolved organic matter characterization of biochars produced from different feedstock materials. *Journal of Environmental Management*, *233*, 393-399.

Rangabhashiyam, S., & Balasubramanian, P. (2019). The potential of lignocellulosic biomass precursors for biochar production: Performance, mechanism and wastewater application-A review. *Industrial Crops and Products*, *128*, 405-423.

Sethupathi, S., Zhang, M., Rajapaksha, A., Lee, S., Mohamad Nor, N., Mohamed, A., … Ok, Y. (2017). Biochars as Potential Adsorbers of CH_4, CO_2 and H_2S. *Sustainability*, *9*, 121.

Shaheen, S.M., Niazi, N.K., Hassan, N.E., Bibi, I., Wang, H., Tsang, D.C., … Rinklebe, J. (2019). Wood-based biochar for the removal of potentially toxic elements in water and wastewater: a critical review. *International Materials Reviews*, *64*, 216-247.

Shen, Z., Hou, D., Jin, F., Shi, J., Fan, X., Tsang, D.C.W., & Alessi, D.S. (2019). Effect of production temperature on lead removal mechanisms by rice straw biochars. *Science of the Total Environment*, *655*, 751-758.

Shen, Z., Zhang, Y., Jin, F., McMillan, O., & Al-Tabbaa, A. (2017). Qualitative and quantitative characterisation of adsorption mechanisms of lead on four biochars. *Science of the Total Environment*, *609*, 1401-1410.

Sikarwar, V.S., Zhao, M., Clough, P., Yao, J., Zhong, X., Memon, M.Z., … Fennell, P.S. (2016). An overview of advances in biomass gasification. *Energy & Environmental Science*, *9*, 2939-2977.

Song, C., Shan, S., Müller, K., Wu, S., Niazi, N.K., Xu, S., … Wang, H. (2018). Characterization of pig manure-derived hydrochars for their potential application as fertilizer. *Environmental Science and Pollution Research*, *25*, 25772-25779.

Srinivasan, P., Sarmah, A.K., Smernik, R., Das, O., Farid, M., & Gao, W. (2015). A feasibility study of agricultural and sewage biomass as biochar, bioenergy and biocomposite feedstock: Production, characterization and potential applications. *Science of the Total Environment*, *512*, 495-505.

Tang, C., Weligama, C., & Sale, P. (2013). Subsurface Soil Acidification in Farming Systems: Its Possible Causes and Management Options In J. Xu and D. L. Sparks (eds.) *Molecular Environmental Soil Science* (pp. 389-412). Dordrecht: Springer Netherlands.

Tang, Y., Alam, M.S., Konhauser, K.O., Alessi, D.S., Xu, S., Tian, W., & Liu, Y. (2019). Influence of pyrolysis temperature on production of digested sludge biochar and its application for ammonium removal from municipal wastewater. *Journal of Cleaner Production*, *209*, 927-936.

Tripathi, M., Sahu, J.N., & Ganesan, P. (2016). Effect of process parameters on production of biochar from biomass waste through pyrolysis: A review. *Renewable and Sustainable Energy Reviews*, *55*, 467-481.

Uchimiya, M., Wartelle, L. H., Klasson, K. T., Fortier, C. A., & Lima, I. M. (2011). Influence of pyrolysis temperature on biochar property and function as a heavy metal sorbent in soil. *Journal of agricultural and food chemistry*, *59*(6), 2501-2510.

Usman, A., Sallam, A., Zhang, M., Vithanage, M., Ahmad, M., Al-Farraj, A., … Al-Wabel, M. (2016). Sorption Process of Date Palm Biochar for Aqueous Cd(II) Removal: Efficiency and Mechanisms. *Water, Air, & Soil Pollution*, *227*, 449.

Vithanage, M., Herath, I., Joseph, S., Bundschuh, J., Bolan, N., Ok, Y.S., … Rinklebe, J. (2017). Interaction of arsenic with biochar in soil and water: a critical review. *Carbon*, *113*, 219-230.

Wahi, R., Zuhaidi, N.F.Q.a., Yusof, Y., Jamel, J., Kanakaraju, D., & Ngaini, Z. (2017). Chemically treated microwave-derived biochar: An overview. *Biomass and Bioenergy*, *107*, 411-421.

Wang, B., Lehmann, J., Hanley, K., Hestrin, R., & Enders, A. (2016). Ammonium retention by oxidized biochars produced at different pyrolysis temperatures and residence times. *RSC Advances*, *6*, 41907-41913.

Wang, L., Meng, J., Li, Z., Liu, X., Xia, F., & Xu, J. (2017). First "charosphere" view towards the transport and transformation of Cd with addition of manure derived biochar. *Environmental Pollution*, *227*, 175-182.

Wang, S., Gao, B., Zimmerman, A.R., Li, Y., Ma, L., Harris, W.G., & Migliaccio, K.W. (2015a). Physicochemical and sorptive properties of biochars derived from woody and herbaceous biomass. *Chemosphere*, *134*, 257-262.

Wang, X., Li, C., Li, Z., Yu, G., & Wang, Y. (2019). Effect of pyrolysis temperature on characteristics, chemical speciation and risk evaluation of heavy metals in biochar derived from textile dyeing sludge. *Ecotoxicology and Environmental Safety*, *168*, 45-52.

Wang, Y., & Liu, R. (2017). Comparison of characteristics of twenty-one types of biochar and their ability to remove multi-heavy metals and methylene blue in solution. *Fuel Processing Technology*, *160*, 55-63.

Wang, Y., & Liu, R. (2018). H_2O_2 treatment enhanced the heavy metals removal by manure biochar in aqueous solutions. *Science of the Total Environment*, *628-629*, 1139-1148.

Wei, S., Zhu, M., Fan, X., Song, J., Peng, P.a., Li, K., … Song, H. (2019). Influence of pyrolysis temperature and feedstock on carbon fractions of biochar produced from pyrolysis of rice straw, pine wood, pig manure and sewage sludge. *Chemosphere*, *218*, 624-631.

Wu, W., Li, J., Lan, T., Müller, K., Niazi, N.K., Chen, X., … Wang, H. (2017). Unraveling sorption of lead in aqueous solutions by chemically modified biochar derived from coconut fiber: A microscopic and spectroscopic investigation. *Science of the Total Environment*, *576*, 766-774.

Wu, W., Li, J., Niazi, N.K., Müller, K., Chu, Y., Zhang, L., … Wang, H. (2016). Influence of pyrolysis temperature on lead immobilization by chemically modified coconut fiber-derived biochars in aqueous environments. *Environmental Science and Pollution Research*, *23*, 22890-22896.

Xu, X., Zhao, Y., Sima, J., Zhao, L., Mašek, O., & Cao, X. (2017). Indispensable role of biochar-inherent mineral constituents in its environmental applications: A review. *Bioresource Technology*, *241*, 887-899.

Yang, X., Igalavithana, A.D., Oh, S.-E., Nam, H., Zhang, M., Wang, C.-H., … Ok, Y.S. (2018). Characterization of bioenergy biochar and its utilization for metal/metalloid immobilization in contaminated soil. *Science of the Total Environment*, *640*, 704-713.

Yang, X., Lu, K., McGrouther, K., Che, L., Hu, G., Wang, Q., … Ye, Z. (2017). Bioavailability of Cd and Zn in soils treated with biochars derived from tobacco stalk and dead pigs. *Journal of soils and sediments*, *17*, 751-762.

Yang, X., Ng, W., Wong, B.S.E., Baeg, G.H., Wang, C.-H., & Ok, Y.S. (2019). Characterization and ecotoxicological investigation of biochar produced via slow pyrolysis: Effect of feedstock composition and pyrolysis conditions. *Journal of Hazardous Materials*, *365*, 178-185.

Yang, X., Wang, H., Strong, P.J., Xu, S., Liu, S., Lu, K., … He, L. (2017). Thermal properties of biochars derived from waste biomass generated by agricultural and forestry sectors. *Energies*, *10*, 469.

Yuan, J.H., & Xu, R.K. (2011). The amelioration effects of low temperature biochar generated from nine crop residues on an acidic Ultisol. *Soil Use and Management*, *27*, 110-115.

Zama, E.F., Zhu, Y.-G., Reid, B.J., & Sun, G.-X. (2017). The role of biochar properties in influencing the sorption and desorption of Pb(II), Cd(II) and As(III) in aqueous solution. *Journal of Cleaner Production*, *148*, 127-136.

Zhang, H., Chen, C., Gray, E.M., & Boyd, S.E. (2017). Effect of feedstock and pyrolysis temperature on properties of biochar governing end use efficacy. *Biomass and Bioenergy*,*105*, 136-146.

Zhang, J., Liu, J., & Liu, R. (2015). Effects of pyrolysis temperature and heating time on biochar obtained from the pyrolysis of straw and lignosulfonate. *Bioresource Technology*,*176*, 288-291.

Zhang, J., Zhang, J., Wang, M., Wu, S., Wang, H., Niazi, N.K., … Wong, M.H. (2019). Effect of tobacco stem-derived biochar on soil metal immobilization and the cultivation of tobacco plant. *Journal of soils and sediments*, *19*, 2313-2321.

Zhang, X., Sarmah, A.K., Bolan, N.S., He, L., Lin, X., Che, L., … Wang, H. (2016). Effect of aging process on adsorption of diethyl phthalate in soils amended with bamboo biochar. *Chemosphere*,*142*, 28-34.

Zhang, Z., Zhu, Z., Shen, B., & Liu, L. (2019). Insights into biochar and hydrochar production and applications: A review. *Energy*, *171*, 581-598.